POLITECNICO DI TORINO

Master in Environmental and Land Engineering

Eco-morphological analysis and geomatic survey of the coastal dune of the San Rossore Park

Supervisors
Prof. Carlo Vincenzo Camporeale
Prof. Elena Belcore

Candidate
Muhammad Tahir

ACADEMIC YEAR 2022-2023

Acknowledgements

In the Name of Allah Almighty, The Most Gracious and Most Merciful.

First and foremost, I express my deepest gratitude to Allah Almighty, whose blessings, mercy, and guidance have enabled me to accomplish this important academic milestone.

I extend my heartfelt thanks to Professor Carlo Vincenzo Camporeale and Professor Elena Belcore for their continuous guidance, patience, encouragement, and invaluable support throughout this research. Their mentorship played a fundamental role in the successful completion of this thesis and in my academic growth.

I am profoundly grateful to my beloved parents, Muhammad Javid and Halima Akhtar, whose unwavering support, sacrifices, prayers, and encouragement have made my educational journey possible. Their dedication and belief in me have been the foundation of my achievements and have enabled me to pursue my studies at Politecnico di Torino and complete my degree. I also extend my sincere appreciation to my beloved sisters and brother for their constant love, motivation, and encouragement throughout this journey.

Additionally, I would like to express my sincere gratitude to all my teachers, mentors, colleagues, friends, and seniors who have supported, guided, and inspired me throughout my academic and personal development. Their knowledge, advice, and encouragement have greatly enriched my learning experience.

Finally, I would like to thank everyone who contributed, directly or indirectly, to the completion of this thesis. Their support and goodwill are deeply appreciated.

Thank you.

Summary

This thesis provides a detailed eco-morphological analysis of the coastal dune system in San Rossore Park (Tuscany, Italy). This research integrates geomatic data acquisition with ecological analysis to quantify recent alterations in dune topography and vegetation. We chose San Rossore Park for its dynamic Mediterranean dunes and protected status, which make it an ideal site to study dune responses to environmental and anthropogenic factors. This in turn helps guide conservation measures. The study utilized multi-source datasets includes Uncrewed Aerial Vehicle (UAV) photogrammetry, airborne LiDAR scans, Global Navigation Satellite System (GNSS), and in-situ bathymetric surveys. Annual UAV flights from 2021 to 2024 generated high-resolution point clouds and orthophotos of three coastal study sites. We merged RTK-corrected nearshore bathymetric points with georeferenced LiDAR data to produce precise digital elevation models (DEMs) covering the dunes and adjacent beach. These DEMs provide a baseline for detecting terrain and vegetation changes.
The methodology integrated terrain and vegetation change detection. We used multi-temporal DEM differencing to calculate elevation changes (Erosion or Accretion) across the survey years. We applied a statistical Level of Detection (LoD) threshold to remove any changes that fell within the uncertainty threshold. We analyzed visible-band imagery using the Visible Atmospherically Resistant Index (VARI) to assess vegetation greenness. We first separated ground points from non-ground points and then used a supervised classification to distinguish vegetated areas from bare sand. After that compared maps from different years to identify where vegetation cover had expanded or reduced.
Key results show divergent trends among the three areas. Area 1 remained essentially in equilibrium with only minor sand shifts and little net change in vegetation cover. Area 2 experienced pronounced foredune erosion and landward shoreline, accompanied by a notable loss of vegetation along the seaward dune face. Area 3 underwent major sand deposition in one interval followed by erosion in the next, resulting in minimal net topographic change by 2024. Vegetation cover, after an initial decline, ultimately showed a modest net increase. These contrasts highlight that even within one park, some dune sectors remained stable while others suffered significant erosion or recovery.
Overall, the findings demonstrate the values of high-resolution geomatic monitoring for understanding coastal dune dynamics. The combined LiDAR and bathymetry approach captured fine-scale changes in topography that conventional methods might miss. Furthermore, non-ground LiDAR points enabled the assessment of vegetation changes over the study period. The study confirms that dune morphology and vegetation are interlink like the zones of sand accretion generally corresponded to vegetation growth, whereas erosional hotspots led to vegetation loss. These insights highlight the importance of continuous monitoring to provide early warning of dune erosion or habitat decline. This helps timely management actions and supports long-term ecosystem stability.

Table of Contents

Summary ... 3

List of Figures ... 6

List of Tables ... 7

List of Symbols, Abbreviation &Nomenclature ... 8

1 Introduction ... 11

2 Materials and Datasets ... 16

2.1 Study Area ... 16

2.2 Overview of Acquired Data ... 17

2.3 Coordinate Systems ... 20

2.4 Software Used ... 21

2.5 Measures uncertainties ... 21

3 Methodology ... 22

3.1 Workflow Overview ... 22

3.2 Preprocessing in CloudCompare ... 24

3.3 Elevation Change Detection ... 25

3.3.1 Raster Clipping to Study Area Extents ... 26

3.3.2 Multi Temporal DEM Differencing ... 26

3.3.3 Level of Detection (LoD) ... 26

3.3.4 Thresholding Elevation Changes ... 27

3.3.5 Histogram Analysis of Filtered Changes ... 27

3.3.6 Reclassification into Erosion and Accretion Categories ... 27

3.3.7 Area Calculation and Statistical Analysis ... 28

3.4 Vegetation Change Detection ... 28

3.4.1 CSF Filtering for Non-Ground Points ... 29

3.4.2 Rasterization and RGB Band Separation ... 29

3.4.3 VARI Index Calculation ... 30

3.4.4 Supervised Classification of Vegetation and Non-Vegetation ... 30

3.4.5 Multi Temporal Differencing and Change Mapping ... 31

3.4.6 Quantification of Vegetation Change ... 32

4 Results ... 34

4.1 Overview of Results Presentation ... 34

4.2 Elevation Change Detection Area 1 35
4.3 Elevation Change Detection Area 2 44
4.4 Elevation Change Detection Area 3 53
4.5 Vegetation Change Detection Area 1 64
4.6 Vegetation Change Detection Area 2 68
4.7 Vegetation Change Detection Area 3 74
5 Discussion 82
5.1 Area 1: Geomorphological and Vegetation Changes 82
5.2 Area 2: Geomorphological and Vegetation Changes 83
5.3 Area 3: Geomorphological and Vegetation Changes 85
5.4 Synthesis and Comparative Analysis Across Areas 88
5.5 Evaluation of Methodological Approaches 90
5.6 Limitations and Uncertainties 95
5.7 Implications for Dune Conservation and Monitoring Strategies 99
6 Conclusion 103
7 References 105
8 Appendix 107

List of Figures

Figure 1 Study Areas with their map coordinates 16
Figure 2 Morphology of the Area 1 in 2023 overlapped with the bathymetry points 20
Figure 3 Workflow Diagram 23
Figure 4 Area 1 DoD at LoD 1 36
Figure 5 Area 1 DoD at LoD 95 36
Figure 6 Classified Elevation Change Map of Area 1, Threshold LoD1 38
Figure 7 Significant Change Histogram of Area 1 with LoD1 39
Figure 8 Classified Elevation Change Map of Area 1 at LoD95 41
Figure 9 Significant Change Histogram of Area 1 with LoD95 42
Figure 10 Area 2 DoD at LoD 1 44
Figure 11 Area 2 DoD at LoD 95 44
Figure 12 Classified Elevation Change Map of Area 2 at LoD1 46
Figure 13 Significant Change Histogram of Area 2 with LoD1 47
Figure 14 Classified Elevation Change Map of Area 2 at LoD95 49
Figure 15 Significant Change Histogram of Area 2 with LoD95 50
Figure 16 Area 3 DoD at LoD 1 54
Figure 17 Area 3 DoD at LoD 95 54
Figure 18 Classified Elevation Change Map of Area 3 at LoD1 56
Figure 19 Significant Change Histogram of Area 3 with LoD1 58
Figure 20 Classified Elevation Change Map of Area 2 at LoD95 59
Figure 21 Significant Change Histogram of Area 3 with LoD95 61
Figure 22 VARI raster layer - greenness intensity distribution in Area 1 65
Figure 23 Vegetation vs. non-vegetation classification map, Area 1 66
Figure 24 Vegetation change maps of Area 1 67
Figure 25 VARI raster layer - greenness intensity distribution in Area2 70
Figure 26 Vegetation vs. non-vegetation classification map, Area 2 71
Figure 27 Vegetation change maps of Area 2 73
Figure 28 VARI raster layer - greenness intensity distribution in Area 3 76
Figure 29 Vegetation vs. non-vegetation classification map of Area 3 77
Figure 30 Vegetation change maps of Area 3 80
ANNEX 1 Histograms of Area 1 Elevation Changes excluding peak classes at LoD1……..107
ANNEX 2 Histograms of Area 1 Elevation Changes excluding peak classes at LoD95 107
ANNEX 3 Histograms of Area 2 Elevation Changes excluding peak classes at LoD1 108
ANNEX 4 Histograms of Area 2 Elevation Changes excluding peak class at LoD95 108
ANNEX 5 Histograms of Area 3 Elevation Changes excluding peak class at LoD1 109
ANNEX 6 Histograms of Area 3 Elevation Changes excluding peak class at LoD95 109

List of Tables

Table 1 Summary of Point Density of LiDAR Datasets in Clipped AOIs (2021-2024) 18
Table 2 Summary of Bathymetry Datasets: Number of Points (2021-2024) 19
Table 3 Parameters for Terrain Surface 24
Table 3a SVM training samples by area 33
Table 4 RMSE results and the chosen interpolation method per area/year 34
Table 5 LoD1 Threshold values 35
Table 6 LoD95 Threshold values 35
Table 7 Elevation Change Summary of Area 1 at LoD1 38
Table 8 Elevation Change Summary of Area 1 at LoD95 41
Table 9 Elevation Change Summary of Area 2 at LoD1 46
Table 10 Elevation Change Summary of Area 2 at LoD95 49
Table 11 Elevation Change Summary of Area 3 at LoD1 56
Table 12 Elevation Change Summary of Area 3 at LoD95 60
Table 13 Vegetation Change Summary, Area 1 68
Table 14 Vegetation Change Summary, Area 2 74
Table 15 Vegetation Change Summary, Area 3 81
ANNEX 7 DoD Areal change summary of Area 1 at LoD 1 110
ANNEX 8 DoD Areal change summary of Area 1 at LoD 95 110
ANNEX 9 DoD Areal change summary of Area 2 at LoD 1 110
ANNEX 10 DoD Areal change summary of Area 2 at LoD 95 110
ANNEX 11 DoD Areal change summary of Area 3 at LoD 1 111
ANNEX 12 DoD Areal change summary of Area 3 at LoD 95 111

List of Symbols, Abbreviation &Nomenclature

Abbreviation / Symbol	Full Term	Description / Context
UAV	Uncrewed Aerial Vehicle	Drone platform for dune surveys.
LiDAR	Light Detection and Ranging	Airborne laser scanning for elevation.
ALS	Airborne Laser Scanning	LiDAR acquisition modality (airborne).
GNSS	Global Navigation Satellite System	Satellite positioning for surveys.
RTK	Real-Time Kinematic	Centimetric GNSS corrections for accuracy.
WGS1984	World Geodetic System 1984	Global geographic reference datum.
UTM	Universal Transverse Mercator	Projected metric coordinate system.
EPSG:32632	EPSG code 32632	UTM Zone 32N reference system.
DEM	Digital Elevation Model	Rasterized surface of elevations.
DSM	Digital Surface Model	Elevation including vegetation/objects.
DTM	Digital Terrain Model	Bare-earth elevation model.
DoD	DEM of Difference	Raster differencing for change detection.
LoD	Level of Detection	Threshold to filter noise in changes.
LoD1	Level of Detection (1σ)	Minimal detectable change (~68% conf.).
LoD95	Level of Detection (95%)	Significant change at 95% confidence.
RMSE	Root Mean Square Error	Overall magnitude of interpolation error.
σ	Standard deviation	Spread of residual errors around mean.
μ	Mean (bias)	Systematic offset of residual errors.
IDW	Inverse Distance Weighting	Distance-weighted raster interpolation.
Kriging	Ordinary Kriging	Geostatistical interpolation using variograms.

C2M	Cloud-to-Mesh	Validation distances point→ mesh in CloudCompare.
CSF	Cloth Simulation Filter	Ground/non-ground separation in point clouds.
SfM (SFM)	Structure-from-Motion	Photogrammetric 3D reconstruction approach.
VARI	Visible Atmospherically Resistant Index	RGB-based vegetation index (no NIR).
NDVI	Normalized Difference Vegetation Index	Classic NIR-based vegetation index.
NDWI	Normalized Difference Water Index	Spectral index highlighting water.
RGB	Red-Green-Blue	Visible bands used for VARI/classification.
NIR	Near-Infrared	Spectral band absent in dataset.
SVM	Support Vector Machine	Supervised classifier for vegetation map.
GIS	Geographic Information System	Environment for spatial analyses.
DSAS	Digital Shoreline Analysis System	Tool for shoreline trend analyses.
M3C2	Multiscale Model to Model Cloud Comparison	Precise 3D change measurement algorithm.
AOI	Area of Interest	Clipped common extent for analysis.
LAS	LAS point cloud format	Standard LiDAR point cloud file.
CSV	Comma-Separated Values	Bathymetry/GNSS points file format.
GeoTIFF	Georeferenced TIFF	Raster export format for DEMs/indices.
ArcGIS Pro	ArcGIS Pro (Esri)	Main environment for raster processing.
CloudCompare	CloudCompare	Point-cloud processing and validation.
Raster Calculator	ArcGIS Pro Raster Calculator	Used for height/geoid corrections.
RSiQ	Root Sum in Quadrature	Error propagation method for LoD.
AI	Artificial Intelligence	ML-based pattern recognition in studies.
OBIA	Object based Image Analysis	Object-level classifier used in literature.
GCP	Ground Control Point	Survey control used for UAV/SfM.

GSD	Ground Sampling Distance	Image resolution (e.g., 10 cm).
DUVES	Dune Vegetation State Index	Visible-band index cited in review.
ICP	Iterative Closest Point algorithm	Algorithm for aligning 3D data
IMU	Inertial Measurement Unit	Georeferences mobile mapping system sensors

1 Introduction

1.1 Background & Motivation

Coastal sand dunes are highly dynamic features formed where land meets the sea, occupying nearly one-third of the Earth's ice-free shorelines (Luijendijk et al., 2018). They deliver critical ecosystem services, including coastal protection by buffering wave impacts and stabilizing shorelines, and supporting biodiversity by creating unique habitats for specialized plant and animal communities (Duffy et al., 2018). Vegetation plays a central role in dune formation and evolution: pioneer dune plants trap and bind windblown sand, promoting vertical growth of foredunes and accretion of dune volume. In turn, higher dunes with dense vegetation are more resistant to storm erosion, serving as natural barriers that protect inland areas from flooding and erosion (Jackson et al. 2019). Coastal dunes attract tourism and recreational activities, thereby offering both cultural and economic benefits to coastal communities. However, dunes are inherently sensitive to change. Alterations in climate patterns (e.g. rising sea levels, changing storm regimes) and anthropogenic pressures (development, trampling, off-road vehicles) can rapidly destabilize dune systems. Recent global analyses reveal a complex picture: for example, many dune fields worldwide have experienced a 'greening' (increase in vegetation) since the 1980s, which can enhance dune stability, even as coasts face higher flood risk (Jackson et al. 2019). Understanding these processes requires integrated study of both the ecological (vegetation, habitats) and geomorphological (sand transport, dune morphology) aspects of dunes. As one review notes, "coastal dunes contain rich information on climate change, sea level change, and environmental change," making them valuable indicators for coastal vulnerability and global change studies.

Despite their importance, coastal dunes worldwide are under threat and require careful monitoring. Increased storminess and extreme weather can erode dunes quickly, while human activities (urban development, tourism) can degrade vegetation cover and disrupt natural sand dynamics. There is thus a pressing need to monitor dunes at high resolution over time in order to detect subtle changes in morphology and vegetation, and to inform management decisions. Advances in geomatics (e.g. Uncrewed Aerial Vehicles (UAV's) and satellite remote sensing) now allow detailed, repeat surveys of dunes. Such methods can capture fine scale morphological changes that were previously undetectable. Ecologists now emphasize linking these physical measurements with vegetation data, since interactions between sand and plants ultimately determine dune stability. Modern approaches integrate aerial imagery, structure from motion (SFM) photogrammetry, and field surveys of plant communities to build comprehensive three-dimensional models (sometimes called digital twins) of coastal systems (Duffy et al., 2018). These digital models can reveal how dunes evolve through seasonal storm cycles and climatic trends, and how vegetation zonation responds to changing substrates.

Coastal sand dunes are dynamic geomorphic systems at the land-sea interface, acting as natural buffers that absorb storm wave energy and protect inland areas (Jackson et al., 2019). Vegetation on dunes binds windblown sediment, increasing dune height and volume and enhancing storm-resistance (Jackson et al., 2019). Dunes also supply sand to beaches during storms and provide critical habitat, supporting biodiversity and offering recreational space

(Duffy et al., 2018). However, dunes are highly sensitive to climatic factors (wind, waves, sea-level rise) and human impacts (development, vehicles), which can fragment and erode them (Flores-de-Santiago et al., 2023). Recent studies emphasize that dunes record long-term changes in coastal dynamics and climate, making their monitoring vital for understanding environmental evolution (Ma et al., 2024). For example, (Jackson et al. 2019) found a "global greening" trend in dune vegetation (1984-2017), suggesting increased dune stabilization under changing climate. Yet, anthropogenic pressures and rising sea levels (projected +0.65 m by 2100) threaten dune integrity (Flores-de-Santiago et al., 2023). In summary, dune morphology and vegetation are closely linked to coastal resilience, but they remain highly vulnerable. Monitoring these systems therefore requires high-resolution, frequent surveys to capture subtle morphological shifts (often only centimeters per year) as well as vegetation changes (Flores-de-Santiago et al., 2023, Duffy et al., 2018).

Remote sensing and geomatic tools have become essential in such studies, overcoming the limits of sparse field surveys. Satellite imagery (Landsat, Sentinel) provides broad coastal coverage, while high-resolution platforms (UAVs, LiDAR, SfM photogrammetry) capture detailed dune topography and vegetation at sub-meter scales (Flores-de-Santiago et al., 2023). These techniques enable the creation of accurate digital surface/terrain models (DSMs/DTMs) of dunes, revealing 3D morphology and detecting change (Laporte-Fauret et al., 2019). Vegetation indices (e.g. NDVI, NDWI) derived from multispectral data help map dune vegetation and infer dune stability (Christofi et al., 2025, Talavera et al., 2022). For instance, NDVI can reveal vegetated foredunes and being indicator of erosion-prone areas (Christofi et al., 2025). Advanced approaches now integrate AI (Artificial Intelligence) with GIS (Geographic Information System). For example, machine learning algorithms can classify land cover and vegetation from UAV imagery (Belcore et al., 2024), and AI-based pattern recognition can exploit multi-spectral and multi-temporal datasets (Flores-de-Santiago et al., 2023). Overall, the literature shows a trend toward multimodal sensing, combining optical (RGB, multispectral), LiDAR, radar, and GNSS data, to achieve comprehensive coastal mapping (Flores-de-Santiago et al., 2023, Ma et al., 2024). These modern geomatics methods allow rapid, cost-effective surveying of wide dune regions at fine spatial (down to 0.05-0.2 m vertically) and temporal resolutions (Flores-de-Santiago et al., 2023, Ma et al., 2024). They have transformed coastal research, providing "detailed and accurate information that would otherwise be difficult to acquire" (Flores-de-Santiago et al., 2023).

UAV and LiDAR technologies in particular have greatly advanced dune analysis. Low-cost drones equipped with high-resolution cameras now routinely capture dune morphology over kilometers in a single flight (Laporte-Fauret et al., 2019). For example, (Laporte-Fauret et al. 2019) used a Phantom 2 and Phantom 4 UAV to photogrammetrically map a 4 km dune-beach section in France, generating a 0.1 m resolution DSM with 0.05 m vertical accuracy. Their approach (permanent GCPs and repeatable flight plans) allowed multi-temporal surveys (post-storm) to quantify dune erosion and aeolian buildup over months. Similarly, (Duffy et al. 2018) demonstrated that even kite-based photogrammetry (using Structure from Motion, SfM) can detect sub-decimeter changes in dune shape. LiDAR (airborne or UAV-mounted) adds the ability to penetrate vegetation and obtain ground elevation beneath plants. In one recent study, UAV-LiDAR plus genetic-algorithm regression predicted dune ground

elevation (beneath grass cover) with mean error <10 cm (Pinton et al., 2023). However, LiDAR is costlier, so many studies complement it with UAV photogrammetry and GNSS. For instance, (Ma et al. 2024) combined LiDAR, GNSS-surveyed profiles, and satellite data to characterize dune change from point, profile, and surface viewpoints. Across the literature, UAV digital photogrammetry stands out for flexibility and fine detail (0.02-0.10) m resolution (Flores-de-Santiago et al., 2023, Laporte-Fauret et al., 2019), while LiDAR offers dense terrain points and vegetation penetration (Pinton et al., 2023).

Another important facet of monitoring is the change detection: mapping how dune topography evolves over time. Change detection methods typically involve differencing time-series DEMs to identify erosion and deposition (Flores-de-Santiago et al., 2023, Duffy et al. 2018). For example, (Flores-de-Santiago et al. 2023) created very high-resolution DEMs (spatial resolution < 5 cm) using UAV SfM and airborne LiDAR at three time points (Apr, Jun, Oct 2021) and computed a DEM-of-difference (DoD) to quantify beach-dune sediment shifts. Such DoD grids, especially when combined with DSMs from different sensors, reveal spatial patterns of erosion (negative changes) and accretion (positive changes) across the dune-beach system. (Flores-de-Santiago et al.) note that geomorphic DoDs often outperform point-profile surveys in capturing distributed changes. Likewise, (Duffy et al. 2018) applied a Monte Carlo SfM change analysis (M3C2 algorithm) to show that changes as small as ~20 mm could be reliably detected. Researchers combine several datasets and different techniques together to better understand how the coast and dunes are changing instead of just reply on one method. Tools like DSAS (Digital Shoreline Analysis System) used in the Altamura Island study extracted shorelines from multi-year satellite images and analyzed long term shoreline migration along transects (Flores-de-Santiago et al. 2023). A key advantage of DEM-based techniques is their ability to measure both surface morphology and sediment volume changes, unlike basic profile measurements. Thus, modern change-detection relies on repeat high-res DEMs (via UAV/LiDAR) plus rigorous co-registration and subtraction techniques (Duffy et al. 2018, Flores-de-Santiago et al., 2023).

Previous studies in the San Rossore/Migliarino area (Tuscany) are relatively few but informative. Bertoni et al. (2014) described an innovative integrated survey at Migliarino-San Rossore Park: combining geomorphology, sedimentology, vegetation surveys, UAV flights, and even a wireless sensor network for dune monitoring. Their goal was a cost-effective, multidisciplinary system to measure dune volume, wind, moisture, etc. a valuable pilot but mostly methodological. More recently, Belcore et al. (2024) focused on vegetation mapping in San Rossore: they developed a hierarchical object based machine learning model applied to UAV multispectral imagery. This model classified 12 plant species and two substrate types, achieving ~76% overall accuracy. Their work demonstrated that high-resolution UAV data (10 cm GSD) and texture analysis are powerful for distinguishing dune plants. However, (Belcore et al.) also noted limitations and the need for further refinement. To date, ecological and geomorphic aspects have often been studied separately in this region: e.g. species level vegetation mapping or habitat mapping (some works used Worldview 3 imagery with fuzzy classifications), and hydrodynamic studies of foreshore dunes (e.g. using hyperspectral sensing). Few studies have combined high-resolution morphological surveys with vegetation surveys in Tuscany. Notably absent are recent analyses of dune beach sediment budgets or

multi-year volumetric changes specific to San Rossore. One gap is also the lack of published work on nearshore bathymetry or GNSS-tracked profiles in this park; coastal monitoring here has largely emphasized terrestrial dunes and vegetation. Thus, previous Tuscan studies provide important methods (wireless sensors, UAVs, OBIA classifiers) but leave open a need for integrated, multi-sensor dune dynamics assessment.

Overall, the literature highlights remote sensing's value for dune morphology and vegetation but also notes some important gaps. In the Tuscany context, comprehensive studies integrating UAV photogrammetry, LiDAR scanning, GNSS topographic surveys, and shoreline analysis are scarce. For example, while (Belcore et al.) mapped vegetation and others proposed sensor networks, no study to date has fully merged high-resolution terrain change analysis with species-level mapping in San Rossore. Also, few works examine dune shoreline coupling or sediment transport between beach and dune in this area. On methods, many studies use photogrammetry or LiDAR separately; there is room for multi-platform fusions (e.g. combining UAV-SfM DEMs with satellite sentinel time series). Moreover, change detection methodologies (e.g. DoD, DSAS) have been applied in Mexico (Flores-de-Santiago et al., 2023), and China (Ma et al., 2024) but not yet locally. Likewise, vegetation-dynamics indices (like the DUVES index (Talavera et al., 2022)) have been formulated but not tested in Tuscany. Due to increasing climate pressures, a renewed evaluation of dune resilience in San Rossore has become essential.

As (Innangi et al. 2025) note, combining UAV remote sensing with ecological data provides "a valuable tool for ecosystem monitoring, supporting conservation management" under rising environmental pressures. Similarly, (Talavera et al. 2022) emphasize that quantitative indices of dune vegetation state can greatly aid future coastal management aimed at conserving dune habitats. For example, (Ma et al. 2024) stress that analyzing dune dynamics systematically offers "necessary technical support and a scientific basis for the protection of tourism resources and ecological environments in nature reserves, as well as the prevention and control of coastal hazards". In the San Rossore context, this means identifying areas where dunes are eroding or where vegetation is stressed, so that timely interventions (e.g. beach nourishment, planting) can be planned. Moreover, the integration of spatial and ecological datasets into multi-temporal 3D terrain models for this park provides a scalable foundation for a future coastal digital twin that could be expanded and updated with new data over time.

Monitoring of coastal dune evolution using multi-temporal DEMs is inherently affected by measurement uncertainties. Failure to address these uncertainties can lead to misinterpretation of apparent elevation changes. It is well established in geomorphological change detection that accounting for DEM uncertainty is crucial to avoid overestimation of erosion or deposition (Alfonso-Torreño et al., 2021). A common approach is to define a minimum detectable change threshold so that any elevation difference smaller than this threshold is considered insignificant (i.e. assumed to be noise) (Alfonso-Torreño et al., 2021).

This research aims to fill these gaps by applying a fully integrated remote-sensing approach, combining multi-year UAV-LiDAR and GNSS datasets with DEM differencing and LiDAR-based vegetation analysis, to quantify dune morphological change and vegetation dynamics in San Rossore Park. Overall, the study will provide a scientific baseline and methodological

framework that can benefit dune conservation efforts not only in Tuscany but in comparable coastal regions.

1.2 Research Gap and Objectives

No study has thoroughly brought together high-resolution geomatic survey methods with a detailed ecological assessment of vegetation on the San Rossore dune system. In particular, there is still a lack of information on how recent environmental changes have influenced dune landforms and the distribution of habitats across the area. This raises the research question: how can we quantitatively map and analyze the combined geomorphic and ecological characteristics of the San Rossore dune system using modern survey technology, to support its conservation? In other words, there is a need for an integrated ecomorphological analysis that produces a "digital twin" of the dune landscape, capturing both its shape and vegetation dynamics. Addressing this problem will help fill local knowledge gaps and may serve as a model for similar coastal systems.

In response to these challenges, the study will pursue the following objectives:

- Acquire high resolution spatial data of the San Rossore coastal dune (e.g. UAV photogrammetry, LiDAR, or satellite imagery) to map its topography and surface morphology.
- Vegetation distribution along the dune profile (from beach to inland), and analyze how plant cover relates to dune shape and stability.
- Compare different year survey to recent morphological or vegetation changes along the dune, measuring uncertainties.
- Integrate multi-temporal topographic and vegetation data into high-resolution 2.5D and 3D raster and mesh models, enabling spatial analysis and visual interpretation of dune morphology and vegetation dynamics across the study areas.
- Evaluate the implications of the ecomorphological findings for coastal management, such as identifying vulnerable zones or informing restoration strategies.

The thesis is divided into six chapters. Chapter 2 describes the study area, the data sources used ,and any preprocessing steps. Chapter 3 explains the methodological approach, covering both the geomatic survey techniques and the procedures for vegetation sampling and change analysis. Chapter 4 presents the results of the study includes high resolution maps of dune morphology and vegetation cover, statistical evaluations of their interrelations and changes over time. Chapter 5 discusses the findings in the context of dune management, outlines the implications for conservation, and suggests directions for further research. Finally, Chapter 6 presents the conclusions, highlighting the main contributions, management-oriented recommendations for San Rossore, acknowledged limitations, and clear directions for future research.

2 Materials and Datasets

2.1 Study Area

The San Rossore coastal dune system in Tuscany, Italy, exemplifies the challenges and opportunities of dune monitoring. The focus is the coastal dune area at San Rossore, in the Municipality of Pisa (Tuscany, Italy). Geographically, it lies on the Ligurian Sea margin of the Tyrrhenian Basin (about 43°46′N, 10°17′E). The Migliarino-San Rossore-Massaciuccoli Park is a protected regional park extending from the mouth of the River Arno northwards for about 20 km of shoreline.

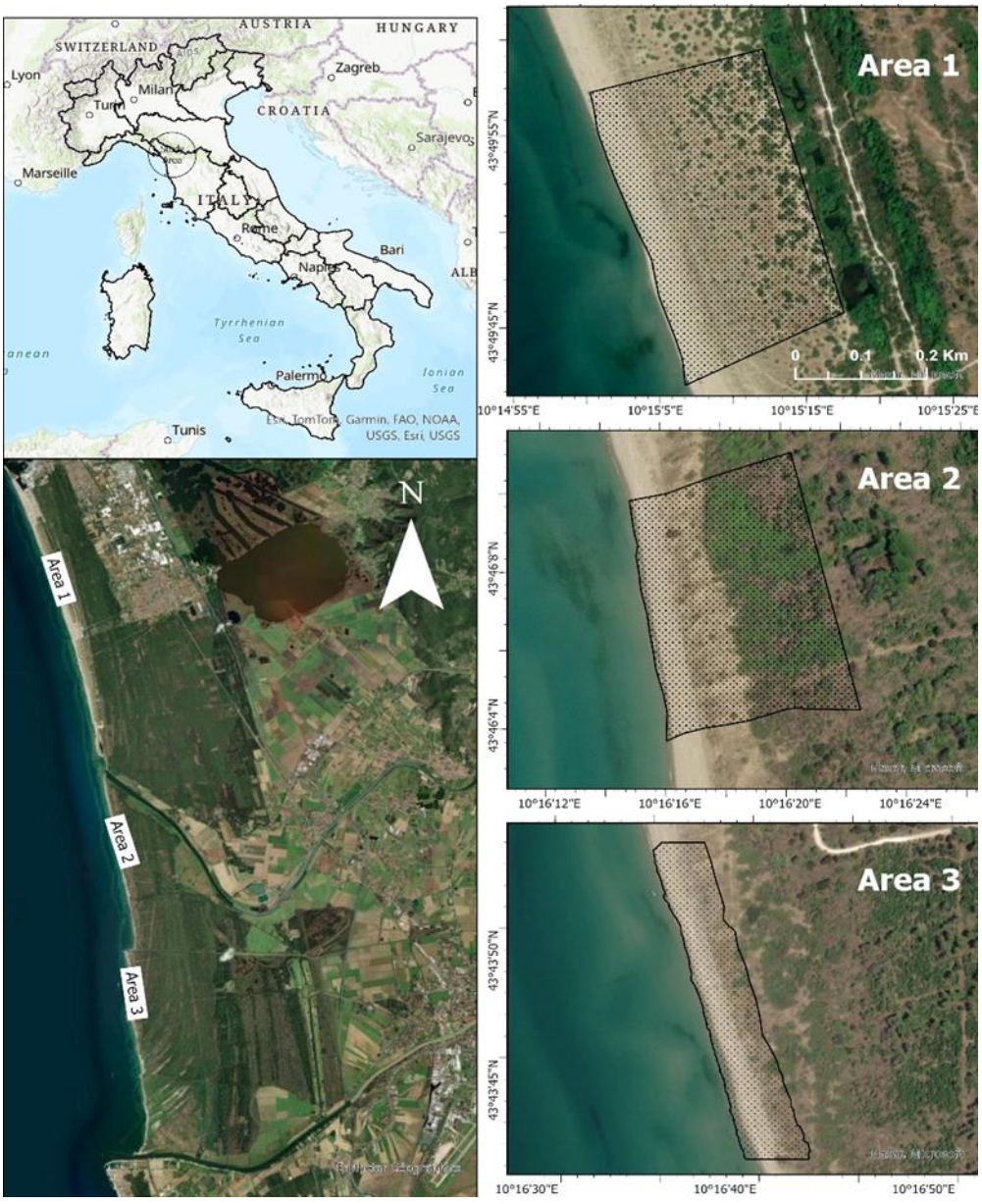


Figure 1 Study Areas with their map coordinates

The dune ridge runs parallel to the beach, separated occasionally by lagoons or wetlands. The maximum dune height reaches a few tens of meters above sea level at stabilized foredunes, tapering to lower, mobile foredune fronts at the shoreline. The area climate is typical Mediterranean, with strong winter storms that can reshape the beach dune interface.

Historically, some dune areas here have been altered by land use and sea level trends. Vegetation on these dunes exhibits classic zonation: pioneer species (e.g. Ammophila arenaria) dominate the first dune ridges, while inland dunes host shrubs (Rosmarinus, Cistus) and maritime pine (Pinus pinea) in fixed parabolic dunes further from the sea. The Park is ecologically rich, supporting several protected plant communities and wildlife, yet it is also visited for tourism and recreation. As such, the coastal dunes at San Rossore constitute an important natural barrier for the Tuscan coast, warranting detailed scientific study. The significance of this study lies in its contributions to scientific understanding and coastal management. By creating a detailed ecomorphological dataset of the San Rossore dunes, the study will enhance understanding of how Mediterranean dune systems function and respond to change.

The study consists of three coastal sub-areas located along the San Rossore shoreline (Figure 1). Area 1 occupies the northernmost sector of this shoreline near Torre del Lago. It includes a relatively wide dune field that is densely vegetated and backed by continuous coastal pine forest. Area 2 lies roughly at the center of the study coastline, adjacent to where the Serchio River meets the Tyrrhenian Sea. It covers a wider dune sector with a more heterogeneous surface pattern, including alternating patches of bare sand and vegetation within the dune interior. Finally, Area 3 defines the southern extremity of the study area near to Spiaggia Gombo, situated between Serchio and Arno River. The landward side of area 3 transitions into more open terrain, with sandy surfaces and scattered shrub. These areas are situated adjacent to the Migliarino-San Rossore-Massaciuccoli Regional Park, a protected coastal corridor known for its ecologically significant dune systems and dynamic shoreline processes.

2.2 Overview of Acquired Data

The datasets used in this study consist of preprocessed high-resolution topographic Aerial Laser scanning surveys and in-situ bathymetric surveys, collected over the 2021-2024 period for each coastal study area. The data acquisition was carried out by another group, while this work focuses on data processing and analysis. For each site, two primary data types were available:

The primary source of topographic information for this study is a set of airborne LiDAR (Light Detection and Ranging) datasets collected between 2021 and 2024 over three selected test areas.

Each of the three study areas, originally defined as rectangular zones of approximately 500 × 400 meters, was surveyed annually over four consecutive years using airborne laser scanning (ALS) technology. The surveys were conducted with a drone-mounted LiDAR system equipped with a dual-frequency GNSS receiver and Real Time Kinematic (RTK) correction, achieving high georeferencing precision approximately 2 to 3 cm horizontally and 3 to 4 cm in the vertical component. This level of geodetic accuracy ensures spatial consistency among the multi-year UAV-LiDAR and GNSS datasets used in this research.

The LiDAR data for each acquisition were delivered in standard LAS format, which stores 3D points location (X, Y, Z coordinates WGS84/32N), intensity (0-1) and return number (1-3). A total of 11 LAS files were collected (one per area per year), each containing millions of individual points, allows for a robust temporal analysis of dune evolution. This design is particularly suited for capturing both seasonal variability and longer-term morphological

changes in the study zone, which spans a total of 1.6 km of coastline, roughly 5.3% of the park's total coastal length. Such repeat LiDAR coverage facilitates the construction of a time series of Digital Elevation Models (DEMs), critical for detecting erosion, accretion, and other dynamic surface changes. However, for the purpose of consistent temporal analysis and to eliminate discrepancies due to variable flight footprints, only the common overlapping portion of each area, present in all four years, was selected for analysis. This subset was defined by clipping the full dataset to the intersection of annual coverage, thereby ensuring a stable spatial baseline for change detection. Consequently, the point densities and total number of returns reported in the analysis refer to these clipped common areas, not the entire 500 × 400 m zone. A detailed breakdown of the LAS datasets is presented in Table 1, which lists the number of points, file type, and computed average point density (pts/m²) for each Area-Year combination.

Area	Year	file format	# Of Points (pts)	Area (AOI) (m^2)	Point Density (pts/m^2)
A1	2021	.LAS	69,269,143	124,525	556
	2022	.LAS	95,506,214		767
	2023	.LAS	110,314,442		886
	2024	-	-		-
A2	2021	.LAS	16,429,462	15221	1079
	2022	.LAS	6,357,286		418
	2023	.LAS	8,188,586		538
	2024	.LAS	13,197,348		867
A3	2021	.LAS	13,394,460	16923	791
	2022	.LAS	11,544,939		682
	2023	.LAS	15,223,546		900
	2024	.LAS	30,909,729		1826

Table 1 Summary of Point Density of LiDAR Datasets in Clipped AOIs (2021-2024)

As shown, point density varied notably between acquisitions and among areas, ranging from a minimum of 418 pts/m² (A2, 2022) to a maximum of 1826 pts/m² (A3, 2024). This variation directly influenced the resolution and accuracy of the DEMs. A more in-depth evaluation of these limitations is provided in the Discussion chapter.

One known limitation of airborne traditional LiDAR in coastal zones is its inability to penetrate water surfaces by the NIR beam laser pulse, making it ineffective for capturing subaqueous features such as the nearshore bathymetry. To overcome this gap, additional bathymetric data were acquired during field campaigns using a dual-frequency GNSS receiver operating in Real Time Kinematic (RTK) mode, which enabled highly accurate georeferencing of underwater elevation points. The RTK system delivered positional accuracies of approximately 2-3 cm in the horizontal and 3-4 cm in the vertical (up) component, ensuring consistency with the coordinate system and precision level of the LiDAR data.

Area	Year	Extension	# Of Points (pts)
A1	2021	.CSV	86
	2022	.CSV	200
	2023	.CSV	115
	2024	-	-
A2	2021	.CSV	84
	2022	.CSV	134
	2023	.CSV	66
	2024		-
A3	2021	.CSV	164
	2022	.CSV	162
	2023	.CSV	109
	2024	.CSV	269

Table 2 Summary of Bathymetry Datasets: Number of Points (2021-2024)

These GNSS-derived bathymetric points were used to complement the terrestrial point cloud by extending elevation coverage below the waterline, particularly in areas where dune-beach interaction with the nearshore zone is morphologically significant. Overall, the integration of airborne LiDAR and RTK-based bathymetric data provided a detailed, high-resolution topographic foundation for the analysis of coastal dune dynamics across the full 2021-2024 monitoring period. To overcome this limitation, LiDAR and bathymetry were merged in CloudCompare (Figure 2), bathymetry points were interpolated to a 0.25 m grid (Rasterize tool), producing a unified elevation surface compatible with the terrestrial DEM for change detection and visualization in ArcGIS Pro.



Figure 2 Morphology of the Area 1 in 2023 overlapped with the bathymetry points

2.3 Coordinate Systems

Accurate geospatial referencing is a critical foundation for any geomatic analysis, particularly in studies involving multi temporal elevation data and the integration of datasets from different sources and sensors. In the present study, all spatial datasets were processed using a consistent geodetic framework to ensure positional alignment and comparability over time. All UAV-LiDAR point clouds and derived raster products were processed in a consistent projected coordinate reference system (WGS 84 / UTM Zone 32N, EPSG:32632). This ensured accurate positional alignment among multi-year datasets and allowed reliable spatial comparison of elevation changes. The use of a single projected system in metric units was essential for DEM differencing and area-based change analysis.

The vertical reference systems posed more complexity due to inconsistencies across datasets. Specifically, while the majority of LiDAR datasets from 2021 and 2022 were already referenced to orthometric heights, the 2023 dataset was referenced to ellipsoidal heights so direct comparison between years would have introduced vertical bias. To address this issue, the ellipsoidal height LiDAR data were converted to approximate orthometric heights within ArcGIS Pro using the Raster Calculator. This was done by subtracting an average geoid undulation value computed over the areas starting from the Italian Military Institute (IGM) grid for the study area, effectively aligning the vertical reference across all years.

$$Elevation\ Correction = Raster.tif_{ellipsoidal} - Average\ Undulation \text{ (IGM)}$$

2.4 Software Used

A combination of open-source and commercial software tools was used to manage, process, and analyze the datasets. CloudCompare 2.14.alpha was employed for point cloud inspection, filtering, classification, and preliminary rasterization, as well as for accuracy assessment through cloud to mesh comparisons. ArcGIS Pro 3.5.0 served as the main environment for geospatial processing, including raster clipping, change detection, classification, and cartographical output. Microsoft Excel complemented these tools by providing a platform for data cleaning, error calculations, and basic statistical summaries. This integrated software environment ensured both the precision of point cloud analysis and the reproducibility of GIS based spatial modelling, while also supporting effective visualization and interpretation of results.

2.5 Measures uncertainties

All geomatic measurements inherently include a degree of uncertainty, arising from both the characteristics of the sensors and the conditions under which surveys and data processing are performed. In our study, uncertainty primarily derives from four components: UAV-mounted LiDAR acquisition, GNSS positioning, point-cloud classification, and surface interpolation. Data acquisition was carried out using a drone-mounted LiDAR system coupled with a dual-frequency GNSS receiver operating in Real-Time Kinematic (RTK) mode. Under these conditions, the expected georeferencing accuracy is on the order of 2-3 cm horizontally and 3-4 cm vertically. Nevertheless, minor residual errors remain unavoidable and may be introduced by factors such as satellite geometry, platform stability during flight, and local environmental conditions.

Further uncertainty is introduced during ground and non-ground separation using the Cloth Simulation Filter. This step is particularly sensitive in sectors characterized by complex dune topography or discontinuous vegetation, where low or sparse plants may be partially misclassified. Such effects can locally influence the reconstructed ground surface and, consequently, the derived elevations. Additional uncertainty arises during the interpolation of merged LiDAR and bathymetric point clouds into gridded Digital Elevation Models. In this phase, interpolation performance depends strongly on point density, spatial distribution, and small-scale terrain variability. To explicitly quantify these effects, independent validation was performed using withheld bathymetric points, from which Root Mean Square Error (RMSE) values were calculated for each DEM.

When Digital Elevation Models from different survey years are compared, the uncertainties associated with each surface are propagated into the resulting DEM of Difference. As a consequence, some apparent elevation changes may reflect cumulative measurement error rather than genuine geomorphological variation. For this reason, statistical significance was enforced through the computation of Level of Detection thresholds based on the root-sum-in-quadrature of the RMSE values of each DEM pair. Only elevation differences exceeding the corresponding LoD thresholds were retained. It ensures that mapped erosion and accretion patterns represent detectable terrain change rather than measurement noise.

3 Methodology

3.1 Workflow Overview

We followed a systematic workflow in our analysis. Each annual LiDAR point cloud was first preprocessed by applying the Cloth Simulation Filter (CSF), which separated ground from non-ground returns. Next, we combined the ground points with RTK-derived bathymetric data (collected via dual-frequency GNSS) to create seamless topographic-bathymetric surfaces for each area and year. These combined datasets were interpolated into high-resolution Digital Elevation Models (DEMs) using both Inverse Distance Weighting (IDW) and Kriging techniques. We assessed model accuracy by validating against 30% of the bathymetric points (withheld from interpolation) using Cloud-to-Mesh comparisons to compute the root mean square error (RMSE). The interpolation method with the lowest RMSE was retained for final DEM construction. We then clipped these DEMs to the predefined study area boundaries to remove edge artifacts and standardize the spatial extent across years. At the same time, we rasterized the non-ground points into RGB images and processed these in ArcGIS Pro to calculate the Visible Atmospherically Resistant Index (VARI). We applied supervised classification to distinguish vegetation and non-vegetation (dry shrubs, etc.) and used multi-temporal raster differencing to assess changes in vegetation cover. Together, the elevation and vegetation products enabled a comprehensive analysis of dune morphology and ecological change throughout the 2021-2024 period.

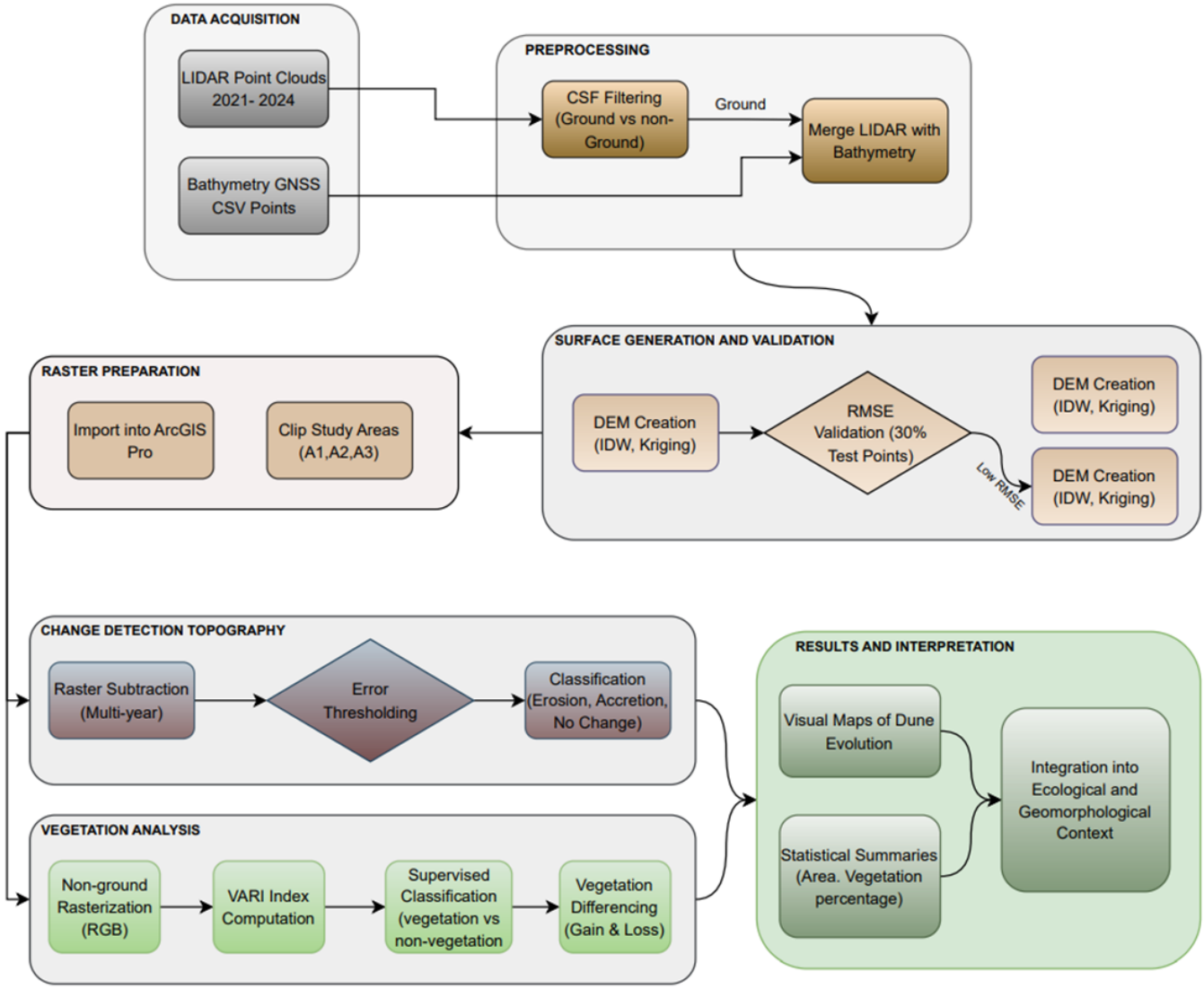


Figure 3 Workflow Diagram

3.2 Preprocessing in CloudCompare

We used CloudCompare (an open-source point-cloud processing tool) to preprocess the LiDAR and bathymetric data. We applied the same standardized procedure to each year's dataset to ensure consistency and reproducibility.

At first LiDAR point clouds, provided as LAS files, were imported into CloudCompare. Each file contained high density elevation points collected via airborne laser scanning technology. Subsequently, bathymetric point data were introduced in CSV format, representing discrete ground control points sampled directly along the shoreline. To objectively evaluate the accuracy of the interpolation methods applied later, the bathymetric data were partitioned into two subsets, 70% of the points were used for training and the remaining 30% for validation. The division was performed randomly in advance, allowing rigorous validation of the interpolation results.

After importing the data, we first preprocessed each year's raw LiDAR point clouds by applying the Cloth Simulation Filter (CSF) to separate ground points from non-ground points. The CSF approach conceptually simulates a flexible "cloth" dropping onto an inverted point cloud surface; points that the cloth contacts are classified as ground, while points remaining above the draped cloth are labeled as non-ground (Bailey et al., 2022). In practice, the point cloud representing the study area was inverted and a virtual cloth was allowed to settle over it under gravity. The areas where this cloth rests correspond to the terrain, and everything above the cloth represents features like vegetation (and any other structures).

The CSF algorithm is advantageous for complex terrains because it can accommodate undulating topography by adjusting the cloth's shape. Several parameters of the CSF were tuned to achieve optimal ground separation. Key parameters include the cloth resolution (which controls the grid size of the cloth mesh) and the cloth rigidity, among others (Bailey et al., 2022). A finer cloth resolution helps the cloth conform to small terrain features, while the rigidity parameter dictates how smoothly the cloth can bend over uneven terrain. The classification threshold defines the vertical distance that the algorithm uses to decide whether a point belongs to the ground surface or should be considered as off-ground. The number of iterations determines how often the cloth simulation runs, enabling the virtual cloth to gradually conform to the terrain surface. In our methodology, parameter values were chosen based on the terrain complexity of the study area, for instance in area 2, a 0.45m cloth resolution was used to capture fine terrain variations, and selecting the steep terrain scene type ensured the cloth could drape over steep areas without over smoothing important features.

Area	Scene	Classification threshold	Max iterations	Cloth resolution
A1	Relief	0.20	500	0.50
A2	Steep	0.20	500	0.45
A3	Steep	0.20	500	0.45

Table 3 Parameters for Terrain Surface

The non-ground points were exported directly as a raster to analyze vegetation change but the ground points were merged with the training subset of bathymetric data into a unified,

integrated point cloud. This merging was executed using CloudCompare built-in merging functionality, carefully ensuring spatial alignment and consistency in coordinate reference systems (WGS84 datum) across all input data. This integration is essential to accurately represent coastal topography, especially in dynamic zones where land and nearshore environments interact. Once the merged point cloud was prepared, rasterization was performed to produce a continuous Digital Elevation Model (DEM). CloudCompare rasterization tool was utilized, leveraging interpolation methods designed to translate discrete point data into gridded surfaces. Two interpolation techniques, Inverse Distance Weighting (IDW) and Ordinary Kriging, were applied. IDW interpolation estimates unknown elevation point values using a weighted average of surrounding points, assigning greater weight to closer observations. Conversely, Kriging provides a statistically rigorous approach, explicitly considering spatial correlation among points to generate elevation predictions.

Following raster generation, each resulting raster dataset was converted into a triangulated mesh within CloudCompare. Mesh generation is a critical step for accurate validation, as it transforms raster data into a continuous surface model that can be precisely compared against independent control points. This mesh provided the reference surface needed for subsequent quantitative accuracy assessment.

For validation, the reserved 30% of bathymetric points, which had not been used during rasterization, were then loaded into CloudCompare. These points, characterized by an average vertical precision of approximately ±3 cm and a horizontal precision of about ±2 cm, provided a reliable basis for accuracy assessment. The accuracy assessment was conducted using CloudCompare Cloud to Mesh (C2M) distance tool, which computes precise vertical distances between each validation point and the mesh surface. The C2M tool provides a statistical summary including the mean error, standard deviation, and the Root Mean Square Error (RMSE), eq. 1.

$$RMSE = \sqrt{\sigma^2 + \mu^2} \qquad (1)$$

σ = standard deviation of the residuals (spread of errors around the mean)

μ = mean of the residuals (systematic bias)

RMSE, a robust measure widely employed in geomatics and remote sensing analyses, quantifies the overall magnitude of interpolation error and is essential for objectively comparing the performance of the interpolation methods.

3.3 Elevation Change Detection

The interpolated Digital Elevation Models (DEMs) and non-ground point layers were exported from CloudCompare in GeoTIFF format, with a uniform pixel size of 0.25 m, and projected in the UTM Zone 32N coordinate system (WGS84). This resolution was selected as a balance between computational efficiency and spatial detail, considering the high LiDAR point density. The chosen 0.25 m pixel size was deemed appropriate for preserving geomorphologically relevant features while ensuring consistency across all years. Once imported into ArcGIS Pro, the rasters were reprojected (if needed) to the local coordinate

system and aligned to a consistent vertical reference system (orthometric height), ensuring spatial coherence of all elevation layers prior to differencing operations.

3.3.1 Raster Clipping to Study Area Extents

In ArcGIS Pro we used the Clip Raster tool (Data Management toolbox) to constrain each DEM to the exact study area polygon. The clipping geometries were polygons defining Areas A1, A2, and A3 (provided as centroid coordinates and mapped extents). Clipping ensures that all rasters share a common footprint and that any unreliable edge points (e.g. where LiDAR coverage tapered off) are removed e.g. 2023_A2. We chose the "Inside" clipping type so that only pixels inside each polygon were retained. This step produced final rasters that precisely match the study area boundaries. Using the same clip mask and extent for all years in a given area guarantees that subsequent change analyses compare like with like.

3.3.2 Multi Temporal DEM Differencing

The first step in analyzing dune morpho-dynamics was to perform multi temporal elevation change detection by subtracting digital elevation models (DEMs) from different survey dates. For each pair of DEMs (later survey minus an earlier survey), a change detection raster was generated to represent elevation differences over time. This raster subtraction, called DEM of Difference, (DoD), yields positive and negative values indicating areas of surface change, a positive value means elevation gain (surface accretion or deposition) while a negative value indicates elevation loss (surface erosion) between the two time periods (Chirico et al., 2020). By repeating this process for sequential DEM pairs, a series of elevation change maps was obtained, each highlighting how the coastal dune's topography evolved over the respective time span. These DEM differencing operations were conducted in a GIS environment, ensuring that each raster was co-registered and aligned to a common grid before subtraction to avoid spurious differences from misalignment.

3.3.3 Level of Detection (LoD)

Direct DEM differencing captures all elevation changes, including very small differences that may fall within the margin of measurement error. To distinguish meaningful topographic changes from random noise, we applied Level of Detection (LoD) thresholds based on the propagated vertical errors of the two input DEMs. In this study, we computed two thresholds for each DEM comparison, LoD1 and LoD95. LoD1 was defined as the root sum of squares of the vertical errors of the two DEMs (essentially a combined RMSE for the difference), while LoD95 was set as the 95% confidence interval of that error combination. In formula form, for two DEMs with vertical accuracies (root mean square error) $RMSE_1$ and $RMSE_2$, we have:

$$LoD1 = \sqrt{RMSE_1^2 + RMSE_2^2} \quad (2)$$

$$LoD95 = 1.96 * \sqrt{RMSE_1^2 + RMSE_2^2} \quad (3)$$

3.3.4 Thresholding Elevation Changes

Once the LoD1 and LoD95 values were established for a given DEM difference raster, we applied these thresholds to filter the raw elevation change data. The aim was to set all changes whose magnitude fell below the detection limit to zero (representing "no significant change"). This was accomplished in ArcGIS Pro using the Raster Calculator with a conditional expression.

Con (Abs ("DEM Difference") <= LoD1, 0, "DEM Difference")
Con (Abs ("DEM Difference") <= LoD95, 0, "DEM Difference")

This expression evaluates each cell's absolute change value. If the magnitude of change is less than or equal to LoD1, the cell value is replaced with 0 (effectively labeling it as no change); otherwise, the cell retains its original elevation difference value. We executed an analogous operation for LoD95 (using the LoD95 value in place of LoD1) to produce a more strictly thresholder raster. The result of this thresholding process is two sets of filtered DEM's of difference rasters, one in which all changes not exceeding LoD1 are nulled out, and another in which only changes above the larger LoD95 threshold remain. Through this step, we effectively isolated significant elevation changes by removing those differences that could be attributed to survey uncertainty. By performing the thresholding in an ArcGIS Pro, we preserved the geospatial integrity of the data, the output rasters remain aligned with the original DEMs and can be directly compared or analyzed further. In this study, we examined both thresholds as part of the methodology.

3.3.5 Histogram Analysis of Filtered Changes

After applying the LoD based thresholding, we evaluated the distribution of the remaining elevation changes by generating histograms of the filtered difference rasters. Histograms were produced for both the LoD1 filtered and LoD95 filtered change maps to assess how the threshold level affected the frequency distribution of elevation changes. These histograms plot the number of raster cells (vertical axis) against binned elevation change values (horizontal axis), allowing a visual assessment of the predominance of erosion vs. accretion and the amount of area mapped as no-change (zero difference). The LoD1 filtered histogram generally showed a broad distribution with many small positive and negative values (since LoD1 permits detection of smaller changes), whereas the LoD95 filtered histogram exhibited a pronounced spike at zero and relatively fewer cells in non-zero bins. This is because the stricter LoD95 threshold forces most minor changes to zero, resulting in a larger portion of the area being classified as unchanged. By comparing these distributions, we confirmed that thresholding was effectively removing the noise. In the LoD95 case, only the tails of the distribution (representing substantial elevation gains or losses) remain, and the center of the distribution collapses into the zero bin.

3.3.6 Reclassification into Erosion and Accretion Categories

With threshold change rasters (for either LoD1 or LoD95), the next step was to classify the spatial patterns of elevation change into meaningful categorical classes. To simplify

interpretation, we labeled the raster into three qualitative categories: erosion, no change, and accretion. Erosion corresponds to significant negative elevation change (surface lowering), no change corresponds to a zero value (within the LoD threshold), and accretion corresponds to substantial positive change (surface raise). This categorization aligns with standard geomorphic interpretations of DEM differences, where negative DoD values indicate erosion and positive values indicate deposition.

In ArcGIS Pro, we implemented this classification using the Reclassify tool. The thresholder raster was reclassified by defining value ranges that map to each category. Specifically, all cells with values < 0 were reclassified as "Erosion" class, cells with value = 0 as "No change", and cells with values > 0 were classified as "Accretion" class. In practice, this was achieved by setting the reclassification rules such that any negative value (down to the minimum in the raster) is assigned a new code representing erosion, zero remains zero (is assigned a distinct code for no-change), and any positive value (up to the maximum) is assigned a code for accretion. This produced an integer raster map of change classes. After reclassification, the study area's surface change is expressed in a categorical map: each raster cell is labeled as either an erosion cell, an accretion cell, or an unchanged cell. This greatly aids interpretation and visualization, as it condenses the complex numeric differences into a clear picture of where the dune has eroded, remained stable, or grown.

3.3.7 Area Calculation and Statistical Analysis

In addition to visual maps, quantifying the area of erosion and accretion is important for understanding the scale of changes and for comparing different time intervals. ArcGIS Pro's tool (Tabulate Area) was used to calculate the surface area of each change category derived from the reclassified rasters. This tool calculates the area occupied by each class within specified zones. In our case, the entire dune system (or the raster extent of the DEM difference) was treated as a single zone, so Tabulate Area effectively summed up the total number of cells in each class and multiplied by the cell area to report the area in square meters of erosion, no-change, and accretion. The output was a table of area statistics for each category per DEM comparison. For example, for a 2021-2023 interval on Area 1 with LoD95, we obtained values such as "erosion area = 141 m^2, no-change area = 124254 m^2, accretion area = 68 m^2," which express 0.17% change in Area in 3-year period. These statistics allow for a quantitative assessment of how much of the dune area experienced significant loss or gain in elevation over time. By repeating this analysis for each sequential period, we could compare the magnitude of erosional vs. depositional activity between intervals. Such comparisons are valuable in evaluating, for instance, whether a particular time period saw widespread erosion or if accretion dominated due to, say, a sedimentation event or effective dune management measures.

3.4 Vegetation Change Detection

Vegetation change detection involves a multi-step workflow to identify and quantify changes in vegetation cover and structure between two different time periods. The overall process includes filtering out ground points from 3D data, preparing raster layers (including spectral

bands and height models), computing a vegetation index, performing a supervised classification of vegetation types, comparing multi temporal results to map changes, and finally quantifying the change areas. The following sub sections describe each step-in detail, following standard practices in remote sensing and GIS for vegetation analysis.

3.4.1 CSF Filtering for Non-Ground Points

The first step focuses on isolating vegetation by removing ground points from the point cloud data. This was accomplished using the Cloth Simulation Filter (CSF) algorithm, which is a popular method for separating ground (terrain) and above ground features in LiDAR or photogrammetric point clouds. By using CSF, we effectively filtered out the ground points and retained only the non-ground points, which in this context predominantly correspond to vegetation canopy. (It is noted that if manmade structures were present in the area, they would also appear as non-ground points; however, the study area is predominantly natural vegetation, so non-ground points overwhelmingly represent vegetation. Any minor non-vegetation objects above ground, if present, were manually identified and assigned non-vegetation so as not to skew the vegetation analysis.)
By applying the CSF filtering, we obtained a cloud of points that correspond to vegetation only. This set of points forms the basis for generating vegetation specific raster products and for conducting change detection focused on vegetation cover.

3.4.2 Rasterization and RGB Band Separation

With ground points removed, the next step was to convert non-ground data into raster format and prepare the spectral bands for vegetation index computation. To create a consistent dataset for vegetation index, the point cloud was rasterized at a high resolution in CloudCompare. A grid cell size of 0.25 m was chosen for all years, meaning the point cloud was aggregated to create an orthomosaics with 25 cm by 25 cm pixels. This resolution preserves fine detail of vegetation structure while smoothing out point level noise.
The rasterization was performed by projecting the colored points onto a two-dimensional plane (the horizontal X-Y plane) and assigning each pixel an RGB value based on the points falling within that cell. If multiple points fell in the same cell, their color values were combined (e.g., averaged) to determine the pixel's RGB value. This process produced three visible bands Red, Green, and Blue (RGB) orthorectified image of the above-ground features. The image was then clipped to the exact extent of the study area to remove any extraneous data outside the region of interest, ensuring that subsequent analysis focused only on the area under investigation.
We separated these RGB bands into individual single-band raster layers. This band separation is a preparatory step to facilitate the calculation of vegetation indices that use specific spectral bands as input. Each band was retained at the same spatial resolution as the raster layer. By having the red, green, and blue reflectance values available in separate rasters, we ensured that spectral computations (such as the vegetation index described in the next section) could be performed accurately on a per pixel basis.

3.4.3 VARI Index Calculation

To enhance the distinction of vegetation in the imagery, we computed the Visible Atmospherically Resistant Index (VARI) from the orthomosaics, eq. 2. VARI is a vegetation index designed for use with standard color images (which lack a Near InfraRed, usually used for vegetation monitoring) to highlight green vegetation while mitigating effects of illumination differences and some atmospheric disturbances (Gitelson et al., 2002). It leverages the fact that healthy vegetation typically reflects more green light and less red/blue light compared to other surfaces. The formula for VARI is given by:

$$VARI = (Green - Red)/(Green + Red - Blue) \quad (2)$$

where Red, Green, and Blue represent the bands with digital number values (Gitelson et al., 2002). The index produces higher values for pixels dominated by green tones typically dense, healthy vegetation and negative values for non-vegetated surfaces such as bare soil, dry vegetation, or built areas. An important advantage of VARI is that by including the blue band in the denominator (as a subtraction), it corrects for some atmospheric effects and illumination differences, making it more "atmospherically resistant" than simpler ratios (Gitelson et al., 2002). Using the rasterized bands prepared earlier, the VARI was calculated for each pixel across the study area for each time period.

This VARI layer served multiple purposes in our analysis. It provided a straightforward way to mask out non-vegetated areas: by applying a threshold on VARI (e.g., VARI > 0 for potential vegetation presence), one can distinguish vegetated pixels from others. The use of VARI is ideal here because we only have visible bands available; despite the lack of an infrared band (which is traditionally used in indices like NDVI), VARI allowed us to effectively exploit the RGB data for vegetation mapping.

3.4.4 Supervised Classification of Vegetation and Non-Vegetation

While the VARI index highlights vegetation, a supervised classification was performed to objectively separate vegetation from other land cover types present in the above ground data. For this purpose, a Support Vector Machine (SVM) classifier was applied to the raster dataset. SVM is a supervised machine learning algorithm that is well established in remote sensing for land cover classification due to its robustness and accuracy with limited training data (Esri, 2026). It has the ability to handle high dimensional data and does not require the input features to be normally distributed (Esri, 2026). In addition, SVM is less sensitive to noise and can manage unbalanced training sets effectively (Esri, 2026), which makes it suitable for binary classification like vegetation vs. non-vegetation.

Using ArcGIS Pro's classification tools, training samples were created to represent the two classes: "Vegetation" and "Non-vegetation". Small polygonal training areas were carefully digitized on the RGB imagery (and guided by the VARI output) to capture representative examples of each class. Vegetation training samples (assigned value 1) included pixels covering tree canopies, grass, and shrubbery, whereas non-vegetation samples (assigned value 0) covered surfaces such as bare soil, and other non-green features. These training

samples were input into the ArcGIS Training Samples Manager to assign class labels and values.

Area	Class	No. of polygons	No. of pixels
A1	Vegetation	1	495
	Non-vegetation	1	915
A2	Vegetation	3	784
	Non-vegetation	1	90
A3	Vegetation	7	1,477
	Non-vegetation	3	172

Table 3a SVM training samples by area

The training samples were created manually on the RGB orthomosaics, guided by the VARI raster to ensure that each polygon contained either clearly vegetated or non-vegetated surfaces (Table 5). For each area (A1, A2 and A3), the SVM classifier was trained only on derived samples and then applied to the corresponding clipped VARI raster covering the dune-beach polygon of that area. The VARI value was used as the single input feature. All labelled pixels were used for training and the ArcGIS Pro implementation of SVM does not expose a user-controlled number of epochs, as the optimization iterates internally until convergence. A simple global VARI threshold was considered but a single cut-off value could not reliably separate vegetation from bright bare sand and shaded areas across all years and sub-areas. SVM adapt the decision boundary to the spectral distributions of the manually labelled samples.

After preparing the training samples, the SVM classifier (classify tool in image classification toolbox) was used for classification. VARI layer were used as input features for the classification. This tool analyzes the spectral signatures of the training samples and determine the optimal decision boundary. It separates vegetation from non-vegetation in the multi-dimensional feature space. In the resultant raster, each pixel is classified as either vegetation or non-vegetation based on the SVM's learned decision function. The outcome of this step was a binary vegetation map showing the spatial distribution of vegetated areas (class value = vegetation) and non-vegetated areas (class value = non-vegetation) across the study site.

3.4.5 Multi Temporal Differencing and Change Mapping

A post-classification comparison was performed using the vegetation maps produced for each survey year, to analyze how vegetation patterns evolved over time. Each annual raster was first classified independently using the SVM algorithm to determine vegetation presence. The classified outputs were then compared on a pixel-by-pixel basis to detect changes between consecutive years.

The classified vegetation rasters from each year (e.g., 2021, 2022, 2023, 2024) were reclassified into binary format, with a value of 1 assigned to vegetation and 0 to non-vegetation. This binary simplification was essential for isolating actual vegetation presence and facilitating logical differencing operations. Subsequently, raster subtraction was carried out using the

Raster Calculator tool in ArcGIS Pro. For example, to determine vegetation change between two years, the vegetation raster of the later year was subtracted from that of the earlier year, eq. 3:

$$Change = Vegetation_{later\ year} - Vegetation_{earlier\ year} \quad (3)$$

This operation yielded a new raster layer wherein each pixel was assigned a value representing the direction and magnitude of vegetation change:

- A pixel value of +1 indicated an area that was previously non-vegetated and had become vegetated in the subsequent year, signifying vegetation gain.
- A value of -1 represented an area that was vegetated in the earlier year but became non-vegetated later, indicating vegetation loss.
- A value of 0 denoted no change, either due to persistent vegetation or continuous absence.

To ensure full coverage and eliminate spatial gaps in the raster output, NoData values from the original classified rasters were handled by assigning a default value of 0 (non-vegetation) prior to the differencing step. This treatment enabled consistent comparison across the entire spatial domain of each study area and avoided misinterpretation of null pixels as change. The resulting raster layer, a categorical vegetation change map, visually communicated the patterns of gain and loss across the landscape. By symbolizing the output using a diverging color ramp (e.g., red for loss, green for gain, grey for stability), the spatial distribution and intensity of vegetation transitions became readily interpretable. This enabled identification of zones undergoing afforestation, deforestation, seasonal changes in canopy, or disturbance related dynamics, which we discussed in next chapter.

This post classification differencing technique was applied across all relevant temporal intervals (e.g., 2021-2022, 2022-2023, etc.) for each study area. The method's strength lies in its simplicity, repeatability, and capacity to produce discrete thematic outputs those are easily interpreted and integrated into further statistical and spatial analyses. Since classification errors are isolated to each individual epoch, the resulting change maps are less susceptible to compounded inaccuracies. Eventually, this approach facilitated a detailed understanding of vegetation dynamics within the coastal dune system. It offers insights into ecological resilience, succession processes, and anthropogenic or climatic drivers influencing vegetative cover across the monitored years.

3.4.6 Quantification of Vegetation Change

The final step of the vegetation change detection workflow was to quantify the amount of change in vegetation cover. We calculated the, classified change map, area corresponding to each change category (gain, loss, no change) using a zonal analysis approach. Specifically, the Tabulate Area tool in ArcGIS was utilized to compute the cross tabulated area of each class within the study zone (Esri, 2025). Tabulate Area is a GIS function that calculates the area of overlap between two datasets, in this case, the "zone" dataset can be defined as the entire study area, and the "class" dataset is the raster of vegetation change categories. The tool outputs a table indicating the total area occupied by each class within each zone (Esri, 2025).

For our purposes, we treated the whole study area as a single zone and the change map as the categorical input. The Tabulate Area results provided the total surface area corresponding to pixels classified vegetation gain, vegetation loss, and unchanged vegetation. As the raster cell size is known (0.25 m resolution, or 0.0625 m^2 per pixel), the tool effectively counted the number of pixels in each category and multiplied by the area per pixel to get the results in square meters. This provided a quantitative measure of vegetation change.

In summary, combining the change map with tabulated area statistics finalizes the change detection analysis by showing not only where vegetation shifts occurred, but also how much area was gained or lost. These quantified results are essential for monitoring vegetation dynamics and informing resource management, restoration efforts, or policy decisions regarding land cover change.

4 Results

4.1 Overview of Results Presentation

This chapter presents the analytical outcomes of the study, structured by spatial unit and thematic focus. Specifically, the results are organized across the three study sub-areas (Area 1, Area 2, and Area 3) each of which was examined in terms of two key dimensions: topographic (elevation) change and vegetation dynamics. The intent is to systematically illustrate how the coastal dune morphology and vegetation cover have evolved between the years 2021 and 2024.

To decide which method of interpolation we will use for that, we recorded the RMSE for IDW and Kriging interpolation (Table 4) for each area and year. This validation procedure was systematically repeated for each interpolation technique (IDW and Kriging) and for each annual dataset, enabling direct and rigorous comparison. Ultimately, the interpolation method yielding the lowest RMSE value was selected for subsequent analyses, thereby ensuring that only the most accurate and reliable elevation data advanced to the GIS based processing stages. Through this rigorous and systematic preprocessing approach in CloudCompare, combining careful merging of LiDAR and bathymetric data, dual method interpolation, mesh-based validation, and RMSE driven method selection, the resulting elevation datasets were robustly prepared for detailed geomorphological change detection analyses within ArcGIS Pro.

Area	Year	IDW RMSE (m)	Kriging RMSE (m)	Chosen Method
A1	2021	0.186	0.286	IDW
A2		0.223	0.190	Kriging
A3		4.232	0.298	Kriging
A1	2022	2.438	0.569	Kriging
A2		0.515	0.460	Kriging
A3		3.327	0.252	Kriging
A1	2023	2.604	0.645	Kriging
A2		4.565	0.478	Kriging
A3		1.060	0.617	Kriging
A1	2024	-	-	-
A2		2.540	0.469	Kriging
A3		3.321	0.256	Kriging

Table 4 RMSE results and the chosen interpolation method per area/year

Note: These RMSE values apply to nearshore interpolation zones. On land, LiDAR point density was high and DEMs were generated from dense observations with negligible interpolation

In our study, whichever method gave the lower RMSE was chosen for generating the final DEM for that area and year. Generally, we found that kriging tended to yield more accurate results (lower RMSE) in highly variable dune terrain, while IDW was sometimes competitive in flatter zones. Regarding 2024_A1, we don't have any data and 2024_A2, only LiDAR data is available so on the bases of previous year's trend, we choose Kriging.

To computed two thresholds for each DEM comparison: LoD1 and LoD95 we will use the RMSE values of chosen interpolation method (Table 4). Formulas (2) & (3) reflect the assumption that errors in the two DEMs are independent and normally distributed. In formula (3) the factor 1.96 corresponds to approximately 95% confidence for a normal distribution, so LoD95 represents a threshold beyond which changes are significant at the 95% confidence level. In other words, LoD1 is roughly the "1σ" (68% confidence) detectable change level and LoD95 is a more stringent threshold (~95% confidence) for change detection. Using the root sum of squares (also called quadrature summation) of the DEM errors is a statistically sound way to propagate uncertainty from two surfaces.

The resulting threshold values for LoD1 (minimal level of detection) for each DEM pair are summarized in Table 5, and the 95% confidence thresholds (LoD95) are given in Table 6.

Area	**2022-2021**	**2023-2022**	**2024-2023**	**2024-2021**	**2023-2021**
A1	0.599	0.860	-	-	0.671
A2	0.561	0.663	0.669	0.506	
A3	0.391	0.667	0.668	0.393	

Table 5 LoD1 Threshold values

Area	2022-2021	2023-2022	2024-2023	2024-2021	2023-2021
A1	1.174	1.686	-	-	1.315
A2	1.100	1.300	1.312	0.992	
A3	0.766	1.307	1.310	0.771	

Table 6 LoD95 Threshold values

These tables list the numeric thresholds that were used to distinguish significant elevation changes from noise in each case. As expected, DEM pairs with higher survey uncertainty (larger RMSE) yielded higher LoD values, whereas high accuracy data produced lower detection thresholds. This procedure was repeated for all comparisons, ensuring each differencing analysis had its own tailored LoD appropriate to the data quality of the input DEMs.

4.2 Elevation Change Detection Area 1

Area 1's elevation change was assessed by differencing DEMs for consecutive time intervals (2021-2022 and 2022-2023) as well as over the entire 2021-2023 period. Figure 4 shows the significant elevation change raster maps for Area 1 under the LoD1 threshold (for each time

interval), and Figure 5 shows the equivalent maps using the LoD95 threshold. The spatial results are supplemented by quantitative area calculations (in m² and as a percentage of Area 1) for each change category, summarized in tabular form.

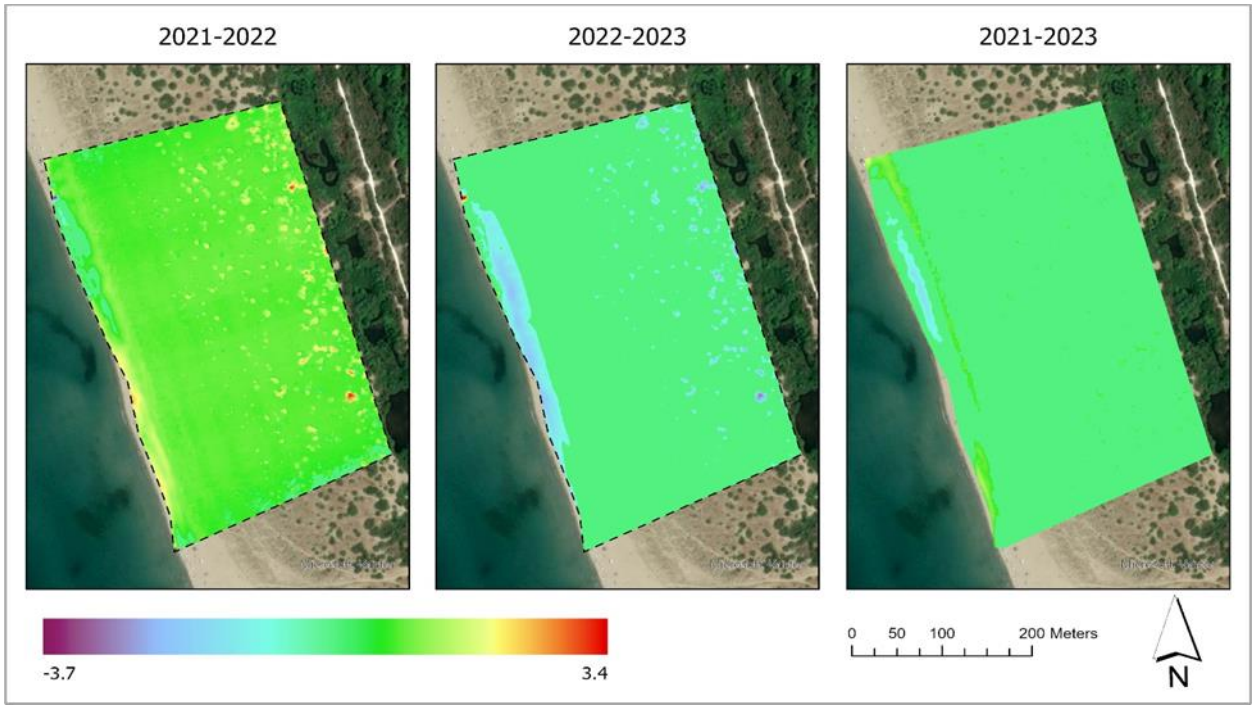


Figure 4 Area 1 DoD at LoD 1

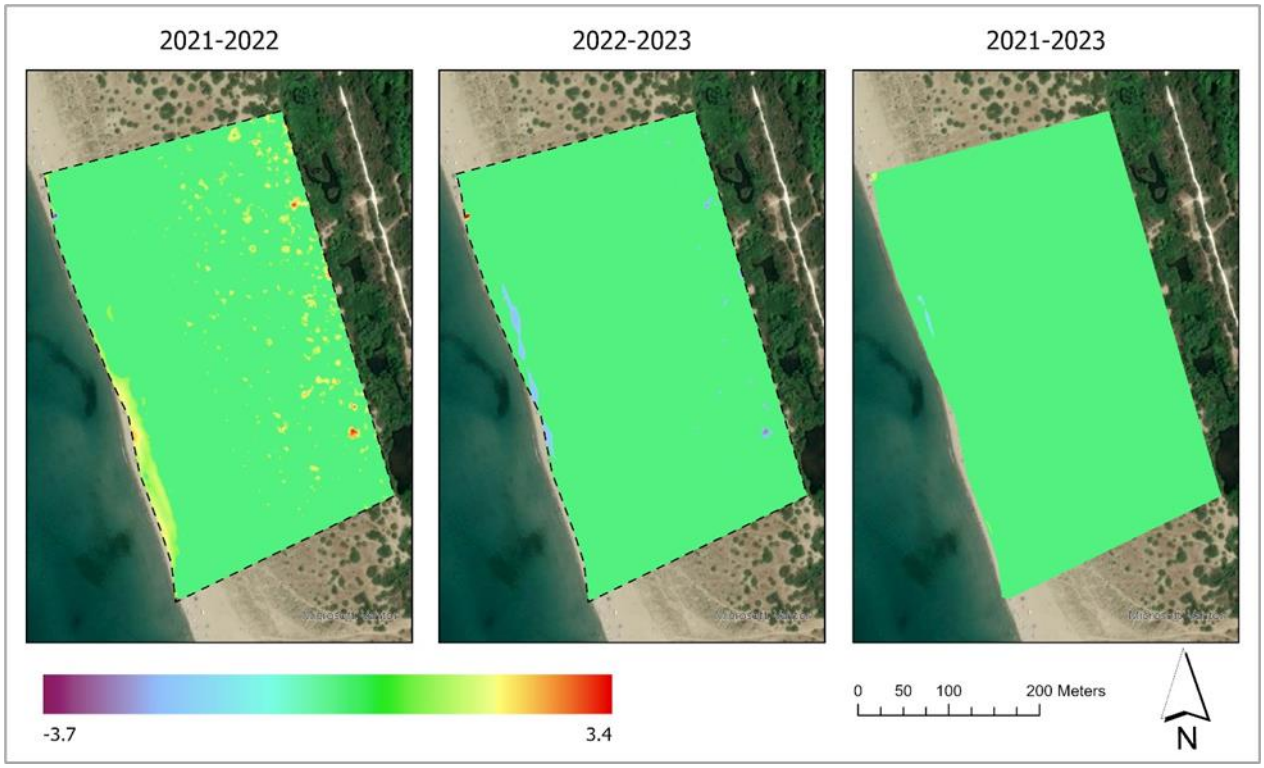


Figure 5 Area 1 DoD at LoD 95

4.2.1 LoD1 Threshold: Spatial Change Patterns and Extent

Using the minimum detection threshold (LoD1), the elevation changes maps reveal clear patterns of widespread but low-magnitude change in Area 1. For the 2021-2022 interval, the LoD1 classified map shows that nearly the entire area experienced accretion. In Figure 6 (left panel), blue shading dominates throughout Area 1, indicating pervasive elevation gains. Only very minor patches of erosion (red) appear, confined to the western (seaward) edge of the area (likely at the beach/dune interface). Virtually minor portion of the area remains gray (no-change) under this lenient threshold, meaning even small elevation differences were marked as change.

Tabulated area results strongly confirm the presence of widespread accretion. During 2021-2022, Area 1 shows a clearly accretional budget, with about 118,993 m^3 of sediment gained but only roughly 147 m^3 lost to erosion (Table 7).

In contrast, the 2022-2023 period shows a reversal in trend, with erosion now dominating, especially along the coastal fringe. Figure 6 (2022-2023) shows a continuous red strip along the western margin, indicating that both the shoreline and the foredune zone experienced elevation drops surpassing the LoD1 threshold. These erosion patterns extend across much of the seaward edge, pointing to dune face retreat or beach lowering. In the central and eastern zones of Area 1, the map is mostly gray, meaning there was no measurable change landward of the foredune based on LoD1 limits. Remarkably, blue pixels representing accretion are nearly absent in this interval, a notable difference from the prior year, implying sediment was lost rather than deposited. In terms of area, the erosion class constitutes a modest fraction of Area 1 (roughly 10-15%) while the remaining classified as no change (Annex 7).

Over the full 2021-2023 period, the LoD1 results show a mixed but muted change pattern. As seen in Figure 6 (right panel), the majority of Area 1 registers as stable (gray) when comparing 2021 to 2023. The only notable changes are confined again to the coastal margin, where alternating patches of erosion and accretion appear. One segment of the shoreline exhibits net erosion (red) while an adjacent segment shows net accretion (blue), indicating spatial heterogeneity in the two-year balance of sediment. These change patches are relatively small in area, and much of the inland portion remains unchanged. Area 1 in 2021-2023 experienced modest volumetric fluctuations, with erosion totaling approximately 1541m^3 and accretion around 4219m^3 (Table 7). This implies that the extensive deposition observed after 2021 was largely counteracted by subsequent erosion by 2023, yielding little net change overall.

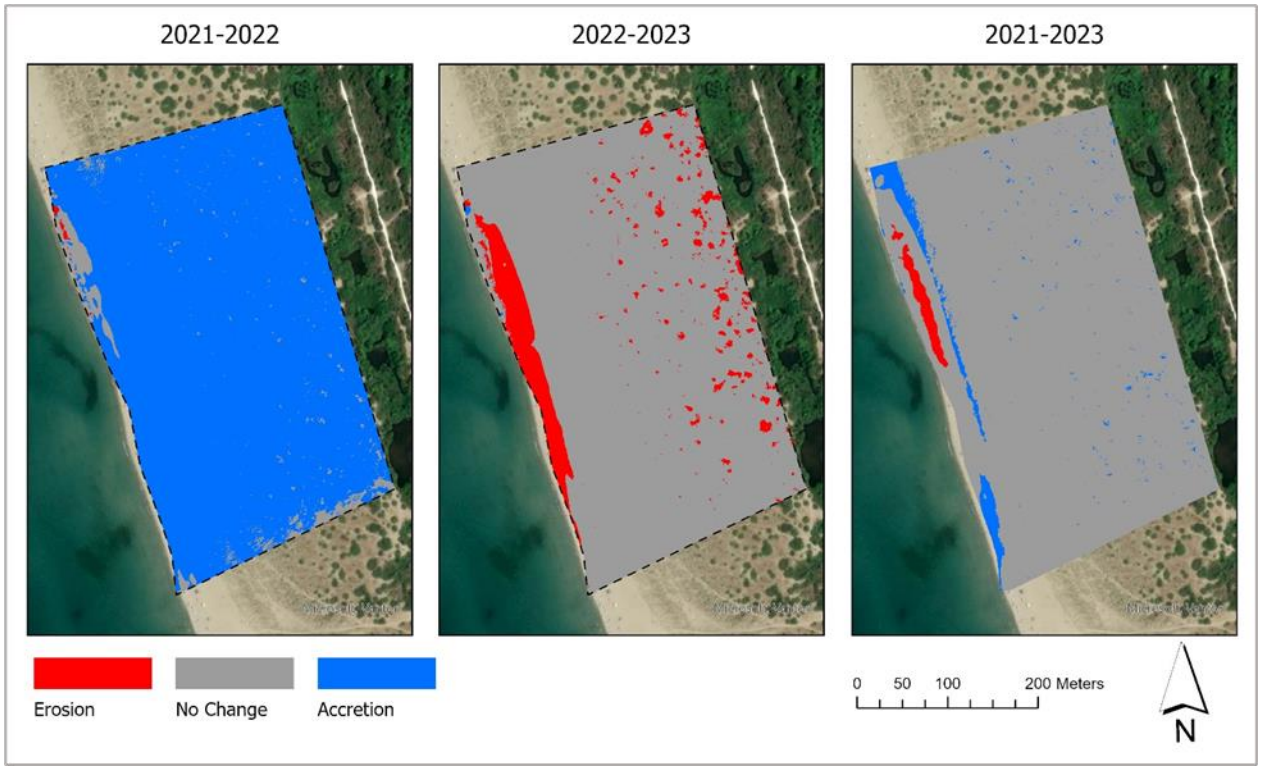


Figure 6 Classified Elevation Change Map of Area 1, Threshold LoD1

A1	Erosion Vol.	Accretion Vol.	Net Vol.
	m^3	m^3	m^3
2021-2022	146.87	118993.53	118846.66
2022-2023	10320.17	69.97	-10250.20
2021-2023	1551.16	4219.99	2668.83

Table 7 Elevation Change Summary of Area 1 at LoD1

Note: Net volume = Accretion Vol - Erosion Vol (m^3); positive values = net accretion, negative values = net erosion.

The distribution of elevation changes for Area 1 was further examined by analyzing the frequency of point values within defined elevation bins for each time interval. The histogram under the LoD1 threshold (Figure 7) displays a broader spread of elevation differences, particularly in the positive elevation ranges. The dominant bin lies between 0.6 m and 1 m, indicating a significant proportion of points associated with accretion during the 2021-2022 interval. In contrast, the 2022-2023 interval exhibits a sharp increase in the negative bins, with a dominant peak in the -0.2 m to 0.0 m range, suggesting a widespread erosion phase in that period. The long tail toward positive values in the 2021-2022 profile indicates localized zones of dune buildup, while 2022-2023 and 2021-2023 curves are more skewed toward zero and negative changes.

The distribution of elevation changes in Area 1 was investigated through frequency histograms, which present the point counts across discrete elevation change intervals for each annual and biennial comparison. Figure 7, which includes the full range of elevation bins,

shows a pronounced concentration of points in the -0.2 m to 0.0 m class for both the 2022-2023 and 2021-2023 intervals. This overwhelming dominance suggests that a large proportion of the surface experienced shallow erosional changes during those periods, which nonetheless exceeded the minimum Level of Detection (LoD1), and are therefore considered significant. Conversely, the 2021-2022 profile is characterized by a broader positive spread, with marked peaks in the 0.6 - 1.0 m class, indicative of substantial surface accretion linked to localized dune buildup processes.

However, the inclusion of the -0.2 to 1.0 m bins in the main histogram visually overshadows other important change categories by compressing the scale and limiting contrast. An additional histogram was generated without the -0.2 to 1.0 m classes (ANNEX 1), enabling a clearer assessment of the remaining variation in elevation change. This refined visualization reveals several critical secondary trends that were previously masked. For the 2022-2023 interval, a progressive increase in point frequency is observed across more negative bins, particularly from -1.2 to -0.8 m, highlighting a broader erosional response in the post 2022 phase, affecting deeper portions of the terrain.

The 2021-2022 histogram, when viewed without the bins closest to zero, clearly emphasizes its accretional signature. It features pronounced spikes in higher positive classes, most notably in the 1.0 to 1.6 m range. These sharp peaks suggest intense and localized deposition events, likely linked to wind-driven accumulation along the dunes. Looking at the full 2021-2023 cumulative histogram, the distribution appears more balanced between negative and positive values. This implies that while the later period was marked by widespread erosion, the earlier accretion phase still played a key role in shaping the net morphodynamic evolution of the area.

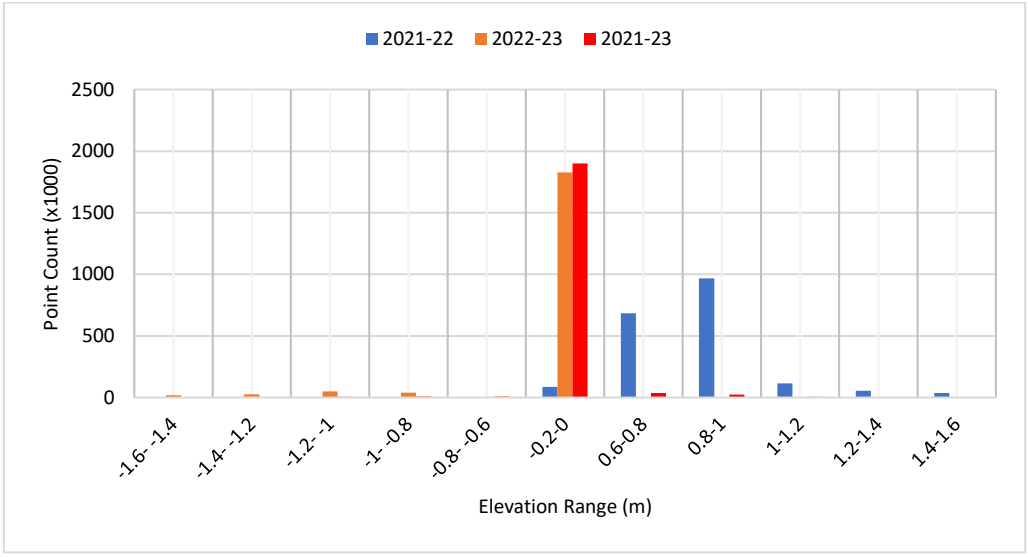


Figure 7 Significant Change Histogram of Area 1 with LoD1

4.2.2 LoD95 Threshold: Refined Detection and Statistical Confidence

Applying the stricter 95% confidence threshold (LoD95) yields a more conservative depiction of change in Area 1. Many of the minor changes flagged under LoD1 are filtered out, leaving

only the most pronounced elevation differences. For 2021-2022, the LoD95-based map (Figure 8, left panel) still indicates accretion as the dominant process, but its spatial extent is greatly reduced. Unlike the widespread blue seen earlier, accretion is now concentrated in specific zones, notably along the western side. Large portions of the interior that showed slight gains under LoD1 now appear as no change (gray) under LoD95. Only the most substantial depositional areas (blue) remain highlighted, and erosion (red) is virtually absent. This refinement is also reflected in the area statistics: accretion is limited to a small portion of Area 1 while the majority (~85-90%) shows no significant change (Annex 8). Erosion is virtually nonexistent for this period at the 95% confidence level (Table 8).

In 2022-2023, the LoD95 change map (Figure 8, 2022-2023) clearly delineates the coastal erosion zone while suppressing smaller-scale changes. A sharp red band is visible along the shoreline, indicating significant elevation losses there (similar to the LoD1 result, but more cleanly defined). However, unlike the LoD1 map, virtually no red patches appear in the interior, the erosion is confined to the coastal fringe. The rest of Area 1 remains gray, reflecting a lack of statistically significant change away from the shore. The net sediment balance is slightly erosional, with an estimated 1,303 $m^3$of material lost, and just 39 m^3accumulated through accretion (Table 8). The maximum area around 98% shows no change at the LoD95 level (Annex 8).

Looking at the cumulative results for 2021-2023, the LoD95 analysis emphasizes the overall stability of Area 1. The right panel of Figure 8 is almost entirely gray, dominated by the no-change class. Only one or two isolated cells show minimal elevation change but their spatial extent is negligible. In essence, at the 95% certainty level, there was no widespread elevation shift in Area 1 over this two-year period. The tabulated data confirm that more than 99% of the area remained unchanged between 2021 and 2023, with erosion and accretion each affecting less than 1% of the surface (Annex 8). This finding confirms that many of the changes observed under LoD1 in the long-term comparison fall within the margin of error and cannot be interpreted as statistically significant at the LoD95 level.

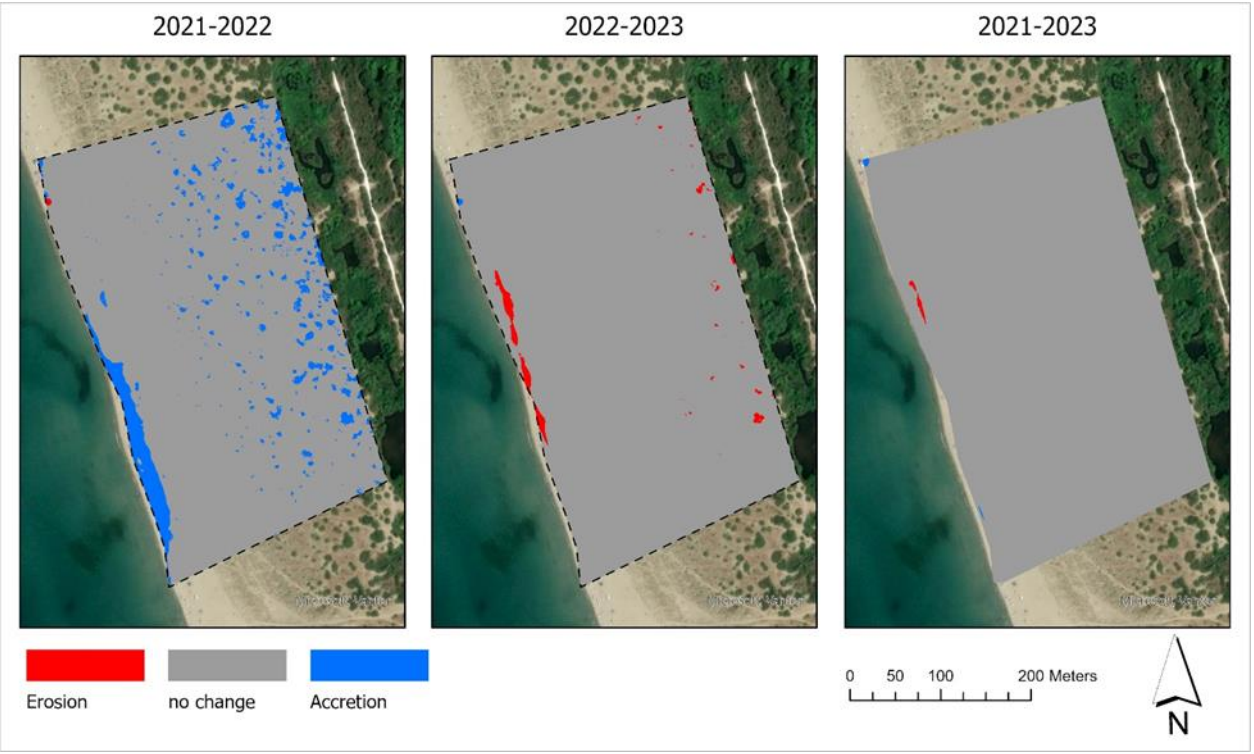


Figure 8 Classified Elevation Change Map of Area 1 at LoD95

A1	Erosion Vol.	Accretion Vol.	Net Vol.
	m^3	m^3	m^3
2021-2022	46.67	9127.28	9080.62
2022-2023	1303.15	39.48	-1263.67
2021-2023	141.43	67.53	-73.90

Table 8 Elevation Change Summary of Area 1 at LoD95

The histogram analysis under the 95% confidence threshold (Figure 9) reveals a markedly narrow distribution of elevation changes in Area 1. The overwhelming majority of points cluster within the -0.2 m to 0.0 m bin across all intervals, especially in the 2022-2023 and 2021-2023 comparisons. This outcome illustrates the effect of applying the LoD95 threshold, which eliminates low-certainty variations and retains only those changes that meet statistical significance. As a consequence, small-scale topographic noise is filtered out, allowing only the more reliable signals of morphological change to remain visible. This dominant peak near zero thus indicates widespread terrain stability or changes that were minimal in magnitude but statistically significant.

However, the visual prominence of the central bin overshadows the presence of other meaningful elevation changes distributed across the terrain. To address this, a secondary histogram was produced without the -0.2 to 0.0 m bin (ANNEX 2), allowing for enhanced visibility of the remaining significant elevation changes across both erosional and depositional

classes. This refined view reveals critical insights. During the 2021-2022 interval, multiple accretional peaks become evident, particularly in the 1.2 - 1.8 m range, indicating the presence of sustained vertical buildup in localized zones, likely corresponding to aeolian sand accumulation along the dune crest. The 2022-2023 period, by contrast, reveals a distinct concentration of points in the erosion bins, including -2.2 to -1.6 m. These deeper changes suggest more aggressive erosion episodes, possibly linked to storm events or seasonal dune scarping along exposed coastal fronts. The 2021-2023 cumulative profile exhibits a balance between both erosional and depositional extremes, although the distribution remains sparse. These histograms complement the raster classifications and area change tables by showing not just the spatial extent of change, but also how those changes are distributed in terms of magnitude. They emphasize how thresholding can impact the interpretation of dune dynamics, LoD1 captures more spatial variability, while LoD95 offers a more conservative estimate of morphodynamic activity.

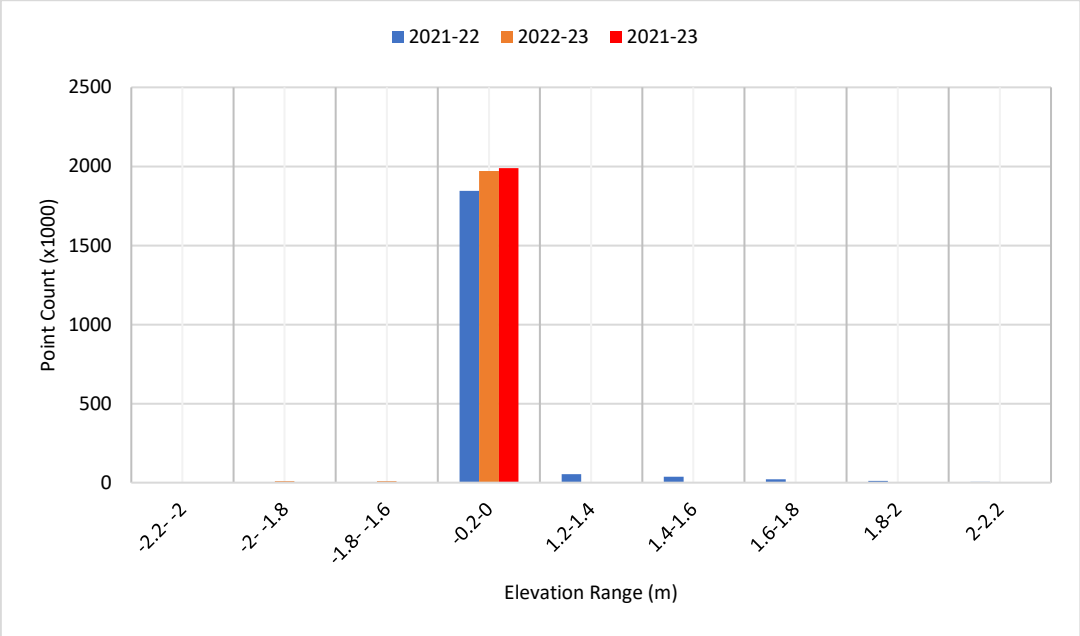


Figure 9 Significant Change Histogram of Area 1 with LoD95

4.2.3 Comparative Insights Between Thresholds

A side-by-side comparison of the LoD1 and LoD95 results for Area 1 highlights the influence of the detection threshold on the apparent extent of change. In all time intervals, the total area classified as changed (erosion or accretion) is substantially greater under LoD1 than under LoD95. For example, in 2021-2022 nearly the entire Area 1 was flagged as undergoing accretion with LoD1, whereas only a relatively small portion was identified as accretion under LoD95 (Tables 7 and 8). Similarly, in 2022-2023 the erosional area is a few times larger when using the lenient threshold than when using the stricter threshold. By 2021-2023, LoD1 still shows some pockets of change while LoD95 finds virtually none. This demonstrates that LoD1 tends to over-estimate the spatial extent of elevation changes by including many marginal or

noise-level differences, whereas LoD95 provides a more filtered representation limited to high-confidence changes.

Although the two thresholds differ in the magnitude of detected changes, they consistently highlight the same primary spatial patterns. Notably, both methods indicate that the western coastal margin is the focal point of significant transformation. The broad accretion across Area 1 in the 2021-2022 LoD1 map, for instance, appears under LoD95 as a set of more localized deposition areas. Still, both thresholds indicate that this interval was marked predominantly by accretion. Similarly, both LoD1 and LoD95 recognize the 2022-2023 period as one dominated by coastal erosion with negligible signs of deposition, differing only in the extent of the mapped erosion.

It is also evident that certain broad trends apparent under LoD1 are diminished or absent under LoD95. For instance, the slight region-wide elevation gain that was indicated by LoD1 for 2021-2022 (resulting in the nearly ubiquitous blue shading) does not manifest in the LoD95 map, suggesting that this broad low-amplitude change was not statistically significant at 95% confidence. Thus, what might be interpreted from the LoD1 results as a uniform accretion or a possible survey bias is largely dismissed by the LoD95 analysis as within the noise level. This comparison underscores the importance of threshold selection: a lower threshold (LoD1) is useful for capturing subtle changes and providing an upper bound on potential change areas, whereas a higher threshold (LoD95) yields a more conservative estimate, emphasizing only changes that exceed rigorous uncertainty criteria

In the context of Area 1, both approaches ultimately convey a consistent narrative of change, initial deposition followed by erosion, while the LoD95 results lend greater confidence to the significance of those changes.

4.2.4 Temporal Evolution Across 2021-2023

The temporal development of elevation changes in Area 1 between 2021 and 2023 reveals a dynamic behavior. During the 2021-2022 period, accretion was the dominant process, particularly concentrated along the seaward dune toe and frontal sectors. In contrast, 2022-2023 saw a shift, with marked erosion occurring in many of the same coastal zones. This reversal indicates that a substantial portion of the material deposited during the earlier phase was later reworked or removed, likely due to seasonal hydrometeorological forcing. Spatial overlap between zones of prior accretion and later erosion further supports the conclusion of a short-term sedimentary cycle. While the full range of elevation changes detected spanned from approximately -3.7m to +3.4m, these extremes were highly localized and represent rare occurrences. The majority of changes, as confirmed by histogram analysis, were concentrated within the ±0.2m interval, reflecting more subtle and widespread adjustments in dune morphology. Overall, the interval 2021-2023 displays a net pattern of stabilization with relatively limited change, suggesting partial recovery or re-equilibration of the dune surface following earlier perturbations.

4.3 Elevation Change Detection Area 2

Area 2's elevation change was assessed by differencing digital elevation models (DEMs) over three consecutive annual intervals (2021-2022, 2022-2023, 2023-2024) as well as the entire 2021-2024 period. To distinguish real geomorphic changes from survey noise, the same change-detection thresholds and classification scheme described for Area 1, were applied here as well.

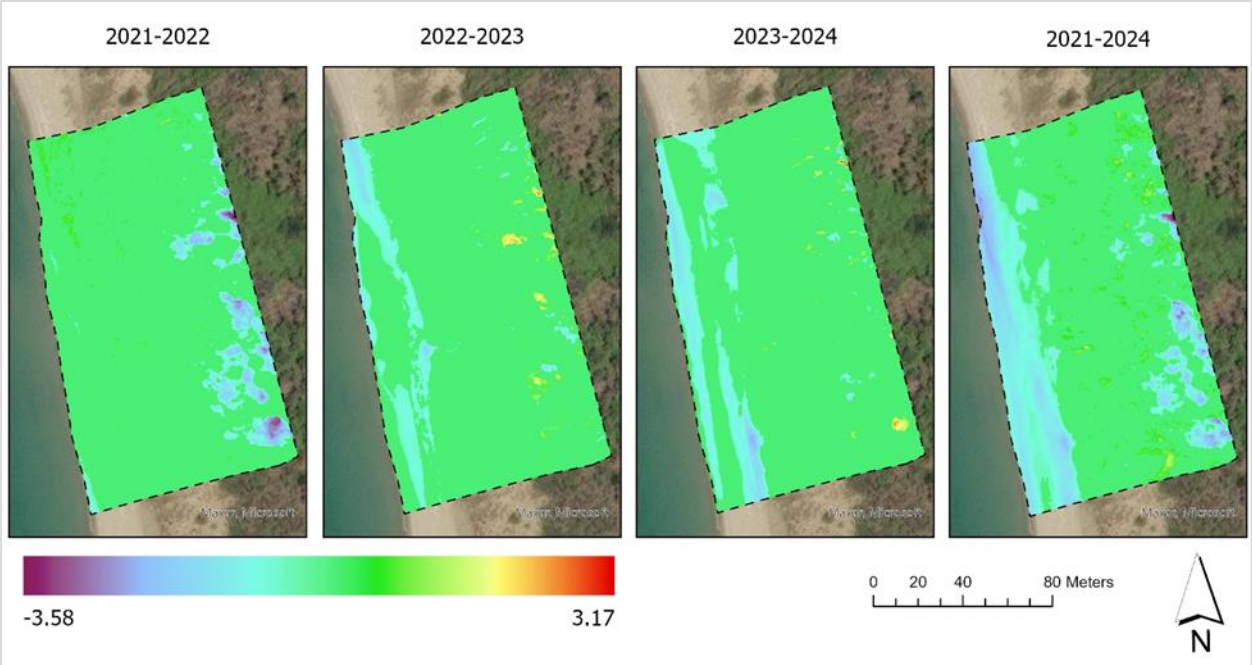


Figure 10 Area 2 DoD at LoD 1

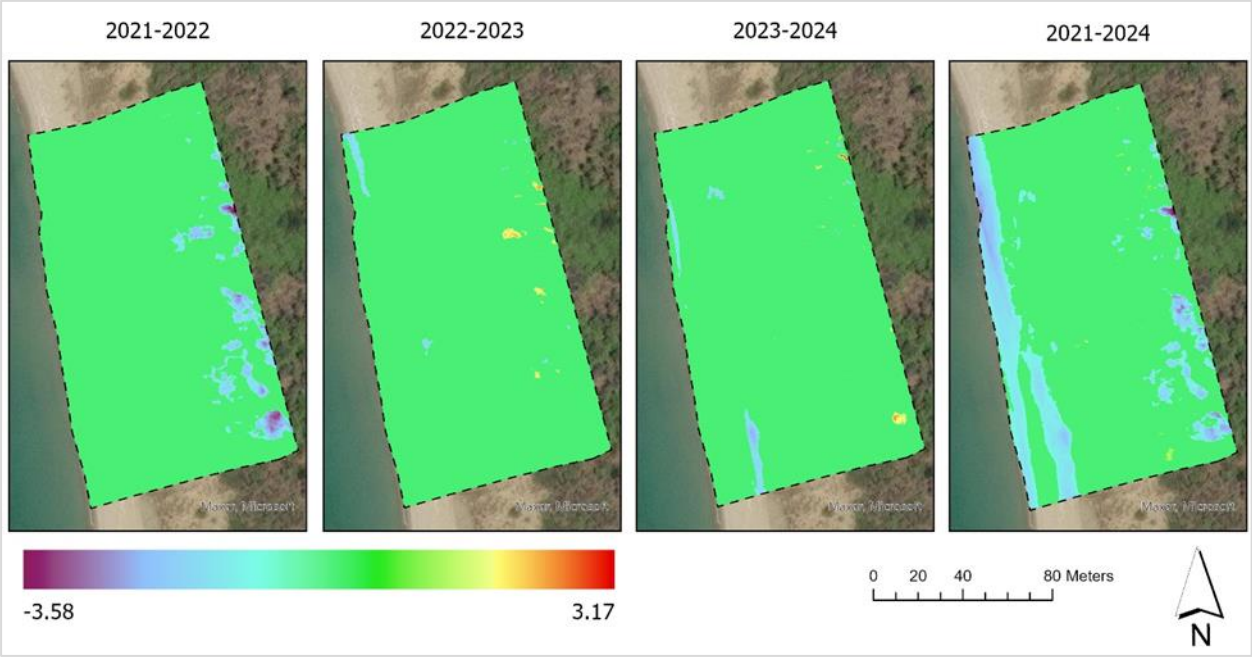


Figure 11 Area 2 DoD at LoD 95

4.3.1 LoD1 Threshold: Spatial Change Patterns and Extent

Using the minimum detection threshold (LoD1), the elevation changes maps for Area 2 reveal relatively localized changes compared to the area's total extent. For the 2021-2022 interval, the LoD1 classified map shows that the vast majority of Area 2 remained stable, with change confined to a few zones. In Figure 12 (2021-2022 panel), a distinct red patch is evident landward margin of Area 2, indicating an erosional hot spot at the beach dune interface. This suggests that during 2021-2022 the dune front underwent noticeable lowering or retreat. Blue patches (accretion) are very scarce, only few tiny spots of blue appear, likely in isolated pockets seaward, implying minor localized deposition. Virtually the entire interior of Area 2 remains gray, denoting "No Change" under this lenient threshold. Volumetric analysis indicates a predominance of erosion, with approximately 1,828 m^3 of material loss compared to just 151 m^3 of accretion, resulting in a net negative change of around -1,677 m^3 (Table 9).

In the 2022-2023 interval, the spatial pattern of change remains predominantly erosional but concentrated at the coastline. Figure 12 (2022-2023 panel) highlights what is nearly a continuous red band tracing along the western seaward edge of Area 2, signifying that the shoreline and foredune zone experienced further elevation losses exceeding the LoD1 threshold. This erosional band stretches along much of the dune front, implying a retreat or lowering of that entire coastal strip during 2022-2023. Landward of this fringe, the area is mostly gray, indicating little to no significant change in the back-dune or interior regions under LoD1. Notably, only extremely limited accretion (blue) is detected in 2022-2023, a couple of very small blue specks can be seen. The volumetric summary shows that erosion with over 1380 m^3 of material loss, while accretion remains limited to just over 326 m^3, resulting in a net negative balance(Table 9). These proportions reinforce that 2022-2023 was marked by net sediment loss focused along the dune margin, with the interior remaining largely stable.

For 2023-2024, the LoD1 results show the most extensive changes of all the single-year intervals. As seen in Figure 12 (2023-2024 panel), the erosion zone expands in both size and continuity along Area 2's seaward boundary. A broad swath of red coloring dominates the frontal dune line, indicating an intensified erosional impact on the dune system during 2023-2024. Conversely, accretion areas (blue) are almost entirely absent in this interval, only few very small patches of blue are visible on the map. The near lack of blue suggests there was virtually no appreciable sediment gain in Area 2 for 2023-2024. Much of the interior again remains gray, but the proportion of gray is somewhat reduced compared to prior years because the erosional areas have grown. During 2023-2024, Area 2 experienced the highest volumetric change of all annual intervals. Erosion exceeds 2000m^3, while accretion remained minimal at just over 200 m^3, reflecting a strongly negative sediment balance (Table 9). Thus, by 2023-2024 the erosional processes not only persisted but affected a broader portion of the area's surface, whereas depositional processes remained minimal.

Over the full 2021-2024 period, Figure 12 (2021-2024 panel), nearly the entire seaward fringe of Area 2 is mapped in red, represent extensive net erosion between 2021 and 2024. The continuous red zone along the seaward margin clearly marks a significant lowering of the dune front over the full study period. A few blue spots are also present, representing areas of net accretion across the three years. However, these depositional zones are limited in extent,

highlighting that the observed gains were insufficient to offset the widespread losses at the dune edge. The 2021-2024 interval recorded a total net loss of approximately 4,777 m^3 in Area 2, with cumulative erosion far exceeding accretion volumes, underscoring a prevailing erosional trend over the three-year period (Table 9). Crucially, the erosion category dominates the multi-year total, on the order of ~30% of Area 2's surface underwent net erosion (significant lowering) in that three-year span, compared to only ~4% of the area showing net accretion (Annex 9). The inland two-thirds of the area stayed effectively unchanged in elevation, highlighting that the major geomorphic adjustments were tightly focused on the coastal dune belt.

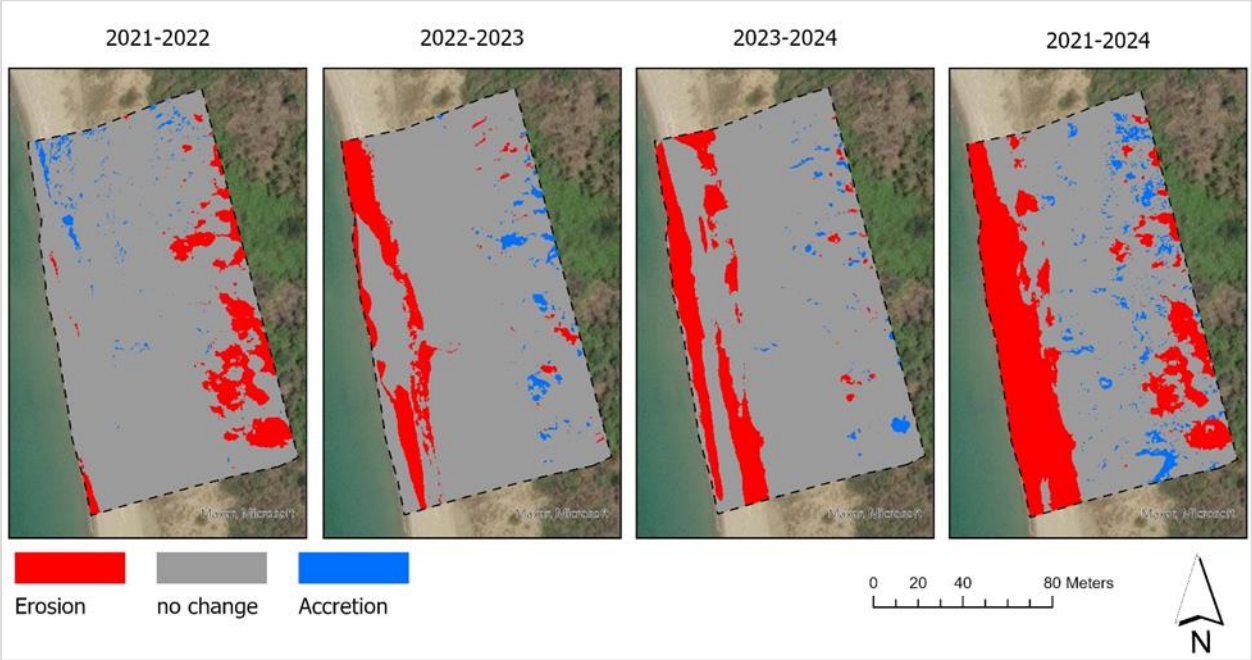


Figure 12 Classified Elevation Change Map of Area 2 at LoD1

A2	Erosion Vol.	Accretion Vol.	Net Vol.
	m^3	m^3	m^3
2021-2022	1827.61	150.75	-1676.85
2022-2023	1380.55	326.14	-1054.41
2023-2024	2065.58	203.06	-1862.51
2021-2024	5176.30	399.25	-4777.04

Table 9 Elevation Change Summary of Area 2 at LoD1

The magnitude and distribution of elevation changes in Area 2 were evaluated using LoD1 threshold-based frequency histograms (Figure 13). The full histogram reveals that the majority of points fall within the -0.2 to 0 m range, pointing to a dominance of low-magnitude elevation changes. In 2021-2022, the distribution shows a clear peak in the -0.2 to 0 m class, with relatively few points beyond that range. The 2022-2023 interval displays an even more concentrated grouping around zero, indicating that changes were generally less pronounced.

By contrast, the 2023-2024 distribution spreads further into negative values, reflecting a greater extent of surface lowering during that period. Overall, the cumulative 2021-2024 distribution confirms that erosion dominates the topographic evolution of Area 2 under the LoD1 threshold, while positive elevation gains remain minimal and largely constrained to small, localized pockets.

When focusing on the remaining elevation intervals, the histogram in ANNEX 3 highlights a consistent skew toward negative elevation changes, especially within the -1.6 to -0.6 m range. This skew is observable across all DoD and is most pronounced in the cumulative 2021-2024 dataset (red bars). The 2023-2024 period shows a broader spread of values within the erosional range, pointing to a notable increase in erosion intensity during the final year of the study. Meanwhile, the frequency of positive elevation changes remains negligible throughout all time intervals. Only a few bars appear in the 0.4 to 0.8 m range, further confirming that substantial accretion is both rare and spatially limited within Area 2. The overall distribution patterns, once the dominant -0.2 to 0 class is removed, reinforce the interpretation of unbalanced geomorphic behavior, where episodic erosion significantly outweighs deposition across the dune system.

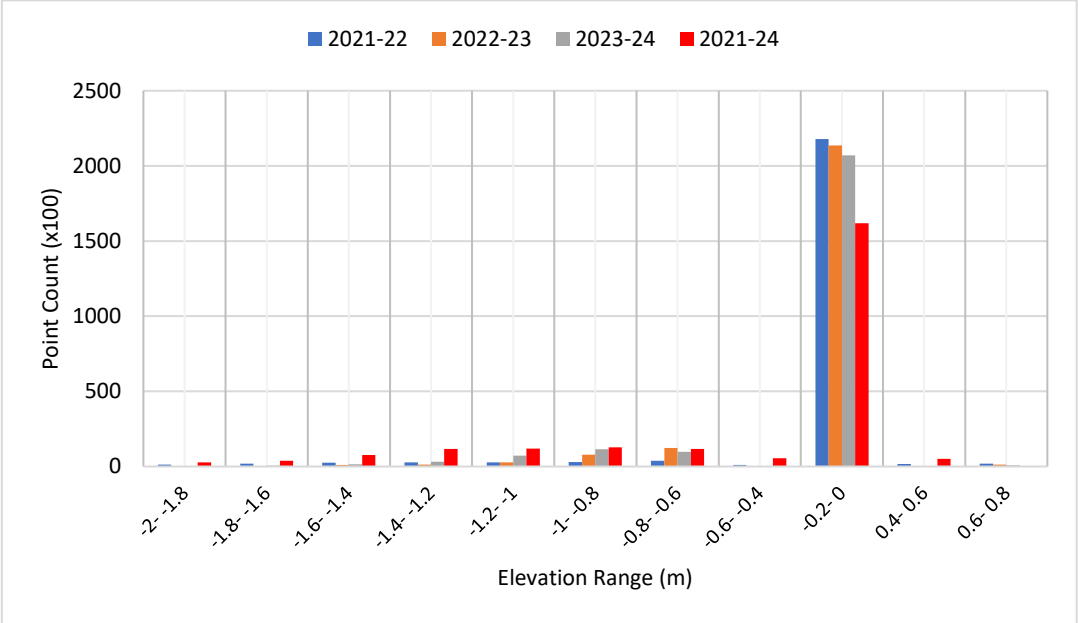


Figure 13 Significant Change Histogram of Area 2 with LoD1

4.3.2 LoD95 Threshold: Refined Detection and Statistical Confidence

Applying the stricter 95% confidence threshold (LoD95) yields a much more conservative picture of change in Area 2. Many of the small magnitude changes that were flagged under LoD1 are filtered out when we require high statistical confidence, leaving only the most pronounced elevation differences. For 2021-2022, the LoD95-based map (Figure 14, 2021-2022 panel) still identifies erosion as the dominant process, but the spatial extent of detected change is greatly reduced compared to the LoD1 map. Instead of a patch of red along the dune front, LoD95 highlights only the core of the erosion area, only a couple of concentrated red patches

along the landward edge where elevation losses were large enough to exceed the 95% confidence limit. the area that showed light erosion patches or slight accretion on seaward side under LoD1 now appears as gray (no change) under LoD95, indicating those changes were below the stricter detection threshold. In fact, virtually no blue is visible in the 2021-2022 LoD95 map, the minor accretion spots from the LoD1 analysis do not register as significant at 95% confidence. The result is that the 2021-2022 LoD95 change map depicts only a small eroded section of the area with the rest of Area 2 deemed unchanged. This interval reveals a distinctly erosional pattern in Area 2, with approximately 1,375 m^3 of material lost and minimal deposition (just 2 m^3), confirming that nearly all the volumetric change was due to erosion (Table 10).

In 2022-2023, the LoD95 change map (Figure 14, 2022-2023 panel) indicates an extremely limited significant change. Virtually the entire map is gray, signifying that Area 2 saw no broad-scale elevation shifts in this interval. The continuous red band of coastal erosion visible under the LoD1 threshold is nearly absent in the LoD95 map. Only a small red patch remains near the shoreline, with a few isolated blue spots indicating accretion. Beyond these minimal features, the 2022-2023 LoD95 result indicates no detectable change across Area 2. Thus, from a high-confidence perspective, 2022-2023 was essentially a year of no measurable geomorphic change in Area 2.

The 2023-2024 interval under LoD95 shows a slight uptick in significant change relative to the previous year, but the overall pattern is still one of highly constrained activity. The LoD95 map for 2023-2024 (Figure 14, 2023-2024 panel) reveals a small but distinct erosion zone along the dune front that passes the 95% threshold. In contrast to 2022-2023, a short segment of the coastline is clearly highlighted in red, indicating that some erosion during 2023-2024 was substantial enough to be considered real change with 95% confidence. This red segment likely corresponds to the most severely eroded portion of the dune. Aside from that, changes remain minimal, the blue (accretion) areas are almost non-existent, with at most few very tiny blue spot visible. The bulk of Area 2, over 98%, remains gray on the 2023-2024 LoD95 map, reflecting no statistically significant elevation change in those parts. As reported in (Annex 10), only 1.9% of the area experienced erosion and only 0.4% attributed to accretion. Therefore, even though 2023-2024 was an erosive year under LoD1, at the 95% confidence level it manifests as just a small erosion hotspot amid an otherwise unchanged landscape.

Over the full 2021-2024 period, the LoD95 analysis captures the cumulative effect of three years of change in a distilled way. Figure 14 (2021-2024 panel) is dominated by the no-change (gray) category inland, but along the coastline it displays a conspicuous band of red that was not present in the shorter interval maps. This red band represents the net erosion of the foredune and beach that has accrued over the entire study period and is large enough to stand out above the uncertainty threshold. Essentially, while year-to-year changes often fell below LoD95, the aggregate change from 2021 to 2024 along the dune front is significant. The spatial extent of this LoD95 confirmed erosion band is fairly substantial in the context of Area 2's size, it runs along a virtuous portion of the seaward edge, marking where the dune has definitively lowered or receded over those three years. On the other hand, very little blue is seen on the 2021-2024 LoD95 map almost no areas show statistically significant accretion when comparing the 2021 and 2024 DEMs. This implies that any apparent build-up of sand that may have been

captured under LoD1 was likely within error margins; only erosional change persists as a sure signal in the long-term. Over the full period, Area 2 underscores a strongly erosional trend, with total losses exceeding 3,700 m^3 and minimal accretion, indicating that nearly all volumetric change was due to erosion (Table 10). Accretion, by contrast, constitutes essentially zero percent of the area at LoD95 (only a trivial 0.1-0.2% of area, on the order of a few tens of square meters, fell into accretion). In other words, at high confidence, Area 2's net three-year change was purely erosional. This long-term LoD95 result underscores that the apparent widespread changes seen with LoD1 were mostly within the noise, and it isolates the true geomorphic change, a significant recession of the coastal edge of Area 2.

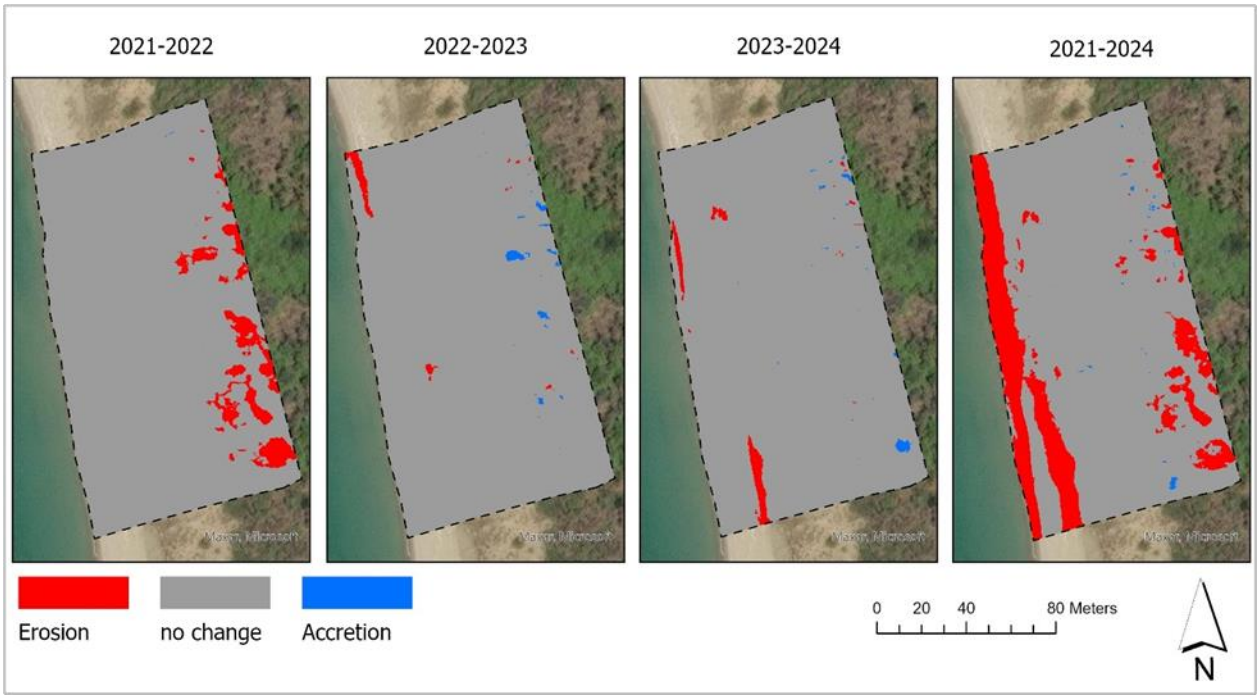


Figure 14 Classified Elevation Change Map of Area 2 at LoD95

A2	Erosion Vol.	Accretion Vol.	Net Vol.
	m^3	m^3	m^3
2021-2022	1375.71	2.01	-1373.69
2022-2023	173.00	135.72	-37.28
2023-2024	351.01	89.90	-261.11
2021-2024	3786.54	38.83	-3747.70

Table 10 Elevation Change Summary of Area 2 at LoD95

To evaluate elevation changes with high statistical confidence, frequency histograms were also generated using the LoD95 threshold, which excludes low-magnitude variations within the 95% confidence interval. As shown in Figure 15, the resulting distributions are sharply concentrated near zero, confirming that most changes across Area 2 were not statistically

significant under this stricter threshold. The vast majority of points across all intervals fall within the narrow -0.2 m to 0 m range, which corresponds to the edge of the noise band defined by the LoD95.

In the 2021-2022 interval, the histogram reveals a modest spread into the negative range. Compared to the LoD1 histogram, the LoD95 distribution appears noticeably narrower. During 2022-2023, the distribution becomes even more compact and peaked at zero, reflecting a year of minimal geomorphic activity. Virtually confirming that this year was characterized by high surface stability. The 2023-2024 shows a similar narrow central peak, with only a very minor extension toward negative values.

Overall the distribution remains tightly clustered around zero change. The cumulative 2021-2024 histogram (red bars) displays a slightly more developed tail into negative elevation classes, notably in the -1.6 m to -1.0 m range. This accumulation of multi-year erosion indicates that while individual annual changes may have been subtle, their compounded effect was sufficient to produce statistically significant surface lowering in certain areas over time. Once again, no meaningful values appear in the positive domain, confirming the absence of high-confidence accretion across the study period.

In ANNEX 4, the distribution tails become distinctly more visible. The cumulative (2021-2024) curve presents a clear concentration of points in the -1.6 m to -1.0 m bins, with non-negligible frequencies also appearing in the -1.6 m to -2.2 m classes. These deeper elevation losses are concentrated in erosion-prone areas and likely reflect localized dune scarp retreat or sediment removal due to extreme wind or tidal events. The 2021-2022 and 2023-2024 intervals also show consistent, though slightly narrower, tails within the same negative range, reinforcing the pattern of recurrent yet spatially limited erosion. Meanwhile, 2022-2023 continues to demonstrate the lowest point counts across all bins, aligning with the visual interpretation that this year exhibited minimal change.

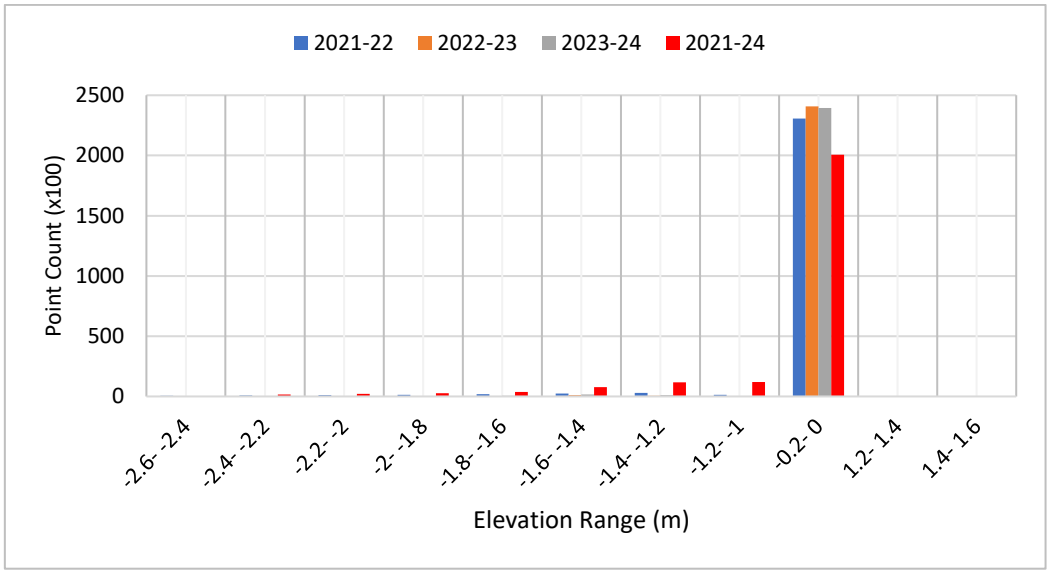


Figure 15 Significant Change Histogram of Area 2 with LoD95

4.3.3 Comparative Insights Between Thresholds

A side-by-side comparison of the LoD1 and LoD95 results for Area 2 highlights the influence of the detection threshold on the apparent magnitude and extent of change. In all time intervals, the total area classified as "changed" (either erosion or accretion) is substantially greater under LoD1 than under LoD95. For example, in the 2023-2024 interval, approximately 15% of Area 2 was flagged as changed using the lenient LoD1 threshold, whereas only about 1.9% of the area was identified as changed under the stringent LoD95 criterion (Annex 9 vs. Annex 10). LoD1 reported nearly eight times more surface area with detectable elevation change than LoD95 for that year. The difference is even more pronounced in 2022-2023, when LoD1 identified changes across roughly 12% of Area 2, while LoD95 flagged only about 1%. Even during 2021-2022, which showed more evident surface change, LoD1 still marked close to 11% of the area as changed, whereas LoD95 recorded only about 5%. By the full 2021-2024 period, LoD1 suggested one-third of the area saw elevation changes, whereas LoD95 confirmed only about half of that (≈18% of area). These comparisons demonstrate that the lower LoD1 threshold tends to over-estimate the spatial extent of change by including many small or marginal elevation differences that a stricter analysis deems insignificant. In essence, LoD1 provides an upper-bound, "sensitive" view of where any possible change might have occurred, while LoD95 provides a pared-down view limited to high-confidence changes.

Despite these differences in mapped extent, both thresholds pinpoint the same key spatial trend. Area 2's changes are overwhelmingly erosional and concentrated along the coastal dune front. The specific locations of change identified under LoD1 generally coincide with those under LoD95, notably, both thresholds consistently indicate that the western (seaward) edge of Area 2 is the locus of virtually all significant activity. Under LoD1, the erosion along the dune margin often appears more continuous or widespread (and small accretion spots pop up here and there in the interior), whereas under LoD95 the erosion zone is distilled to its most severely affected segments and the interior accretion spots vanish. Importantly, neither threshold finds any large accretion dominated area in Area 2 for any interval. Both methods agree that accretion was either minor or absent, the difference is that LoD1 marks a few scattered, very slight accretion patches (e.g. isolated points of slight sand accumulation or measurement noise), while LoD95 effectively shows no accretion at all, implying those patches were below the reliability threshold. In qualitative terms, LoD95 confirms the reality of the changes flagged by LoD1 but filters out the less significant ones. For instance, what appears under LoD1 as a diffuse erosion along the dune toe in 2022-2023 is largely dismissed by LoD95, meaning that the dune likely underwent minor adjustments that year rather than any profound erosion. By contrast, where LoD1 and LoD95 both show change, such as the erosion along the dune face in 2021-2022 and again in 2023-2024, we can be very confident that those are true, meaningful geomorphic changes.

It is also evident that certain broad patterns seen with the lenient threshold are much less pronounced or absent under LoD95. For example, LoD1 indicated a gradually increasing area of change each year (from ~10% up to ~15% annually), suggesting that even subtle adjustments were accumulating over time across a broader area of the dune. However, the LoD95 results reveal that most of that "background" adjustment never exceeded the noise level, only the core erosion zone truly changed. Likewise, under LoD1 one might interpret that a

considerable portion of Area 2's dune system was experiencing low-level dynamics (since a third of the area showed some change by 2024), but the LoD95 analysis refines this view to a more conservative narrative, only the foredune strip underwent significant change, while the rest remained effectively stable. This comparison underscores the importance of threshold selection. In the case of Area 2, both approaches ultimately tell a consistent story of dune erosion without compensating accretion, but LoD95 lends much greater confidence to the areas it flags (at the expense of overlooking minor changes), whereas LoD1 ensures that no possible change goes unmarked (at the expense of including many very small changes of questionable significance). In summary, the threshold comparison for Area 2 reveals that although LoD1 maps a broader extent of erosion, the critical erosion zones are corroborated by LoD95, and no contradictory patterns appear, both thresholds reinforce that Area 2 experienced persistent coastal erosion with minimal genuine accretion during the study period.

4.3.4 Temporal Evolution Across 2021-2024

Examining the temporal evolution of elevation change in Area 2 over the four-time steps (2021-22, 2022-23, 2023-24, and the net 2021-24 change) reveals a pattern of sustained erosional pressure and cumulative dune loss. Unlike Area 1 (which initially experienced deposition and then erosion in a cyclical manner), Area 2 shows no such reversal of fortune, it underwent erosion in virtually every interval, indicating a persistently negative sediment balance. The 2021-2022 period appears to have been one of substantial change for Area 2, the results show noticeable erosion of the back dune (with some of the largest short-term elevation losses occurring in this interval), and only trivial deposition. This suggests that early in the study window, the area suffered significant dune erosion. Moving into 2022-2023, the magnitude of change in Area 2 dropped markedly. Both the LoD1 and LoD95 analyses depict 2022-2023 as a relatively quiet year geomorphically, few locations changed appreciably, and those that did were mostly small erosional nibbles at the dune edge. By 2023-2024, the erosion resumed again. The spatial maps for that interval show the largest erosion zone of any single year, indicating that the coastal dune underwent renewed and more extensive lowering in 2023-2024. This pattern suggests that the brief stability observed in the prior year gave way to a renewed phase of dune-front retreat by the final year of monitoring. Over the three-year span from 2021 to 2024, these year-to-year patterns culminated in a clear net outcome, Area 2's shoreline and foredune have receded and lowered, while the inland portions of Area 2 remained comparatively unchanged. The overlapping of change zones across intervals shows that many of the spots which eroded in 2021-2022 were the same areas to erode further (or remain in an eroded state) by 2023-2024. This spatial persistence points to an ongoing retreat of the dune edge rather than erosion popping up in entirely new locations. There is little evidence in the results of any compensatory accretion elsewhere that might indicate sediment redistribution within Area 2, in other words, the sand that was lost from the dune front was not redeposited in the backdune or other parts of Area 2.

In terms of elevation change magnitudes, the range observed in Area 2 over 2021-2024 is moderate but meaningful. The most extreme changes are found in the erosion hotspots along the dune face. Here, elevation losses on the order of a meter (tens of centimeters to over a meter in some cells) were recorded, exemplifying dune scarping or sand removal at the toe.

These extreme values were relatively rare and highly localized, they represent the maximum incision of the dune. On the accretion side, Area 2 did not experience any comparably large build-ups; the largest positive elevation changes were much smaller, typically only a few tens of centimeters at most (and those were so limited in area that many did not meet the LoD95 significance test). The vast majority of elevation differences across Area 2 fell within a gentle band of a few centimeters up to about 20-30 cm, either as slight erosion or slight accretion. Changes of this low magnitude covered broad swaths of the maps (especially under LoD1), reflecting minor surface adjustments such as shallow sand redistribution or small erosional scouring that are within normal variability. These subtle changes dominate the histograms and account for most of the "changed" area under the lenient threshold, while only the larger changes stand out under the strict threshold. Overall, from 2021 to 2024 Area 2 underwent a net geomorphic degradation concentrated at the dune front, each year contributed incrementally to cutting back the dune. Meanwhile, the interior parts of Area 2 show a pattern of stability, with little to no net elevation change over the three-year period. In summary, the temporal analysis for Area 2 confirms a scenario of progressive coastal erosion without recovery followed by further erosion, resulting in a significant cumulative loss of dune volume and position. Any short-term gains or within-error fluctuations were too small and transient to counter this trend. The outcome by the end of 2024 is a net erosional landscape change for Area 2, setting it apart as an area experiencing ongoing sediment deficit and shoreline retreat over the study period.

4.4 Elevation Change Detection Area 3

Elevation change in Area 3 was assessed by comparing annual DEMs across three one-year periods (2021-2022, 2022-2023, and 2023-2024), as well as over the full span from 2021 to 2024. To maintain methodological consistency, the same classification procedure and level-of-detection (LoD) thresholds applied to the other study areas were used here to distinguish significant elevation change from survey noise.

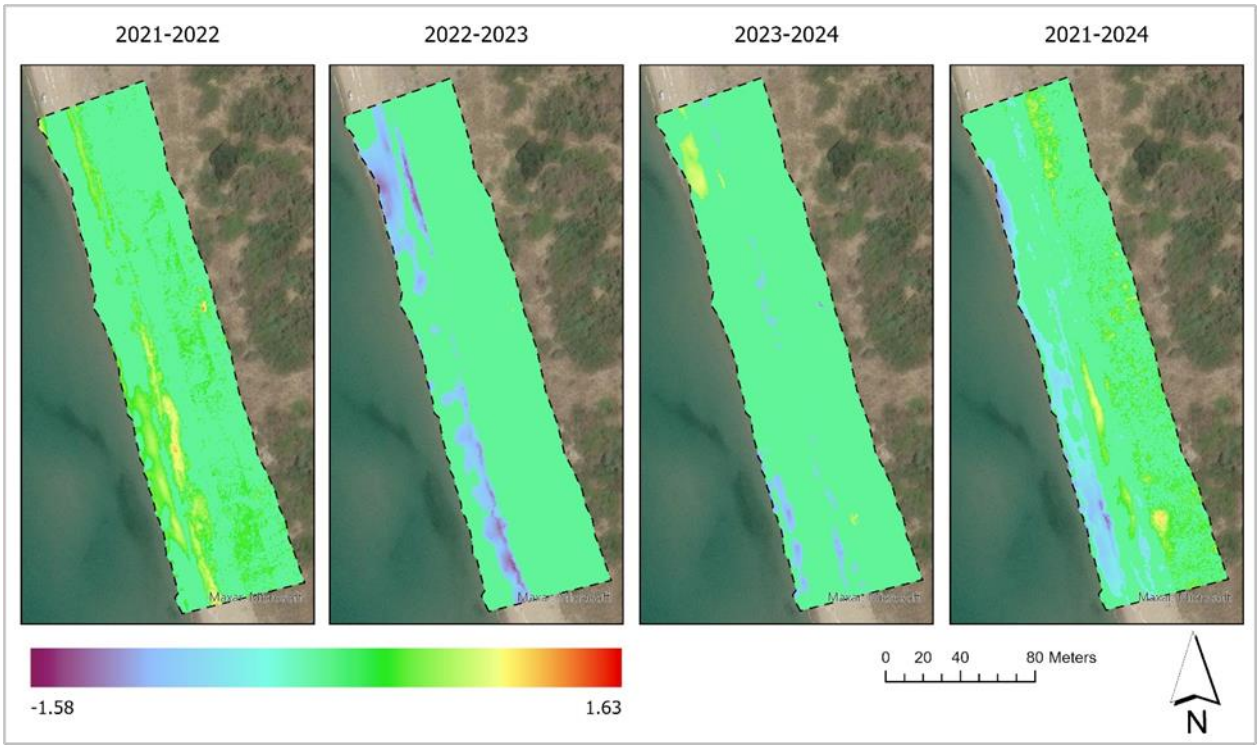


Figure 16 Area 3 DoD at LoD 1

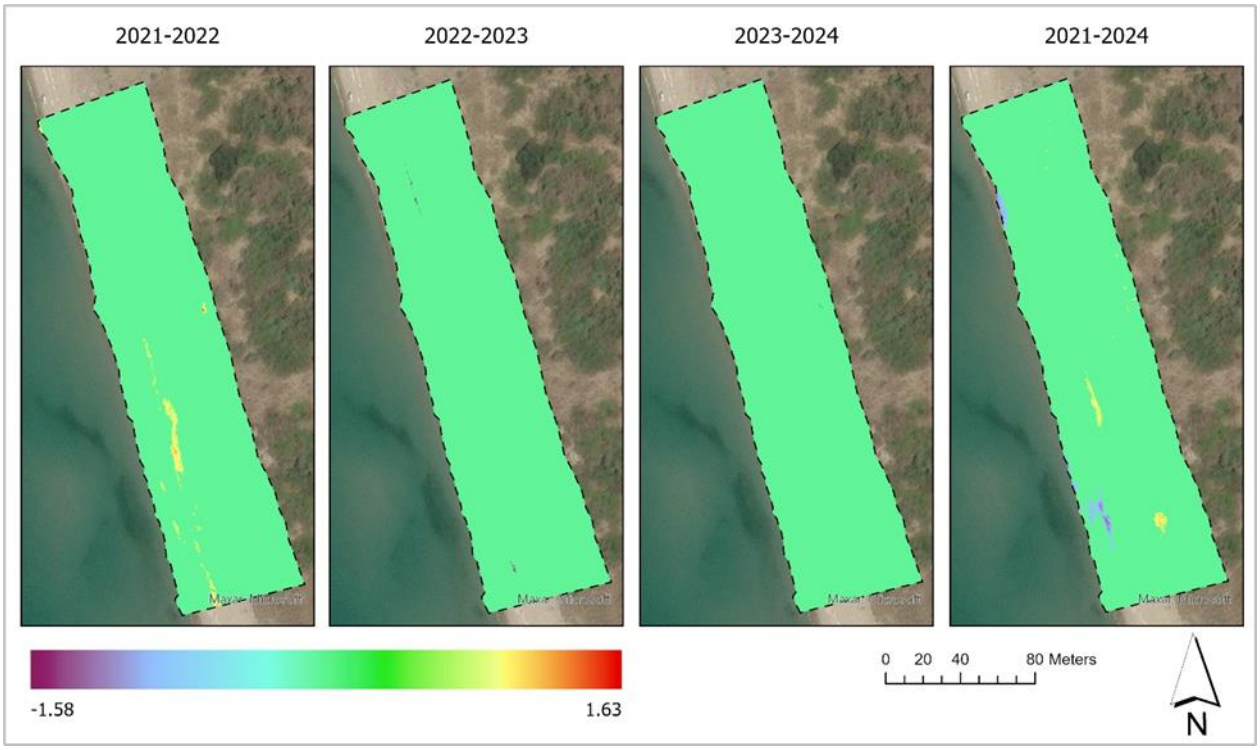


Figure 17 Area 3 DoD at LoD 95

4.4.1 LoD1 Threshold: Spatial Change Patterns and Extent

Using the minimum detection threshold (LoD1), the elevation changes maps for Area 3 reveal more extensive changes in certain intervals relative to the area's total size. For the 2021-2022 interval, the LoD1 classified map shows that while much of Area 3 remained stable, a notable portion experienced elevation gain. In Figure 18 (2021-2022 panel), a distinct blue patch is evident, indicating an accretion "hotspot" where significant sediment deposition occurred. Red patches (erosion) are virtually absent in this period, only an extremely small speck of red is visible, implying that surface lowering was negligible in extent. This suggests that during 2021-2022, Area 3 underwent pronounced sediment accumulation (dune or beach build-up) in one zone, with no corresponding erosion of significance elsewhere. The volumetric summary confirms that erosion in Area 3 during 2021-2022 was minimal, with only about 2 m^3 of material lost, while accretion reached over 2100 m^3. It indicates that nearly all measurable elevation change in this interval was due to sediment accumulation rather than loss (Table 11). In other words, a quarter of Area 3's surface saw detectable elevation gains that year, highlighting a strong positive sediment budget for that interval (Annex 11).

In the 2022-2023 interval, the spatial pattern of elevation changes shifts toward erosion. The corresponding panel in Figure 18 is dominated by gray (no detectable change), except for a prominent red zone. Notably, accretion (blue) is extremely scarce in 2022-2023, virtually no blue patches appear on the map aside from perhaps a couple of tiny isolated specks. This means that almost no appreciable deposition occurred to offset the erosion in that year. In volumetric terms, erosion clearly dominates the change in Area 3, with more than 2120 m^3 of material removed, while accretion is nearly negligible at less than 2 m^3. Overall, the sediment balance indicates an almost entirely erosional response during this interval (Table 11).

For 2023-2024, the LoD1 results show the least amount of change of all the single-year intervals. As seen in Figure 18 (2023-2024 panel), the map is dominated by the gray no-change category, with only very limited colored areas indicative of change. A small patch of red is visible, denoting a localized erosion spot, and similarly a small patch of blue appears, denoting a localized accretion spot. The changes are few and spatially confined, suggesting that 2023-2024 was a relatively quiet year geomorphically for Area 3. The near-absence of widespread color on the map means that the vast majority of the area remained within the LoD1 noise threshold. According to Table 11, the total volumetric change in Area 3 during 2023-2024 was modest. Erosion accounted for approximately 482 m^3 of material loss, while accretion contributed around 239 m^3. These opposing volumes nearly balanced each other, indicating that surface change during this year were relatively limited in scale.

Over the full 2021-2024 period, the LoD1 analysis indicates a moderate cumulative impact, characterized by both erosion and accretion zones within Area 3. In Figure 18 (2021-2024 panel), significant net changes are evident in two contrasting forms, a swath of blue denoting net accretion in part of Area 3, and a neighboring swath of red indicating net erosion in another part. This pattern suggests that across the three-year span, some sections of Area 3 experienced a lasting gain in elevation while other sections underwent a net lowering. The continuous blue patches imply that notable deposition occurred and persisted in those locations over the study period. Meanwhile, the red patches illustrate that considerable erosion took place elsewhere, resulting in a net loss of elevation in those areas from 2021 to

2024. Over the full 2021–2024 period, the volumetric balance in Area 3 was nearly neutral. As shown in Table 11, accretion totaled approximately 1266 m^3 ,slightly exceeding the 1224 m^3 of erosion. This minimal net change of just 41 m^3, indicating that the cumulative elevation changes largely offset one another over the three-year span.

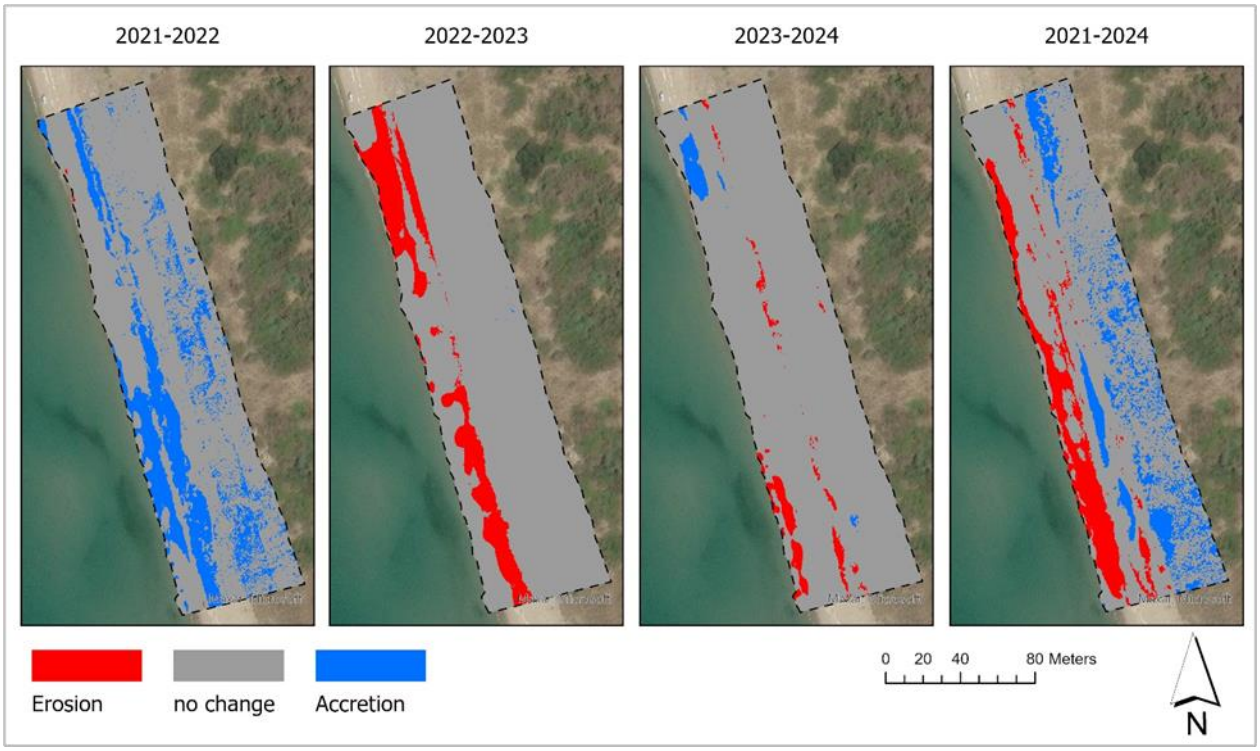


Figure 18 Classified Elevation Change Map of Area 3 at LoD1

A3	Erosion Vol.	Accretion Vol.	Net Vol.
	m^3	m^3	m^3
2021-2022	2.31	2102.96	2100.64
2022-2023	2122.03	1.84	-2120.19
2023-2024	482.37	239.23	-243.14
2021-2024	1224.18	1265.67	41.49

Table 11 Elevation Change Summary of Area 3 at LoD1

The magnitude and distribution of elevation changes in Area 3 were further examined using LoD1 threshold-based frequency histograms (Figure 19). This analysis provides a quantitative view of how much surface change occurred and how it is distributed across different magnitude bins for each time interval and cumulatively. As shown by the combined histogram, a significant majority of point elevations cluster within the narrow interval around 0 m (specifically, in the -0.2 m to 0 m bin), indicating a prevalence of very low-magnitude surface changes that lie just at or below the detection threshold. This strong central peak

reflects that over broad extents of Area 3, only negligible elevation differences were recorded, essentially reinforcing that most of the area was stable or undergoing micro-variations.

The 2021-2022 distribution is notably skewed toward the positive domain. In this year, high concentration of points lies between 0.2 to 0.8 m bins, signifying elevation gain. In contrast, changes of negative magnitude are effectively absent in 2021-2022's distribution. The 2022-2023 interval shows the opposite tendency, its histogram is skewed toward the negative side. A concentration of points occurs in moderately negative elevation change bins (for example, -1.2 m to -0.6 m range), reflecting the dominance of erosion during that year. The distribution for 2022-2023 is tighter around zero than 2021-2022 but with a noticeable tail extending into negative values. Meanwhile, the positive side of the 2022-2023 histogram is essentially flat, virtually no points registered significant positive changes.

The 2023-2024 histogram is comparatively narrow and sharply peaked at zero. This indicates that elevation changes during this year were very minor overall. There is only a very slight extension of the distribution into either tail, signifying that only a few points experienced small erosion or accretion. In essence, the 2023-2024 frequency curve confirms a year of relative geomorphic inactivity, with the vast bulk of observations clustered in the no-change bin and only trivial frequencies in the change bins.

Considering the cumulative 2021-2024 data, the overall distribution incorporates the effects of all three years and thus displays tails in both directions. The multi-year histogram reveals an extended negative tail as well as a positive tail, encapsulating Area 3's combined erosional and accretional changes. On the negative side, one can observe a population of points reaching into deeper erosion classes (for instance, bins -1.0m to -0.4m). These represent the points that experienced the greatest net lowering over the study period, predominantly due to the erosional event of 2022-2023 (and possibly further minor lowering in 2023-2024). On the positive side, there are also bars extending into the higher positive classes (for example, +0.2 m to +0.8 m, and beyond), corresponding to the substantial net elevation gains from the depositional event in 2021-2022. The presence of both tails in the cumulative distribution underscores that Area 3's topographic evolution under LoD1 involved significant contributions from both deposition and erosion at different times. Nonetheless, it should be noted that the tallest bars for the cumulative data are still near zero, reflecting that despite these notable events, large portions of Area 3 saw minimal net change. In summary, the LoD1 histograms portray a bimodal tendency in Area 3's changes, one interval contributed a surge of positive changes, another contributed negative changes, and when summed up, the area exhibits a broad spread of changes on both sides of zero, all superimposed on a dominant background of stability.

A secondary histogram was generated excluding the -0.2 to 0 m bin to better emphasize the less frequent but more substantial elevation changes (Annex 5). In 2021-2022, a distinct positive tail appears in the 0.4 to 1 m range, highlighting the extent of accretion during that year. On the negative side, a cluster of values between -0.6 to -1.2 m is evident, primarily associated with erosion from 2022-2023. Overall, the histogram analysis (Figure 19) supports the interpretation that Area 3's surface change regime was largely dominated by near-threshold variability, with isolated but notable episodes of more significant geomorphic change.

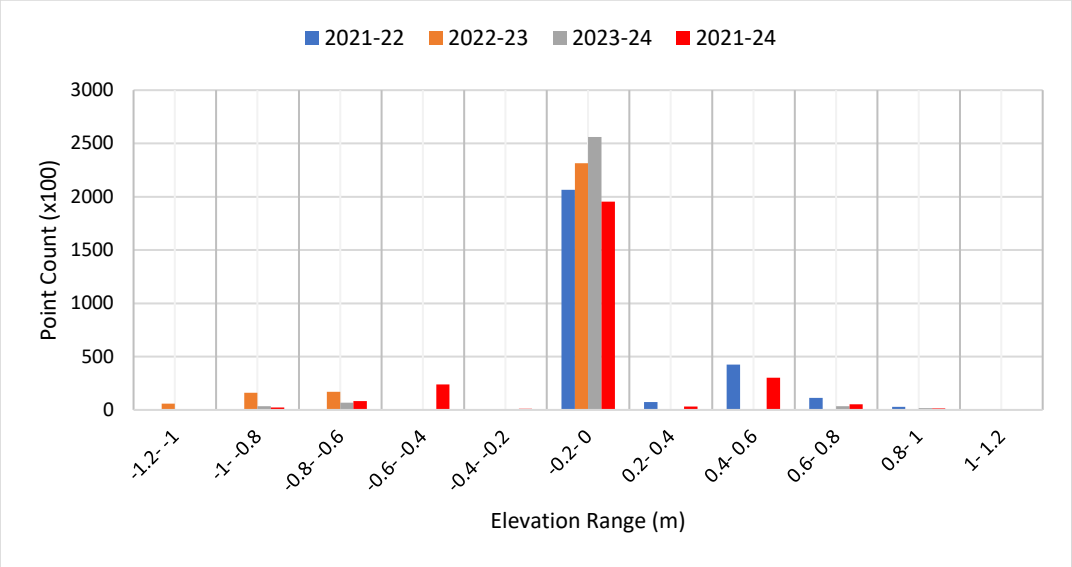


Figure 19 Significant Change Histogram of Area 3 with LoD1

4.4.2 LoD95 Threshold: Refined Detection and Statistical Confidence

Applying the stricter 95% confidence threshold (LoD95) yields a much more conservative picture of change in Area 3. Many of the small-magnitude changes that were flagged under LoD1 are filtered out when we require high statistical confidence, leaving only the most pronounced elevation differences. For 2021-2022, the LoD95-based map (Figure 20, 2021-2022 panel) still identifies accretion as the dominant process, but the spatial extent of detected change is greatly reduced compared to the LoD1 result. Instead of a broad blue patch covering the depositional area, LoD95 highlights only the core of the accretion zone, essentially few concentrated blue patches in the area where elevation gains were largest and most certain. The peripheral areas that showed light accretion or very slight erosion under LoD1 now mostly appear as gray (no change) under LoD95, indicating those changes did not exceed the stricter detection limit. In fact, virtually no red (erosion) is visible on the 2021-2022 LoD95 map at all, the tiny erosional speck noted by the LoD1 analysis does not register as significant at 95% confidence. The result is that the 2021-2022 LoD95 map shows only a small section of Area 3 with real change and classifies the rest of the area as unchanged. The volumetric summary for 2021-2022 confirms that all measurable change in Area 3 was due to accretion, amounting to over 250 m^3 of sediment gain, while no erosion was recorded during this interval (Table 12).

In 2022-2023, the LoD95 change map (Figure 20, 2022-2023 panel) indicates an extremely limited occurrence of statistically significant change. Virtually the entire map is gray, signifying that, at 95% confidence, Area 3 saw no widespread elevation shifts in this interval. The broad red zone of erosion highlighted along a feature in the LoD1 map is almost completely absent in the LoD95 version. Only a minuscule red speck can be discerned at the location of the most intense erosion indicating that only that very limited area had elevation losses large enough to be deemed real change at the 95% confidence level. No blue patches of

accretion appear on the 2022-2023 LoD95 map, which is consistent with the LoD1 result. Apart from this one tiny erosion highlight, 2022-2023 registers as entirely "no change".

The 2023-2024 interval under LoD95 shows a continuation of the minimal-change trend. The LoD95 map for 2023-2024 (Figure 20, 2023-2024 panel) is virtually blank in terms of detected change, it is dominated by the gray no-change category, just as in the previous year. In contrast to the LoD1 analysis which showed a couple of small patches of change. At most, one extremely small red patch can be identified, but its size is so small as to be almost negligible. No significant blue areas (accretion) are present at all. The 2023-2024 outcome indicates an exceptionally stable surface, with volumetric change limited to an extremely small portion of the area (Table 12).

Over the full period, the LoD95 analysis captures the cumulative effect of three years of change in a distilled form. In Figure 20 (2021-2024 panel), the inland portion appears uniformly gray, while a few small colored patches are visible along the seaward margin. The spatial extent of this confirmed change remains very limited relative to Area 3's size, the erosion patch covers only a tiny portion of the dune fringe. The volumetric analysis for the 2021-2024 LoD95 results shows that Area 3 experienced a total net change of approximately -62 m^3 (Table 12). Erosion accounted for the majority of this change around 181 m^3 of material loss, while accretion added only about 119 m^3. In conclusion, at high confidence Area 3's net three-year change was minor and predominantly erosional.

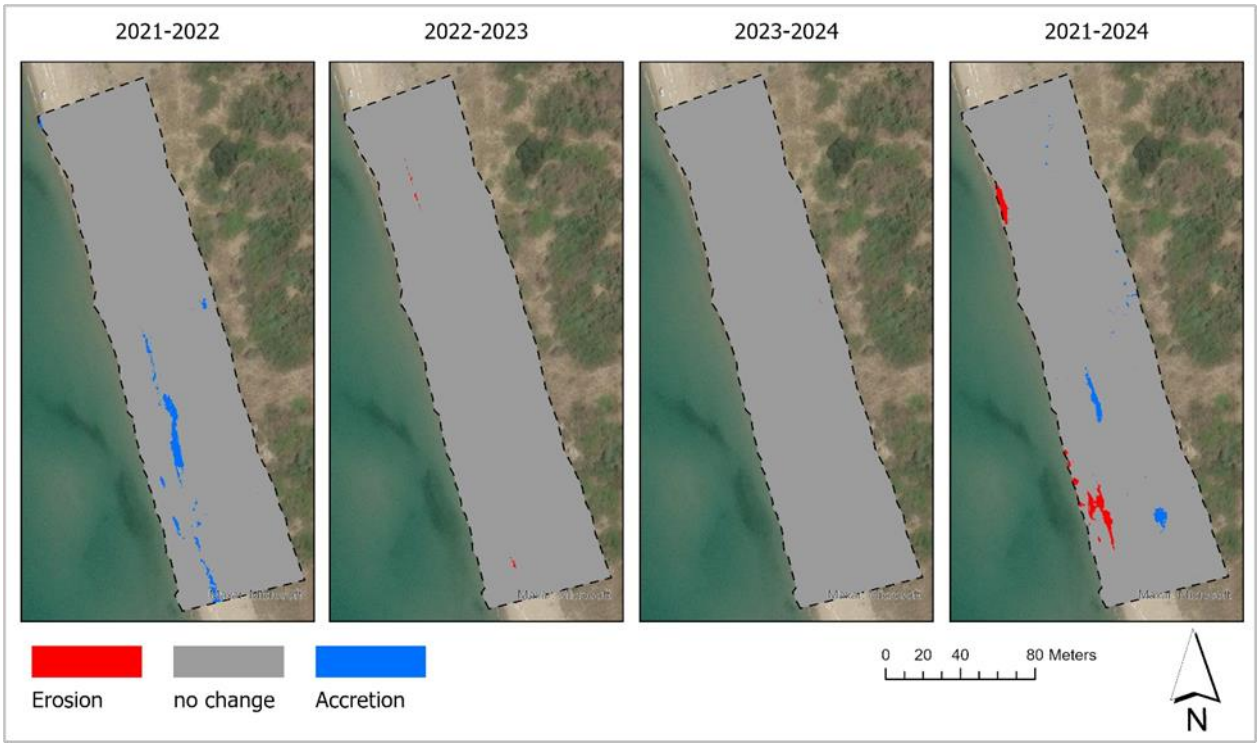


Figure 20 Classified Elevation Change Map of Area 2 at LoD95

A3	Erosion Vol.	Accretion Vol.	Net Vol.
	m3	m3	m3
2021-2022	0.00	256.35	256.35
2022-2023	12.62	0.00	-12.62
2023-2024	0.70	0.00	-0.70
2021-2024	181.35	119.09	-62.26

Table 12 Elevation Change Summary of Area 3 at LoD95

To evaluate elevation changes with high statistical confidence, frequency histograms were also generated using the LoD95 threshold, which excludes low-magnitude variations within the 95% confidence interval (Figure 21). As expected, the resulting distributions for Area 3 are sharply concentrated near zero, confirming that most apparent changes were not significant under this stricter criterion. Across all intervals, the vast majority of points fall within the tight range around 0 m (essentially within ±0.2 m, which represents the approximate LoD95 uncertainty band). This manifests as a very tall, narrow peak at the zero bin in each histogram, reflecting the dominance of "no real change" observations when applying the high-confidence filter.

In the 2021-2022 interval, the LoD95 histogram exhibits a modest extension into the positive domain. This corresponds to the small number of locations that showed true elevation gains beyond the noise level, essentially the core of the accretion zone identified in that year. Compared to the LoD1 histogram for 2021-2022, the distribution under LoD95 is notably compressed, the broad spread of positive changes seen with the lenient threshold has collapsed into a much tighter cluster, with only a tiny tail remaining on the positive side. The negative side of the 2021-2022 LoD95 histogram, by contrast, is almost completely flat; this indicates that none of the slight erosional changes detected under LoD1 were large enough to register as significant at the 95% level. In sum, the 2021-2022 high-confidence distribution confirms a small but real accretion signal and effectively no erosion signal.

During 2022-2023, the LoD95 histogram becomes highly concentrated around zero, with virtually no extension into either positive or negative values. This pattern confirms that the surface remained essentially stable in Area 3 when only changes exceeding the noise threshold are considered. Overall, the histogram indicates that geomorphic activity during this interval was negligible, consistent with the spatial maps. A similar pattern is observed for 2023-2024, where the LoD95 distribution again shows a narrow central peak and almost no deviation beyond the noise range. This reinforces the interpretation that nearly all points experienced no significant elevation change during the final year.

The cumulative 2021-2024 histogram (plotted in a separate color in Figure 21) displays a slightly more developed tail, particularly into the negative domain, compared to the single-year histograms. There is a small but noticeable count of points in the negative elevation change bins, for example in the -0.1 m to -0.6 m range. This tail corresponds to the points that underwent genuine multi-year erosion (as reflected by the red patch on the LoD95 map for 2021-2024). The presence of these frequencies, indicates that when considering the entire study period, a subset of locations in Area 3 experienced a real lowering of the surface on the

order of up to a meter. On the positive side, the cumulative distribution might show a tiny bump in the range of +0.6 m to +1.2 m (and perhaps a few points beyond), attributable to the area of sustained accretion through 2021-2024 (the blue patch). However, this positive tail is very limited, reflecting that the confirmed accretion area was small and the magnitudes of those gains were relatively modest. Overall, even the cumulative LoD95 histogram remains overwhelmingly concentrated at zero change, illustrating that the high-confidence changes in Area 3 were few and small in magnitude.

As with the LoD1 analysis, a secondary histogram was produced for LoD95 with the dominant near-zero class removed to enhance visibility of the tails (ANNEX 6). In this refined high-confidence histogram, the subtle tails become slightly more evident. The cumulative 2021-2024 curve reveals a faint concentration of points in the negative bins around -1.0 m, corresponding to the limited erosion that accumulated over three years. There is also a very minor indication of frequencies in the positive 0.6-1.0 m range, aligning with the net accretion area. These observations reinforce that, while Area 3 did experience some real change, those changes were confined to very small fractions of the area and were not extreme in magnitude. The interval-specific refined histograms underscore the same point, 2021-2022 and 2023-2024 show only tiny tails, and 2022-2023 shows virtually none at all. In effect, the LoD95 frequency analysis confirms that Area 3's significant elevation changes were not only spatially limited but also constituted low-level modifications in the context of the whole study site.

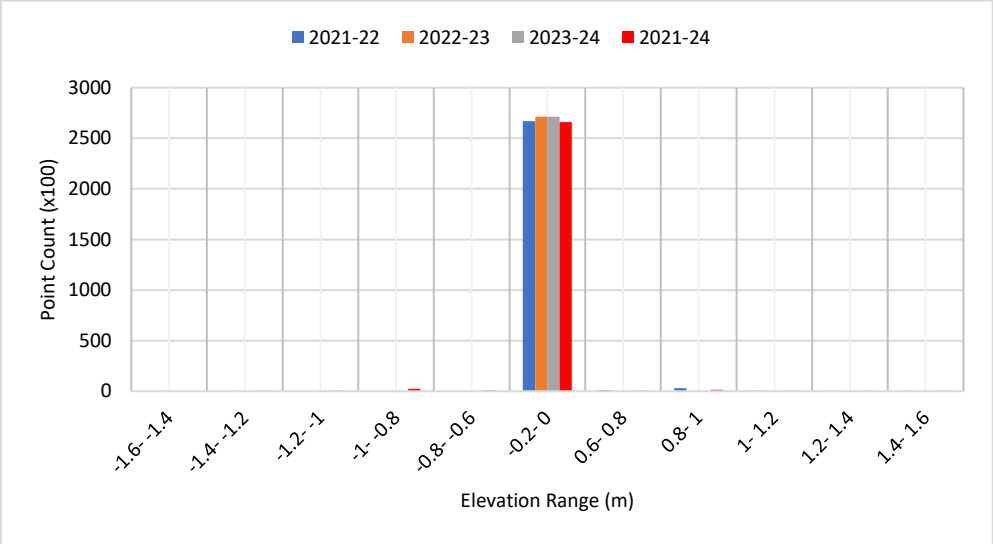


Figure 21 Significant Change Histogram of Area 3 with LoD95

4.4.3 Comparative Insights Between Thresholds

A side-by-side comparison of the LoD1 and LoD95 results for Area 3 highlights the influence of the detection threshold on the apparent magnitude and extent of change. In all time intervals, the total area classified as "changed" (either erosion or accretion) is dramatically larger under LoD1 than under LoD95. For example, in the 2021-2022 interval, approximately 24% of Area 3 was flagged as changed using the lenient LoD1 threshold, whereas only about 1.7% of the area was identified as changed under the stringent LoD95 criterion (Annex 11 vs.

Annex 12). In other words, LoD1 reported roughly fourteen times more area experiencing elevation adjustments than LoD95 did for that year. The contrast is even more extreme for 2022-2023, LoD1 indicated roughly 15% of the area had some change, while LoD95 found only ~0.06% of the area with significant change, a difference by over two orders of magnitude in spatial extent. Similarly, in 2023-2024, LoD1 marked about 5.6% of Area 3 as having detectable change, whereas LoD95 essentially identified 0% (only a vanishingly small fraction) as truly changed. Even over the full 2021-2024 period, LoD1 suggests about 28% of the area saw elevation change, whereas LoD95 confirms only around 2% of the area with high-confidence change. These comparisons demonstrate that the lower LoD1 threshold tends to greatly over-estimate the spatial extent of change by including many small or marginal elevation differences that a stricter analysis deems insignificant. In effect, LoD1 provides an upper-bound, highly sensitive view of where any possible change might have occurred, while LoD95 provides a much more conservative view limited to changes that are well above the noise and thus highly reliable.

Importantly, both LoD1 and LoD95 analyses identify the major accretion event of 2021-2022, though with different emphasis, under LoD1 it appears as a broad extensive zone of elevation gain, whereas under LoD95 it is distilled to its most pronounced core. Likewise, both thresholds recognize that an erosional process affected Area 3 over the study period. LoD1 shows this as a widespread if somewhat diffuse erosion (especially in 2022-2023 and in the cumulative map), while LoD95 confirms that a portion of that erosion was real by highlighting a much smaller zone in the long-term map. Conversely, where LoD1 and LoD95 both show change, such as the heart of the accretion zone in 2021-2022 or the small erosion patch persisting by 2024, we can be very confident those represent true geomorphic alterations. It is also noteworthy that neither threshold finds any large accretion-dominated region beyond the initial 2021-2022 deposition, both methods agree that apart from that one significant deposition event, Area 3 did not experience widespread sediment gains. This comparison underscores the importance of threshold selection, in the case of Area 3, the lenient LoD1 threshold ensured that no possible change went undetected (at the cost of including many very small changes of questionable significance), whereas the stringent LoD95 threshold ensured that any change shown is highly credible (at the cost of overlooking subtle changes). Ultimately, both approaches lead to a generally consistent interpretation for Area 3, they reinforce that a substantial deposition occurred followed by erosion with little net change overall, but they differ in whether the numerous small interim adjustments are emphasized (LoD1) or deemphasized (LoD95).

4.4.4 Temporal Evolution Across 2021-2024

Examining the temporal evolution of elevation change in Area 3 across the four intervals (the three annual steps and the cumulative change) reveals a pattern of alternating phases and an overall near-equilibrium outcome. Area 3 did not exhibit a consistent unidirectional trend (such as continuous erosion or continuous accretion year after year), Instead, it underwent distinctly different conditions in successive periods. The 2021-2022 period was one of substantial positive change for Area 3, the results show a pronounced accretion of the surface in one region, suggesting a significant influx of sediment or sand accumulation during that

time. This might reflect an episode of dune growth or beach progradation, potentially due to favorable environmental conditions (e.g. mild wave climate or abundant sand supply) in that year. In stark contrast, the 2022-2023 period brought a reversal, Area 3 experienced notable erosion focused in roughly the same general area, indicating that a considerable portion of the sediment gained previously was removed. The magnitude of the 2022-2023 losses, while large, was slightly less extensive than the preceding gains, implying that the erosion eroded much, but not necessarily all, of the accumulated sediment from the year before. By 2023-2024, the magnitude of change dropped off dramatically. Both the LoD1 and LoD95 analyses characterize 2023-2024 as a relatively quiet year geomorphologically, with very few significant changes occurring.

Over the entire 2021-2024 span, these year-to-year patterns culminated in a significant net outcome, Area 3 ended up in a roughly balanced state in terms of sediment budget and topography. The overlapping of change zones across the intervals provides insight into how these processes played out spatially. It appears that the area which gained sediment in 2021-2022 is largely the same area (or part of it) that lost sediment in 2022-2023. This spatial coincidence means that much of the sand that was deposited during the first year was subsequently eroded away in the second year. There is little indication from the maps or data that the eroded sand from 2022-2023 was simply redeposited elsewhere within Area 3, no other large blue patches emerge concurrently with the red patch of erosion that year. Thus, it is likely that the material removed in 2022-2023 was transported out of Area 3 (for example, carried further down the coast or offshore) rather than just shifted to a different location inside Area 3. The minor accretion observed in 2023-2024 was highly localized and does not appear to reflect a re-deposition of previously eroded material. Instead, it may represent new sand deposited in a sheltered zone or the early stages of dune recovery. In effect, sediment gained in one year was largely lost the next, with no significant compensatory buildup elsewhere in Area 3. This pattern points to an exchange with the broader coastal system, suggesting that sediment entered and exited the area rather than being redistributed internally.

In terms of elevation change magnitudes, the range of changes observed in Area 3 from 2021 to 2024 was moderate. The most extreme changes were associated with the localized hotspots of deposition and erosion. In the main accretion zone (2021-2022), elevation increases on the order of up to about a meter were recorded, a substantial rise indicating dune or beach buildup. On the erosional side, the most severe losses (primarily in 2022-2023) were of a similar order of magnitude in the opposite direction, on the order of tens of centimeters up to nearly a meter of lowering in the most affected. Under the stricter LoD95 threshold, most of those low-magnitude changes are screened out, highlighting that only the larger changes (which were still moderate in absolute terms) stand out as significant. In summary, while Area 3 did experience meaningful geomorphic changes, the intensity of those changes was moderate and nowhere near catastrophic levels, the landscape adjustments were significant enough to measure but not extreme.

By the end of 2024, the net effect of these alternating changes is that Area 3's topography was not dramatically different from its starting condition in 2021. The portions of Area 3 that initially gained a large amount of sand had, for the most part, lost it again, and no new areas had risen or fallen substantially beyond those transient hotspots. In practical terms, the frontal

zone of Area 3 (for instance, beach face) did not experience a lasting seaward progradation or landward retreat, instead, it saw a temporary advance (due to accretion) followed by a retreat back toward its original position (due to erosion). The interior parts of Area 3 (landward of the main active zone) showed a pattern of stability throughout the study period, with little to no net elevation change, indicating that the erosional and depositional activities were tightly focused and did not propagate far inland. In summary, the temporal analysis portrays Area 3 as a system that experienced a significant but short-lived accumulation of sediment, an almost equal removal of sediment, and then a period of relative calm, effectively resulting in a balanced outcome over the three years. Any short-term gains were largely offset by subsequent losses, leaving Area 3 by 2024 in a state that could be described as dynamic equilibrium. The area did not suffer a permanent deficit of sediment nor a permanent surplus, rather, it oscillated around an equilibrium state, demonstrating resilience in maintaining its overall form despite the temporary fluctuations.

4.5 Vegetation Change Detection Area 1

Area 1's vegetation cover was analyzed over the period 2021-2023 using the Visible Atmospherically Resistant Index (VARI) derived from the orthophotos. The results are presented through greenness intensity maps, binary vegetation classification, change detection maps for consecutive intervals, and a quantitative summary of gains and losses. All observations are based on the spatial patterns seen in the VARI outputs and the classified vegetation maps. The following sub-sections detail the greenness distribution, vegetation classification results, vegetation change mapping, quantitative change summary, threshold-based interpretation, and an overall summary of vegetation changes in Area 1.

4.5.1 Greenness Distribution (VARI)

The greenness intensity raster for Area 1, represented by the VARI values, shows distinct spatial patterns of vegetation vigor across the dune landscape. Higher VARI values (depicted as brighter or more intense green tones) are concentrated in well-vegetated portions of the area, while lower values mark as bare-sand zones. In general, the dune crest and landward areas exhibit the highest greenness, indicating dense or healthy vegetation cover a top and behind the dune. In contrast, the seaward (western) fringe of Area 1, including the beach and foredune toe, registers low VARI values consistent with little to no vegetation. This gradient suggests a transition from lush vegetation on the inland side of the dune to barren or sparsely covered sand toward the shoreline.

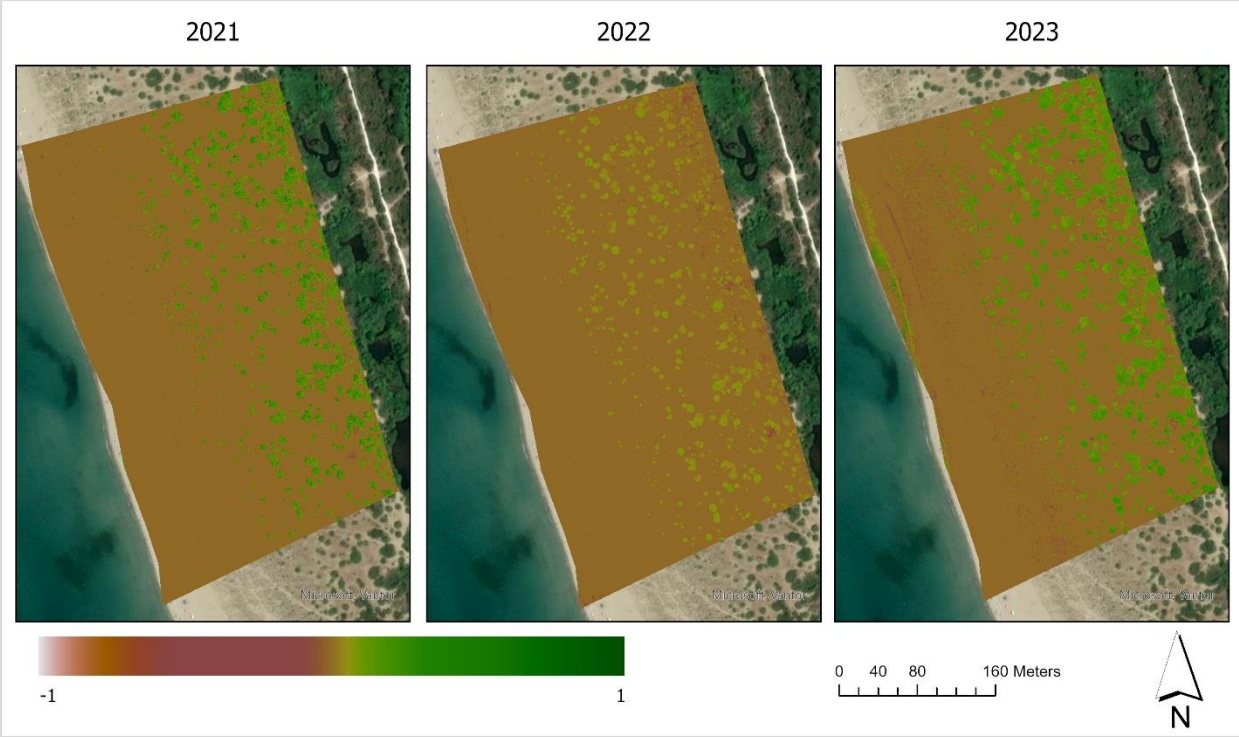


Figure 22 VARI raster layer - greenness intensity distribution in Area 1

Note: VARI > 0 denotes vegetated (greener) surfaces, while VARI ≤ 0 indicates non-vegetated/low-greenness areas.

Comparing the VARI-based greenness maps across the available years reveals only subtle overall changes in vegetation intensity. The spatial pattern of high and low VARI zones remains broadly similar from 2021 to 2023, implying that the core vegetated areas maintained their greenness. Any year-to-year differences in the VARI maps are minor and localized. The key vegetation zones (dune ridge and protected shadow areas) continue to stand out with high VARI in each year, and the open beach consistently remains low. This consistency suggests that, at the landscape scale, Area 1's vegetation greenness intensity did not undergo a dramatic shift over the study period, even if localized pockets show minor fluctuations year to year.

4.5.2 Vegetation Classification Results

The binary vegetation classification map of Area 1 delineates vegetated versus non-vegetated surfaces clearly, highlighting the extent of plant cover within the dune system. In the classification output, vegetated areas appear as a continuous spread over much of the dune's interior and crest, whereas non-vegetated areas correspond to exposed sand on the beach, dune face, and any sparse patches within the study area. The classified map indicates that a substantial portion of Area 1 is covered by vegetation, the dune crest and landward regions are almost entirely classified as vegetated, forming an unbroken belt of plant cover. On the other hand, the seaward margin of the dune, adjacent to the beach, is predominantly classified as non-vegetated, reflecting the presence of bare sand or very sparse pioneer vegetation at the foredune toe. A sharp delineation is visible between the vegetated dune slope and the open

beach, with the boundary roughly corresponding to the dune foot. Within the vegetated zone, coverage appears dense and continuous, with only minimal gaps. Overall, the classification confirms that Area 1's dune is largely vegetated except for the frontal strip along the ocean-facing side, which remains largely bare.



Figure 23 Vegetation vs. non-vegetation classification map, Area 1

4.5.3 Vegetation Change Mapping

Multi-temporal vegetation change maps were generated to visualize where plant cover was gained or lost between successive years. Figure 24 presents the vegetation change detection results for Area 1, with panel (2021-2022) showing changes from 2021 to 2022, panel (2022-2023) from 2022 to 2023, and panel (2021-2023) the net change from 2021 to 2023. In these maps, green areas denote vegetation gain (new vegetation appearing where none was before), red areas denote vegetation loss (previously vegetated areas becoming bare), and gray areas indicate no change in vegetation status. Each sub-panel highlights the spatial distribution of these categories for the corresponding interval.

In 2021-2022 (Figure 24, 2021-2022), the vegetation change map is dominated by gains rather than losses. Green areas occur across several portions of Area 1, pointing to an overall expansion of vegetated cover. The clearest clusters appear along the seaward side of the dune, where stretches that were bare in 2021 are mapped as vegetated in 2022. Smaller, scattered gain patches are also visible on the dune slopes and flatter interiors, consistent with local infilling or denser cover in zones that were previously sparse.

In 2022-2023 (Figure 24, 2022-2023), the pattern reverses, with vegetation losses exceeds gains. The map shows a continuous red band along the western (seaward) boundary of Area 1,

indicating that vegetation present in 2022 was absent by 2023 . Only a few small, scattered green patches are visible, and they remain minor compared with the extent of the red strip. Away from the shoreline, much of the interior stays gray, suggesting that vegetation cover in the backdune sector was largely stable over this interval.

For the whole duration (Figure 24, 2021-2023), the net vegetation change is limited across most of Area 1. Gray tones dominate the map, indicating that the majority of the surface retained the same vegetation status at the beginning and end of the period. The green and red areas are relatively limited and mostly confined to the dune margins. Importantly, several gains observed in 2021-2022 were later reversed in 2022-2023, so they do not appear as net gains in the 2021-2023 map. Despite short-term fluctuations, Area 1's vegetative cover was broadly stable between 2021 and 2023.

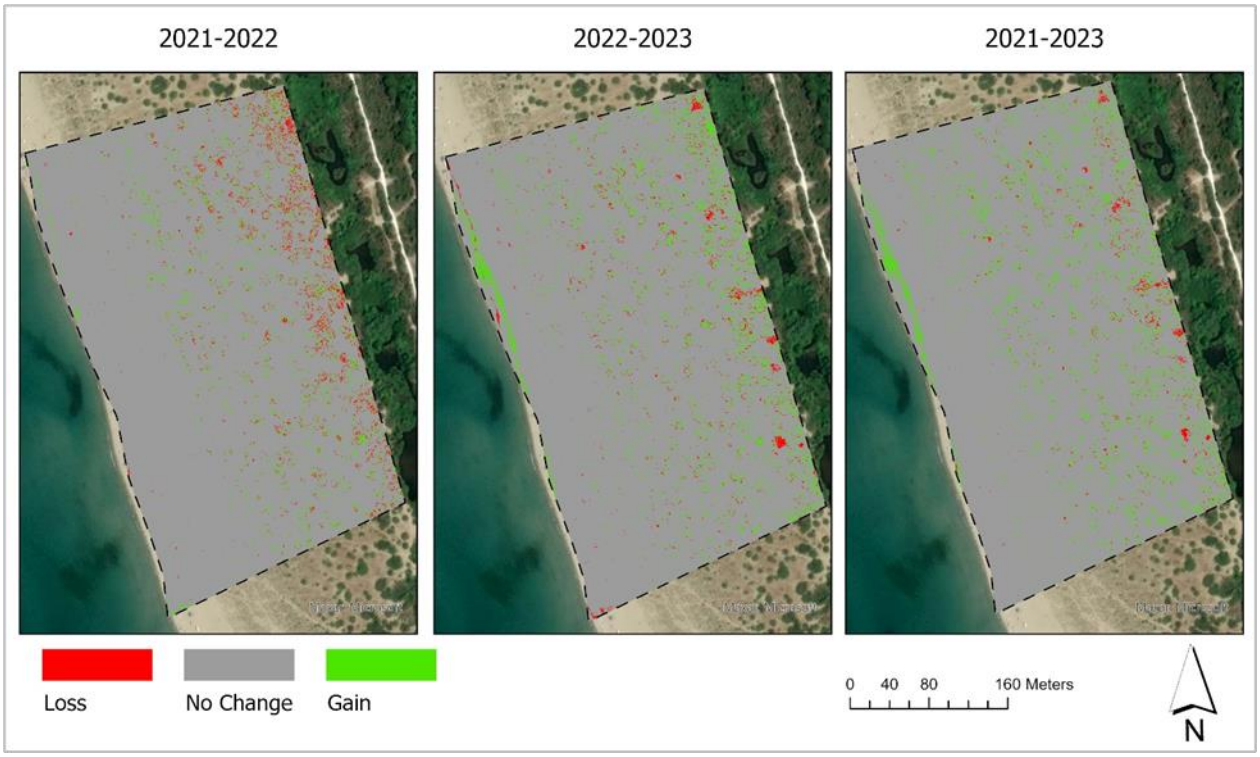


Figure 24 Vegetation change maps of Area 1

4.5.4 Quantitative Change Summary

The tabulated area statistics (Table 13) provide a quantitative breakdown of vegetation gain, loss, and stability in Area 1 for the two one-year intervals and the overall period. These figures confirm the spatial observations from the maps. In the 2021-2022 interval, Area 1 experienced a net increase in vegetated area. Approximately on the order of 3% of the study area showed vegetation gain in 2021-2022, whereas vegetation loss was around 2% of total area. The remainder of the area (roughly 95%) had no change in classification during that first year, meaning it stayed vegetated if it was initially vegetated or stayed bare if it was initially bare. Thus, the quantitative data for 2021-2022 point to a clear positive balance of vegetation change

(significantly more gain than loss), aligning with the visual impression of widespread green patches and scarce red patches in the map for that interval.
In the 2022-2023 interval, Area 1 continued to show a net gain in vegetation cover. Vegetation gain accounted for approximately 5% of the total area, while vegetation loss affected around 1% of the surface. The remaining portion of the area, roughly 94%, maintained its previous vegetation classification without change. This suggests that most of the dune system remained stable, with only peripheral shifts in vegetation status
Over the entire 2021-2023 period, the vegetation dynamics in Area 1 reflected a modest but consistent increase in vegetated surfaces. Vegetation gain occurred across approximately 5% of the study area, while vegetation loss affected just about 1%. The large area remained unchanged in classification, indicating strong spatial stability over time. Above figures confirm that the dune system experienced limited fluctuations at its margins, with an overall tendency toward vegetation gain.

A1	Loss Area	No change Area	Gain Area	Area Changed	Status
	m2	m2	m2	%	-
2021-2022	2691.60	118120.59	3669.33	5.11	Gain
2022-2023	1812.66	116329.35	6339.52	6.55	Gain
2021-2023	1269.81	116437.30	6774.40	6.46	Gain

Table 13 Vegetation Change Summary, Area 1

Spatially, the most active zone of change was at the seaward edge of the dune, where vegetation encroached onto previously bare sand one year and then retreated the next. In contrast, the interior portions of Area 1 (the established vegetated dune fields and persistently unvegetated beach areas) exhibited high stability, with their status remaining constant throughout. The results indicate that while local shifts in the vegetation line occurred at the dune front, the overall extent of vegetated dune habitat in Area 1 did not undergo a progressive increase or decrease during the study period, it oscillated slightly but ultimately remained steady.

4.6 Vegetation Change Detection Area 2

Area 2 vegetation results are summarized here, using the annual VARI-based vegetation masks and the corresponding multi-temporal change maps. The section first describes the spatial distribution of gains and losses for each comparison interval, then reports the associated change totals (m² and % of Area 2). The final paragraph consolidates the interval-specific patterns into an overall view of vegetation dynamics across 2021-2024.

4.6.1 Greenness Distribution (VARI)

The spatial distribution of greenness in Area 2, as indicated by the VARI index, reveals clear patterns of vegetative presence and intensity for each year. Figure 25 illustrates the range from bare sand (low VARI values shown in brown tones) to dense vegetation (high VARI values in

green tones). In 2021, much of Area 2's dune surface is characterized by low VARI values (brown hues dominate), indicating predominantly sparse or no vegetation. Only a few localized patches show higher VARI (green areas), suggesting vegetation clustered in limited sections of the dune, typically around the landward edges and in small pockets on the dune interior. The seaward side of the area (the beach-facing foredune) in 2021 registers very low greenness. By 2022, the greenness intensity across Area 2 increases noticeably. The VARI map for 2022 shows an expansion of green-shaded areas, meaning vegetation became more widespread or healthier that year. Many regions that were previously bare in 2021 exhibit elevated VARI values in 2022. In particular, the central and landward parts of the dune display broader patches of moderate to high VARI (lush green tones), indicating a substantial increase in vegetative cover. The seaward fringe remains comparatively less green, but even there some slight uptick in VARI is visible as scattered vegetation may have colonized parts of the foredune. Overall, 2022 stands out as the peak greenness year, with a richer and more extensive vegetative signature across Area 2 than observed in 2021.

Between 2022 and 2023, the greenness distribution contracts again. The 2023 VARI map exhibits a reduction in green areas relative to 2022, with more of the dune surface reverting to lower VARI values (brown). Some zones that were green in 2022 fade to yellow-brown by 2023, signifying vegetation decline or loss in those parts. Notably, the foredune margin and some interior sections show diminished greenness, patches of high VARI shrink or disappear, and the overall impression is that vegetative robustness was less widespread. The 2024 greenness pattern is similar to, or slightly below, that of 2023. Figure 25 indicates that high VARI areas remain present in 2024 but are limited in extent. The most vegetated spots (green zones) are generally smaller or more fragmented compared to 2022, reflecting that some of the vegetation gain observed earlier has not been sustained. Many regions of the dune are mapped in brown and yellow tones in 2024, denoting bare sand or only sparse ground cover. Importantly, by 2024 the overall greenness of Area 2 appears lower than the initial 2021 condition, a reversal of the temporary greening seen in 2022.

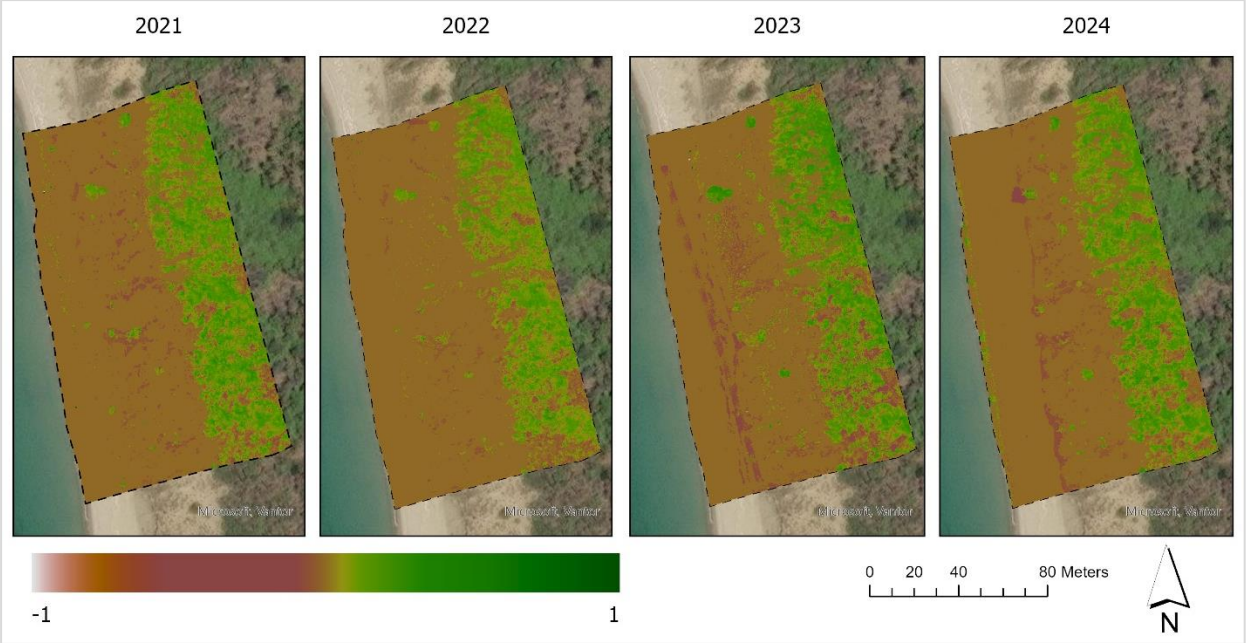


Figure 25 VARI raster layer - greenness intensity distribution in Area2

4.6.2 Vegetation Classification Results

The binary vegetation classification maps for Area 2 (vegetation vs. non-vegetation) further concretize the patterns observed in the VARI greenness index. Figure 26 (Vegetation/Non-vegetation classification for Area 2) shows the explanation of vegetated areas (in green) versus bare or non-vegetated areas (in gray) for each survey year. In 2021, vegetated patches are limited and mostly confined along the backdune (landward side) and a few isolated pockets on the dune slope and interior. The vast majority of the area is classified as bare sand in 2021, and vegetation covers only a small part of it. By 2022, there is a clear expansion in the extent of vegetation. The classification for 2022 displays a marked increase in green-covered area across Area 2. Many regions that were gray (bare) in 2021 turned green in 2022, reflecting successful vegetation establishment or growth within that year. The interior dune surface and sections near the landward boundary show contiguous stretches of vegetation that were not present the year before. Overall, vegetation cover in 2022 occupies a substantially larger portion of Area 2 compared to 2021. Despite this expansion, it is worth noting that even in 2022 a considerable portion of the area remains unvegetated (gray), particularly toward the seaward front, the foredune and beach-proximal zones continue to host sparse vegetation relative to the inland side. Nonetheless, 2022 represents the maximum vegetation extent in the record, with the dune surface at its greenest and most vegetated state.

After 2022, the pattern shifts, several areas that were mapped as vegetation in 2022 are classified as non-vegetated in 2023. This decline is most apparent across parts of the dune interior and along previously vegetated margins, where patches become more fragmented. Consequently, the total vegetated area in 2023 is less than 2022, though still higher than the initial 2021 baseline in some places. Most of the enduring vegetation in 2023 is concentrated

in previously established zones, while the more exposed sections show a rollback of green cover.

The 2024 classification continues the pattern of net vegetation loss. The extent of greenness on the 2024 map is further reduced compared to 2023, signifying additional vegetative retreat. The persistent vegetated zones by 2024 are mainly those core patches that have survived since earlier years (often toward the backdune or around stable clumps of dune vegetation), whereas many areas that briefly became vegetated in 2022 have reverted to bare sand. In sum, the yearly classification results for Area 2 depict a dynamic vegetation cover trajectory, an initial low coverage in 2021, a substantial increase to a peak in 2022, followed by successive declines in 2023 and 2024 that erased the temporary gains and resulted in an overall reduction of vegetated area by the end of the period.



Figure 26 Vegetation vs. non-vegetation classification map, Area 2

4.6.3 Vegetation Change Mapping

The multi-temporal vegetation change maps (Figure 27) provide a detailed visualization of where vegetation was lost (red) or gained (green) in Area 2 during each interval, with unchanged areas in gray. Each panel corresponds to a different comparison: 2021-2022, 2022-2023, 2023-2024, and the overall 2021-2024 change.

The 2021-2022 vegetation change map indicates that most of Area 2 remained stable, but it also contains many scattered green patches marking vegetation gains. These gains are particularly visible across the central and eastern parts of the dune, consistent with an expansion of vegetated cover in 2022. Vegetation losses are limited and occur only as a few small patches near the seaward margin and in parts of the interior. Overall, the pattern is a mixed mosaic, yet it supports a net increase in vegetation during this interval (Table 14).

In the 2022-2023 change map, the pattern notably shifts. Red areas (vegetation loss) dominate many parts of Area 2, reflecting the widespread disappearance of vegetation that had been established by 2022. A nearly continuous band of red is evident along the western seaward edge of Area 2, marking a broad strip where vegetation present in 2022 (especially along the foredune front) was lost by 2023. This indicates a retreat of vegetative cover from the dune face bordering the beach. Additionally, lot of red patches are scattered in interior and landward sections, signifying that many of the vegetated patches across the dune (even away from the edge) suffered losses during 2022-2023. Green patches (vegetation gains) are also present on the 2022-2023 map, but they are relatively few and generally small or scattered. Some green specks appear inland of the main loss zones, suggesting minor new vegetation growth in spots that were bare in 2022. The prevalence of red highlights that 2022-2023 was a period of significant vegetative loss across Area 2.

The 2023-2024 vegetation change map continues to show a loss-dominated pattern, although the contrast appears slightly less pronounced than in the previous interval. Red patches remain widespread, indicating that vegetation present in 2023 was absent by 2024 in several parts of Area 2. Many losses occur in broadly similar zones as before, including along the seaward dune front where more continuous red strips suggest further retreat of vegetation from the coastal margin. Additional red spots are also scattered within the dune interior, reflecting localized reductions. Green gain areas are present as well, but they are generally small and dispersed, often occurring near the margins of loss zones or slightly landward of them. Overall, most of the map remains gray (no change), and the interval still reflects a net vegetation loss, even if gains appear somewhat more frequent than in 2022-2023.

Overall the cumulative change map comparing 2021 to 2024 provides an integrated view of vegetation dynamics over the entire study period. This map is characterized by extensive red areas spread across much of Area 2, indicating where vegetation present in 2021 was no longer present in 2024. The red coloration is especially continuous and pronounced along the seaward (western) boundary of Area 2. Essentially the frontal dune and beach interface show pervasive red, signifying a broad loss of dune vegetation along the coastline from the beginning to the end of the period. Red patches also extend into the interior dunes, confirming that many interior vegetated patches that existed in 2021 were gone by 2024. In contrast, green areas on the 2021-2024 map (representing new vegetation in 2024 that was absent in 2021) are relatively limited. Some green clusters appear in the landward part of Area 2 and in a few interior spots, suggesting new vegetation growth occurred in those locations over the three years. However, these gains are modest both in size and number compared to the widespread losses. Large portions of the map are gray, which correspond to areas that saw no change in vegetation status or vegetation present in both areas. The dominance of red on the overall change map reinforces the finding that vegetation loss outweighed gain in Area 2 from 2021 to 2024. Essentially, the vegetation that was lost (particularly along the dune front and some interior sections) was not fully compensated by the new growth that occurred elsewhere. This aligns with the “Loss” status for the 2021-2024 interval in Table 14, indicating a net decline in vegetated area over the study period.

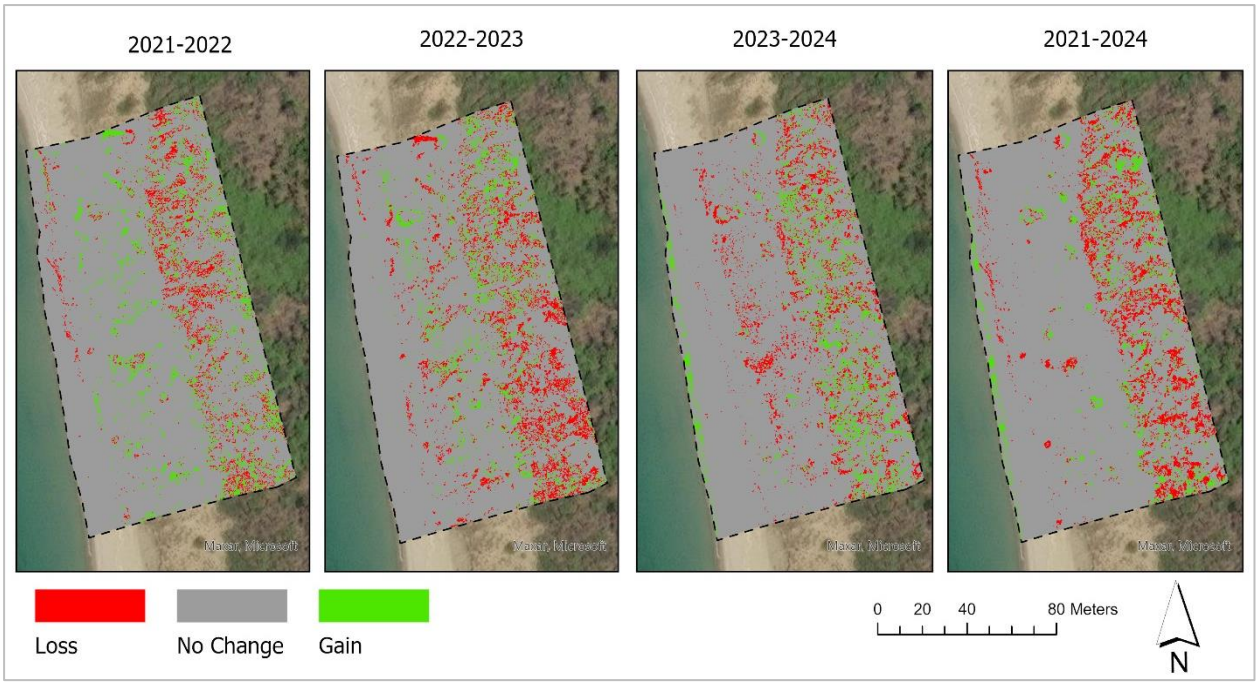


Figure 27 Vegetation change maps of Area 2

4.6.4 Quantitative Change Summary

The area and percentage of vegetation loss, gain, and stability for Area 2 were quantified for each interval, during 2021-2022, approximately 5-6% of Area 2 that was vegetated in 2021 became non-vegetated in 2022 (vegetation loss), while about 6-7% of previously bare sand turned vegetated (vegetation gain). Overall, about 11-12% of the area underwent a change (either loss or gain) in vegetation cover from 2021 to 2022, and the net positive balance is reflected by a "Gain" status for that year in the summary Table 14. This confirms that 2021-2022 saw a modest expansion of vegetation in Area 2, consistent with the maps showing greener than red.

In 2022-2023, the quantitative metrics indicate a net loss of vegetation. Roughly 14% of Area 2 shifted class in this interval (the highest among annual comparisons) driven mainly by losses. About 8-9% of the area transitioned from vegetated to non-vegetated, whereas only around 5-6% moved in the opposite direction. Most of the surface (approximately 85-87%) remained unchanged. Consistent with these proportions, Table 14 assigns a "Loss" status to 2022-2023, confirming an overall contraction of vegetated cover.

The 2023-2024 figures point to the same direction but with a smaller imbalance. Around 12% of Area 2 changed classification during this period, with losses still slightly higher (about 6-7%) than gains (about 5-6%). Roughly 88% of the area remained unchanged year-to-year. The summary for 2023-2024 is marked as a "Loss" scenario in Table 14, in agreement with the change map showing more red than green. While the net decline in this period was less pronounced than in 2022-2023, it nonetheless contributed to the cumulative reduction in vegetation cover.

Considering the entire 2021-2024 period, the aggregated changes reveal a net decrease in vegetation. Over the three-year span, Area 2 saw an 8% of the total vegetation lost (i.e.,

present in 2021 but absent in 2024), versus 4-5% gained (bare in 2021 becoming vegetated by 2024). The net change is a loss of about 541 m² of vegetated area across Area 2 when comparing the endpoints. In total, about 12.69% of Area 2 changed classification at some point between 2021 and 2024 (meaning nearly an eighth of the area transitioned either from vegetated to bare or vice versa). The remaining 87-88% of the area retained its initial state (either continuously vegetated or continuously non-vegetated). The overall balance is clearly negative, and Table 14 labels the 2021-2024 change for Area 2 as a "Loss" scenario. This quantitative summary reinforces the earlier observations, although there were gains in vegetation in certain years and locations, the losses, particularly from 2022 onward, were larger in aggregate, resulting in a net decline in vegetative cover over the study period.

A2	Loss Area	No change Area	Gain Area	Area Changed	Status
	m2	m2	m2	%	-
2021-2022	811.81	13408.18	962.12	11.68	Gain
2022-2023	1318.98	13056.60	806.53	14.00	Loss
2023-2024	1007.12	13347.01	827.98	12.09	Loss
2021-2024	1233.88	13255.63	692.59	12.69	Loss

Table 14 Vegetation Change Summary, Area 2

In summary, Area 2's vegetation exhibited dynamic changes over the 2021-2024 interval, with an initial increase in coverage followed by substantial decline. The greenness (VARI) maps demonstrated a notable greening of the dune in 2022 relative to 2021, highlighting a short-term expansion of vegetation. This was validated by the classification results, which showed that vegetated area in 2022 was considerably greater than the previous year. However, the subsequent maps and change analyses revealed that this gain was not sustained, both 2023 and 2024 saw widespread vegetation loss across the area, erasing the earlier gains. The change detection maps clearly illustrated how the dune's vegetative cover retreated, especially along the seaward edge, with far more areas losing vegetation than gaining it in the later years.

4.7 Vegetation Change Detection Area 3

Area 3's vegetation cover displayed limited yet measurable spatial-temporal variations during the 2021-2024 period. This section presents the results of the vegetation change analysis for Area 3, maintaining the same structure applied in the previous areas. A detailed quantitative summary of the changes (expressed in square meters and percentages relative to Area 3) is also included, followed by a concise overview of the principal outcomes.

4.7.1 Greenness Distribution (VARI)

Figure 28 illustrates the spatial distribution of greenness in Area 3 as indicated by the VARI index for 2021 through 2024. The VARI maps range less than zero shown in brown tones (denoting bare sand or minimal vegetation) to high values in green tones (denoting dense

vegetative cover). This color-coded greenness profile highlights how vegetative vigor and extent change over time on the dune surface.

In 2021, Area 3 is largely characterized by low VARI values, with brown and yellow tones covering most of the dune surface, which points to limited vegetation across wide sectors. Higher VARI values occur only in a few scattered green patches, mostly toward the landward margin, suggesting that vegetation was confined to small zones rather than being continuous. Along the seaward-facing foredune, greenness is consistently low, indicating predominantly bare sand near the beach. In 2022, the map becomes noticeably less green overall, implying a further contraction of vegetated cover. Several areas that appeared moderately green in 2021 shift to brown or neutral tones, and the highest-VARI patches either shrink or disappear. Brown hues therefore become more widespread across the dune, while the seaward fringe remains largely unchanged and sparsely vegetated, consistent with an overall setback in greenness from 2021 to 2022.

In 2023, the greenness distribution rebounds as vegetation recovers and expands. The VARI map for 2023 exhibits an increase in green-shaded areas relative to 2022. Many parts of the dune that were brown in 2022 show a return of green tones by 2023, indicating new vegetation growth or reestablishment. For instance, some central and landward portions of Area 3 that lost vegetation in the prior interval display elevated VARI values again, as plant cover regenerates there. The green patches in 2023 are more numerous and slightly larger compared to 2022, though they remain patchy. This suggests that vegetation became more widespread or healthier in 2023, regaining much of the ground that was lost in the previous year. High VARI values (lush green) appear in the interior and along the backdune signaling the resurgence of dense vegetative cover in those zones. The seaward side of Area 3, while still mostly sparse, also shows a subtle uptick in greenness with a few scattered green specks in 2023. In summary, 2023 marks a notable recovery in greenness for Area 3, with the dune looking greener and more vegetated than it was in 2022 (though not necessarily exceeding the 2021 baseline in all locations).

The 2024 map continues the trend of vegetative improvement. Figure 28 shows that, by 2024, the VARI distribution in Area 3 is comparable to 2023, indicating that greenness was broadly maintained. The green zones identified in 2023 generally persist into 2024 and, in some parts become more intense. Several patches that were previously bare also acquire a green tint in 2024, suggesting new vegetation establishment during the final interval. Meanwhile, the foredune along the coast remains predominantly brownish, indicating that much of the immediate coastal fringe is still open sand with sparse vegetation. Overall, 2024 stands out as the "greenest" year for Area 3 in this series. By the end of the study period, greenness appears slightly higher than in 2021, suggesting that the earlier reduction was compensated by subsequent gains. Despite this improvement, much of the dune surface remains unvegetated or only thinly vegetated. Nonetheless, the VARI maps indicate a net increase in greenness from 2021 to 2024, following an initial dip and a later expansion and densification of plant cover.

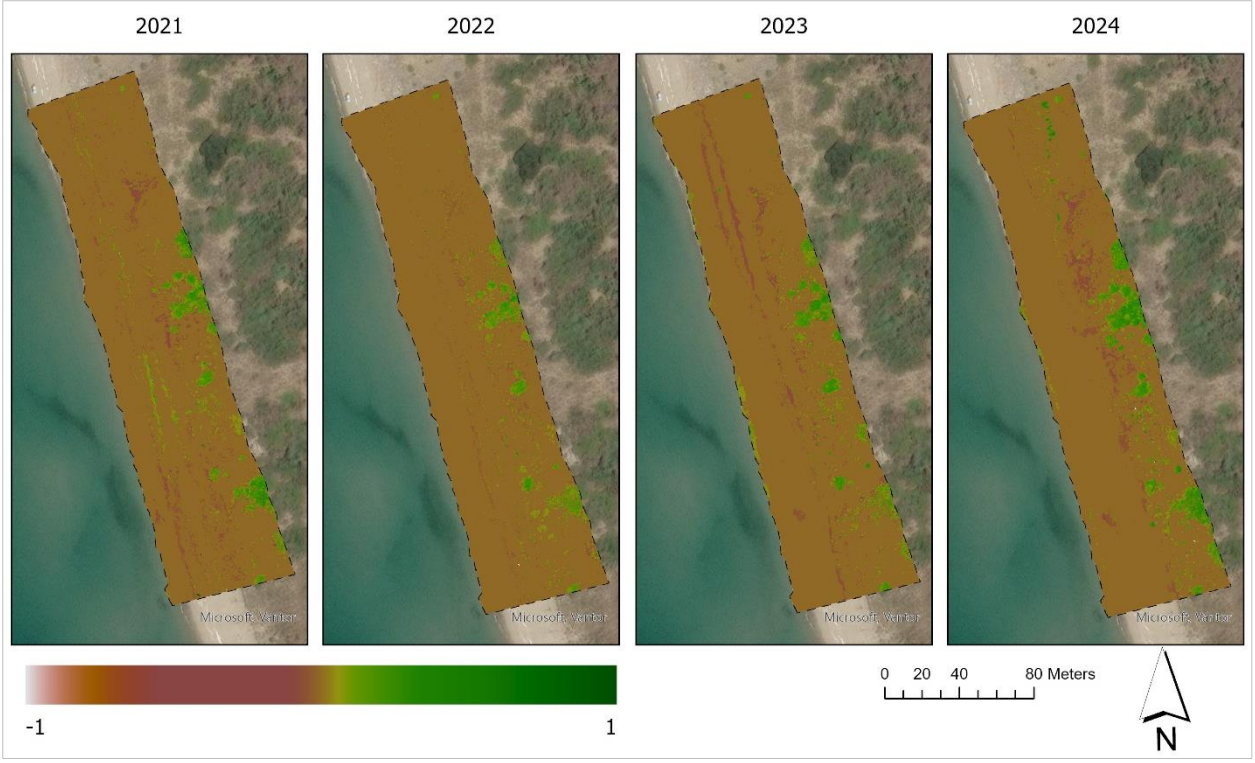


Figure 28 VARI raster layer - greenness intensity distribution in Area 3

4.7.2 Vegetation Classification Results

Figure 29 presents the classified maps, where green areas indicate vegetated surfaces and gray areas indicate non-vegetated (bare) ground. In 2021, the classification reveals that only a small fraction of Area 3 was covered by vegetation at the start of the observation period. Consistent with the VARI greenness observation, Vegetated areas occur primarily near the backdune (landward side) and perhaps a few isolated pockets on the dune interior or ridge where vegetation had taken hold. These patches of green in the 2021 map indicate the presence of dune grasses or shrubs clustered in those favorable spots. In contrast, the vast majority of Area 3 in 2021 is classified as non-vegetated (shown in gray), underscoring that active sand and bare ground dominated most of the area.

By 2022, the classification map shows a further reduction in vegetated area compared to 2021. Instead of the expansion seen in Area 2, Area 3 experienced a contraction of vegetation in this interval. Many regions that were green (vegetated) in the 2021 map turn gray in the 2022 classification, indicating that those areas lost their vegetation cover. The 2022 vegetated patches are fewer and generally smaller, reflecting a setback in vegetative extent. Essentially, some of the limited vegetation that existed in 2021 did not persist into 2022. The majority of Area 3 in 2022 is mapped as non-vegetation (gray), even more so than in 2021, confirming that vegetative cover reached its minimum extent this year. The 2023 classification results indicate a clear rebound in vegetation cover. In 2023, the extent of green (vegetated) area increases markedly from the previous year. The map for 2023 shows that many areas which were gray (unvegetated) in 2022 have turned green, signaling successful vegetation establishment or regrowth within that one-year interval. Notably, vegetation reappears in some sections where

it had disappeared in 2022, suggesting a natural re-colonization of those bare patches. The interior dune surface and portions near the landward boundary of Area 3 exhibit new or expanded vegetated stretches in 2023. Some of these green patches begin to form contiguous clusters that were absent the year before, indicating that individual vegetation patches have grown or coalesced. Overall, vegetation cover in 2023 occupies a substantially larger portion of Area 3 than it did in 2022.

By 2024, several parts of Area 3 that had been empty sand in earlier years are now shown as green, indicating new vegetation growth in those locations over the three-year span. We observe that the vegetated area, while expanded, is still not contiguous across all of Area 3, it remains a patchwork with large gray areas indicating that much of the dune is open sand. The seaward side of Area 3 in 2024 remains largely unvegetated, the front line of the dune still has difficulty supporting vegetation, and those zones stayed gray through all years. By 2024, the landward and central parts of Area 3 appear noticeably greener than the seaward fringe, suggesting that vegetation established more successfully in the more sheltered. Overall, the year-by-year classifications point to a dynamic but broadly positive evolution, vegetation cover was limited in 2021, dropped to its lowest extent in 2022, and then increased markedly in 2023 and 2024. Throughout this period, some vegetative patches proved stable (surviving all four years), while others were transient. Large portions of the area (especially the beach-facing side) remained non-vegetated throughout, highlighting the spatial variability in where plants can successfully persist on the dune.

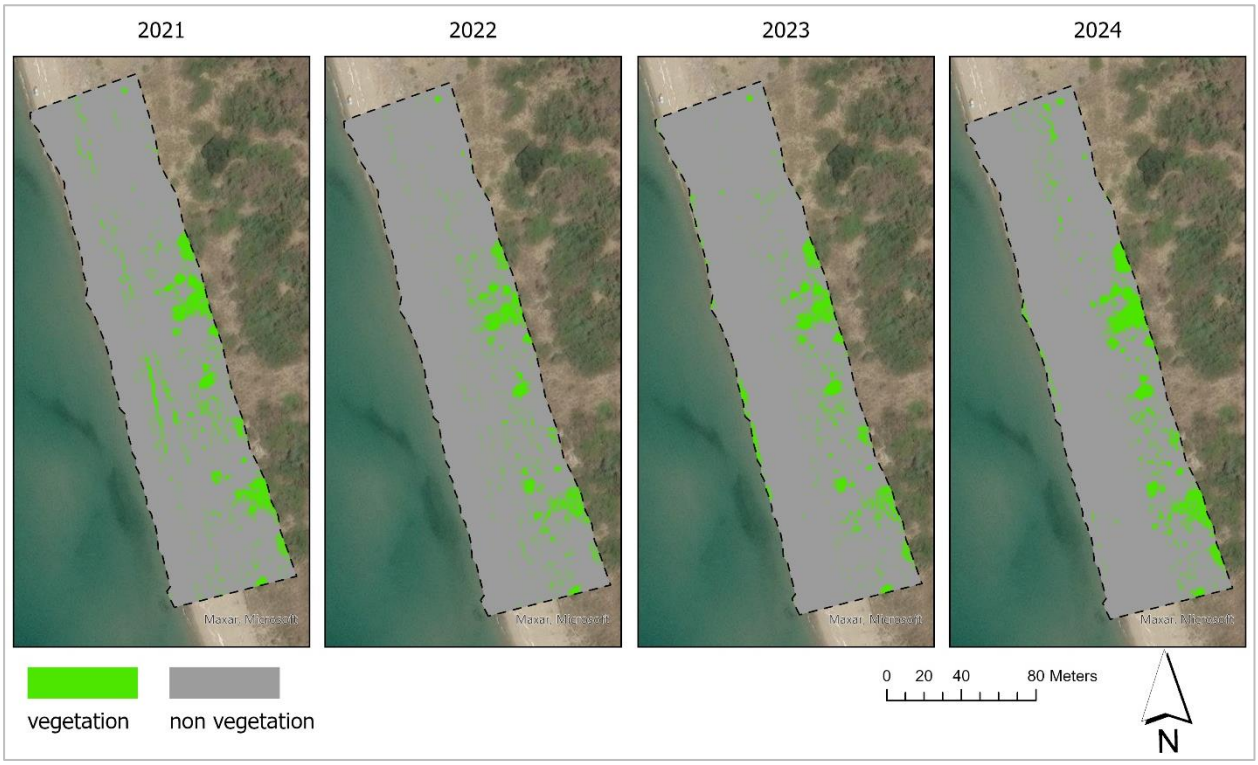


Figure 29 Vegetation vs. non-vegetation classification map of Area 3

4.7.3 Vegetation Change Mapping

The multi-temporal vegetation change maps (Figure 30) provide a detailed visualization of where vegetation cover was lost (shown in red) or gained (shown in green) in Area 3 during each interval, with areas of no change (stable vegetation status or consistently bare ground) shown in gray. Four panels are presented, these maps complement the year-by-year classification results by pinpointing the exact locations of vegetative transitions and highlighting the dominant change trends in each time interval.

The vegetation change map for the 2021-2022 (Figure 30, 2021-2022 panel) interval reveals that the majority of Area 3 remained unchanged in terms of vegetation status over that first year (extensive gray areas dominate the map). In the 2021-2022 panel, red areas (vegetation loss) are noticeable in several parts of the dune, outnumbering the green areas. They tend to be scattered and moderate in size. For example, Red spots appear in the dune interior, likely marking the loss of isolated vegetation pockets that existed in 2021 but did not survive the year. Green patches (vegetation gain) are relatively fewer and generally smaller compared to the red patches. These green areas indicate spots where new vegetation became established on previously bare sand between 2021 and 2022. The green gains seem to be scattered and do not form large contiguous zones, for instance, just inland of the foredune. The overall impression from the 2021-2022 change map is that vegetation losses slightly outweighed the gains during this period.

The vegetation change map for 2022-2023 (Figure 30, 2022-2023 panel) exhibits a notable shift in pattern compared to the prior interval. In this panel, green areas (gains) are more widespread than red areas, indicating that between 2022 and 2023, vegetation expansion was the dominant process. A number of green patches appear across Area 3, marking where plants successfully colonized terrain that was bare in 2022. These gains are especially evident in the interior and landward sectors of the dune. For instance, the 2022-2023 map shows clusters of green inland of the foredune and in central dune areas. The green patches are still mostly discontinuous, but they are more numerous than in the previous year's map, reflecting many small-scale vegetation establishments. Meanwhile, red patches (losses) do exist in the 2022-2023 panel, but they are relatively limited in extent and number. Some red appears along the edges of the vegetated zones from 2022. The overall mosaic for 2022-2023 is one where gray (no change) still covers the bulk of Area 3, but among the changed areas, green outshines red. This indicates a net increase in vegetation cover over that interval.

Figure 30, (2023-2024) indicating that vegetation continued to expand between 2023 and 2024. In several places, gains appear along the edges of existing vegetated patches, which is consistent with a gradual outward expansion of those plant clusters. A few new green spots appear in sections that were still bare in 2023, reflecting fresh colonization in 2024. Red areas (vegetation losses) are also present in the 2023-2024 map, but as in the prior year, they are relatively minor in comparison to the greens. These red patches likely correspond to small-scale losses, for example where a patch of vegetation present in 2023 failed to survive into 2024. Notably, along the seaward foredune, the pattern from previous years holds, that zone remains largely gray (unchanged bare sand), with perhaps some persistent red indicating that any vegetation that managed to grow there in 2023 did not persist (underscoring the difficulty of sustaining plants at the very front). Overall, the balance of changes in 2023-2024 is weighted

toward gains. Most of Area 3 still shows no change (gray), highlighting that large expanse either remained bare throughout or stayed vegetated continuously, but where change is observed, it tends to be positive (new vegetation). In fact, the margin by which gains exceeded losses in 2023-2024 appears slightly larger than that of 2022-2023, indicating that the vegetative expansion accelerated slightly in the final year. The 2023-2024 change map, therefore, reinforces the trend of recovery, it shows a continued spread of vegetation on the dune, building upon the previous year's gains and further diminishing the proportion of area that saw vegetative decline.

The cumulative change map (Figure 30, 2021-2024 panel) comparing the start and end states (2021 vs 2024) provides an integrated view of vegetation dynamics over the entire study period in Area 3. The 2021-2024 overall change map for Area 3 shows a mixed pattern of red and green scattered across the dune, reflecting the spatially heterogeneous nature of the changes. Several red patches are visible, indicating lasting vegetation losses over the study period. These red zones are relatively modest in size and tend to appear in specific locations, such as portions of the seaward (western) edge of Area 3 and some spots within the dune interior.

The presence of red along the coastal side suggests that some vegetation that existed on the foredune or near the beach in 2021 did not survive to 2024, essentially, the frontal dune saw a net retreat in vegetation at those points. Similarly, red in the interior might mark where certain vegetated pockets present at the beginning were absent by the end (perhaps transient patches that died out). On the other hand, the map also highlights numerous green patches distributed around Area 3, corresponding to areas of net vegetation gain. These green areas are especially evident in the landward and central parts of the dune system, aligning with the notion that those regions experienced new colonization and growth that was not there in 2021. The pattern of green vs. red is fairly balanced over the whole area, neither color overwhelmingly dominates the other, which is consistent with the relatively small net change in vegetated area. Importantly, very large portions of the map are gray, confirming that the majority of Area 3 did not change state at all between 2021 and 2024. The overall change map thus conveys that, over three years, Area 3 experienced both gains and losses in different places, but on the whole the gains slightly exceeded the losses.

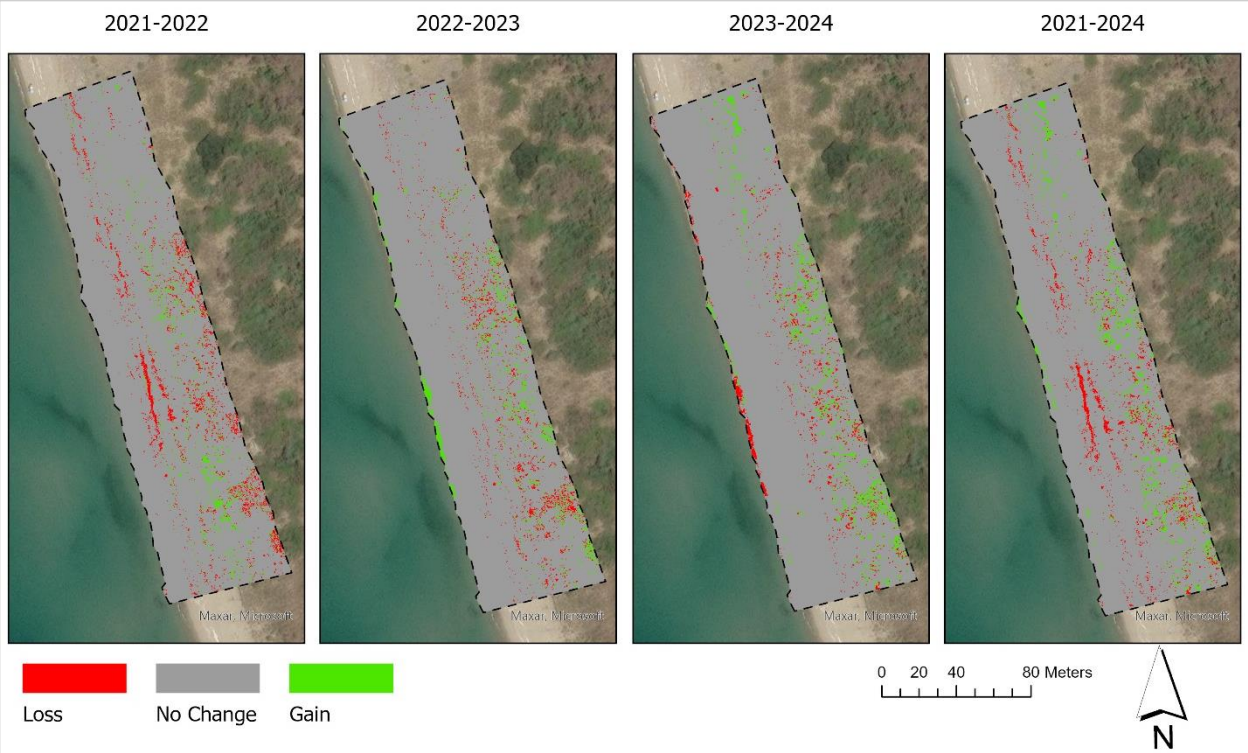


Figure 30 Vegetation change maps of Area 3

4.7.4 Quantitative Change Summary

The quantitative analysis of vegetation changes in Area 3 provides numerical confirmation of the patterns observed in the maps. Table 15 outlines the spatial extent and percentage of vegetation gain, loss, and no change during each time interval and over the full 2021-2024 period. The table also indicates the net outcome for each interval as either "Gain" or "Loss" based on which process dominated. Below is a summary of the key quantitative findings for Area 3:

In the 2021-2022 interval, approximately 6.7% of Area 3 underwent change. This means roughly 93-94% of the area remained in the same state (either consistently vegetated or consistently non-vegetated) from 2021 to 2022. About 4% (over 706 m^2) (about 4.0%) experienced vegetation loss (i.e. areas that were vegetated in 2021 became bare sand by 2022), while gain occurred over 2.4% (around 429 m^2), resulting in a net loss of vegetated area. The majority of the area remained unchanged, and Table 15 categorizes this interval as a "Loss" phase. In summary, the numbers confirm that there was a modest contraction of vegetation in the first year, more area transitioned from vegetated to bare than vice versa, producing a slight negative change in overall vegetative extent (consistent with the visual impression of the maps, where red loss areas outweighed green gains for that interval).

The second interval saw a reversal to net growth in vegetation. Between 2022-2023, change affected around 6.3% of the area, meaning roughly 94% of the area remained unchanged year-to-year. This magnitude of change is similar to the previous interval (on the order of only ~6% of the landscape affected), indicating that most of Area 3 continued to be stable in terms of vegetation status. Vegetation gained over 566 m^2 (3.3%) and lost over 492 m^2 (2.9%), indicating

a net gain of 74 m^2, the vegetation gains slightly exceeded the losses. The "Gain" status in Table 15 for 2022-2023 confirms that Area 3's vegetative cover bounced back in this period, recouping and slightly building upon what was lost previously.

In the final annual interval 2023-2024, Area 3 continued to experience a net vegetation gain, about 6.9% of the area experienced transition. The distribution of change was tilted toward gains, around 2.8% of Area 3 (approx. 469 m^2) that was vegetated in 2023 became non-vegetated in 2024 (losses), whereas about 4.1% of the area (approx. 702 m^2) that was bare in 2023 turned vegetated by 2024 (gains), yielding a net gain of 1.3%. The net change for 2023-2024 (Table 15) was a positive gain of vegetation cover, larger in magnitude than the net gain of the previous year. This quantitative outcome reinforces the earlier observation that 2024 had the greatest vegetated extent. It also suggests that any vegetation losses that did occur in that last interval were relatively minor in area compared to the spread of new vegetation.

Across the entire 2021-2024 period (Table 15), a total of 1,236 m^2 of Area 3 experienced vegetation change, representing 7.3% of the dune surface. Vegetation gained over 633 m^2 (3.7%) and lost over 603 m^2 (3.5%), producing a small net increase of the total area. The net result is a marginal positive change , a net gain on the order of +30 m^2 of vegetated area over three years across the entirety of Area 3. In percentage terms, this net gain is extremely small (around 0.2% of the total area), effectively indicating that the vegetated portion of Area 3 in 2024 was only a hair larger than it was in 2021. It's also worth highlighting that approximately 92-93% of Area 3 remained in the same state for the entire duration, despite visible changes along the margins, the core distribution of vegetation vs. bare sand was largely stable.

A3	Loss Area	No change Area	Gain Area	Area Changed	Status
	m2	m2	m2	%	-
2021-2022	706.10	15764.75	428.60	6.71	Loss
2022-2023	491.58	15842.05	565.83	6.26	Gain
2023-2024	468.74	15728.78	701.93	6.93	Gain
2021-2024	603.05	15663.44	632.98	7.31	Gain

Table 15 Vegetation Change Summary, Area 3

In summary, vegetation in Area 3 showed minor but measurable shifts. An initial decline was followed by consecutive gains in later years, leading to a modest net increase in vegetated area by 2024. Although the total change was limited in extent, the results confirm a trend of slow but progressive vegetative recovery.

5 Discussion

5.1 Area 1: Geomorphological and Vegetation Changes

5.1.1 Geomorphic Changes:

Area 1 exhibited a dynamic but oscillatory behavior over the study period, with one year of widespread sand accumulation followed by a year of erosion that largely negated those gains. In the 2021-2022 interval, virtually the entire area underwent accretion under the lenient detection threshold (LoD1), indicating significant dune buildup across A1. This accretion was especially concentrated along the seaward dune toe and frontal zones, where elevation increases on the order of 0.6-1.0 m were common. The 2021-2022 results show a strongly accretional signal under LoD1, more than 95% of Area 1, is mapped as elevation gain, while erosion is essentially absent (Annex 7). This pattern indicates widespread deposition across the dune surface during that interval. The following year shifts toward erosion, most of the recorded changes fall within the -0.2 to 0 m class, implying a shallow but spatially extensive lowering. Under LoD1, roughly 8% of Area 1 is classified as erosion and accretion is negligible, consistent with a broadly erosional phase. Although, these losses were shallow and spatially uniform enough that they exceeded the minimal detection threshold but remained relatively small in magnitude. Taken together, the two annual intervals point to a compensating sequence, widespread deposition in 2021-2022 followed by shallow lowering in 2022-2023, resulting in a small net change by 2023. This is also reflected in the two-year comparison, where only about 4% of the area shows persistent change and the rest returned to essentially its original elevation, with a slight bias toward net accretion. Overall, A1's sediment budget remained near equilibrium, with sand gains and losses balancing out. Such behavior is indicative of dune resilience, the system absorbed a pulse of sand and then released it, possibly in response to climatic variability (calm year followed by a stormy year).

Applying LoD95 substantially reduces the mapped change. In 2021-2022, the extensive low-magnitude accretion seen under LoD1 collapses into a small number of more concentrated depositional zones. For 2022-2023, the LoD95 output retains only a limited erosional feature near the foredune margin, suggesting that a large fraction of the shallow lowering captured by LoD1 is near the detection limit. Under the stricter confidence criterion, the clearest persistent adjustments are concentrated at the seaward fringe rather than across the entire dune interior.

5.1.2 Vegetation Changes:

The vegetation dynamics in Area 1 closely mirrored these geomorphic fluctuations. Overall, A1's vegetation cover remained largely stable, with only minor, reversible changes concentrated at the dune's seaward edge. A binary classification of vegetation shows that most of A1 (especially the dune crest and landward side) is continuously vegetated, forming an unbroken belt of plant cover, whereas the immediate foredune toe and beach are mostly bare sand. Against this backdrop, multi-temporal maps reveal a cycle of vegetation expansion followed by contraction at the dune front. From 2021 to 2022, vegetation cover expanded in A1. Green (gain) patches appear along the previously bare seaward flank, indicating that

pioneer vegetation colonized sections of foredune that had built up during the accretionary phase. These new vegetated spots suggest that the sand deposited in 2021-2022 provided fresh substrate for plant establishment (for instance, Ammophila or other dune grasses) on parts of the dune face that were bare the year before. Vegetation gains in this interval outpaced losses, yielding a net increase in vegetated area (Table 13) and a "greening" of the foredune.

The 2022-2023 interval the spatial pattern of change shifted but still resulted in a net gain in vegetation. Especially as a continuous band of decline along the western (seaward) edge of A1. The contiguous red strip on the 2022-2023 change map signifies that much of the pioneer vegetation established the previous year did not survive into 2023. Essentially, the vegetated foredune fringe retreated landward: plants that had colonized the dune toe were stripped away, likely by the same erosional forces that removed sand (e.g. storm surge or wave swash). Indeed, the vegetation loss zone corresponds to where the dune face was eroded. Meanwhile, the interior dune remained largely unchanged (gray), meaning the dense vegetation on the crest and backdune persisted unaffected. By 2023, the net vegetation change in A1 was minimal, the small gains of 2021–2022 had been offset by losses in 2022–2023, leaving most of the area in its original state (either continuously vegetated or continuously bare). This pattern underscores the tight coupling between sand movement and plant cover in A1. Zones of sand accretion coincided with vegetation growth, whereas the subsequent erosion led to vegetation die-back. The fact that these changes were largely reversed over two years points to a resilient equilibrium. A1's dune ecosystem can tolerate short-term disturbances with its overall vegetation footprint remaining intact. We interpret that the established vegetation on the dune crest likely stabilized that portion (which saw little net change), while the new colonization on the mobile foredune toe was more vulnerable and ephemeral.

Area 1 shows clear year-to-year fluctuations, but the net outcome over the longer period remains small for both elevation and vegetation. This overall stability indicates that A1 maintained a broad balance between sand deposition and sand removal. Vegetation on the landward dune helps stabilize the surface, so the most pronounced erosion tends to be confined to the more exposed seaward edge. Vegetation can also colonize newly accreted surfaces when conditions are favorable, helping to bind deposited sand and reinforce dune stability. Overall, Area 1 behaves as a relatively stable dune sector that can absorb interannual variability without showing sustained degradation.

5.2 Area 2: Geomorphological and Vegetation Changes

5.2.1 Geomorphic Changes:

Area A2 displayed a markedly different trajectory, characterized by persistent and progressive erosion of the foredune and a net negative sediment budget over the 2021-2024 period. Unlike A1, Area 2 did not experience a compensatory cycle of accretion; instead, each successive year saw further dune degradation concentrated at the seaward side. Under the LoD1 threshold, the 2021-2022 elevation change map for A2 already indicated localized erosion as the dominant process, a distinct erosional "hotspot" appeared along the dune's landward margin (seen as a red patch in the 2021-2022 panel of Figure 12). This corresponds to noticeable lowering or retreat of the backdune toe during that first interval. Only very

minor accretion was detected (tiny blue specks seaward of the eroded zone), implying little to no sand was added to the system in 2021-2022. The interior of the dune thus stayed within the noise level, while the back dune face suffered localized cutbacks. In 2022-2023, a nearly continuous band of erosion stretched along most of A2's ocean-facing edge, effectively tracing the entire foredune line with elevation losses beyond LoD1. The continuity of the red strip suggests a coherent response along the dune front rather than a few isolated blowouts. In 2022-2023, erosion affected roughly 10-11% of Area 2, while accretion remained below 2%, so the balance stayed clearly negative. The small depositional pockets that do appear are limited and do not meaningfully compensate for the losses. The strongest annual signal occurs in 2023-2024, the erosional band becomes wider and more continuous and the LoD1 map is dominated by red along the frontal dune, with very little blue. Around 14-15% of the area is classified as erosion (the highest annual share), whereas accretion is confined to about 1% or less. Over the full 2021-2024 comparison, the pattern consolidates into a clear net lowering along much of the seaward fringe. Approximately one-third of the surface shows detectable change over the three-year span, and most of that changed area corresponds to net erosion (about 30% of Area 2) rather than net accretion (around 4%). The scattered inland accretion patches are small and discontinuous and do not offset the frontal-dune lowering, implying that removed sediment was not substantially retained within Area 2. It's likely that, much of the eroded sand was transported out of the area (offshore or alongshore), leading to a net coastline retreat. Indeed, analysis indicate that the dune front migrated landward in A2 between 2021 and 2024.

The LoD95 results make the point even clearer. Close to the shoreline the uncertainty is higher, so the 95% threshold removes most small fluctuations and retains only the strongest signals. For example, in 2023-2024 the mapped changed area drops from roughly 15% under LoD1 to about 1.5% under LoD95, yet the retained changes still cluster along the seaward dune margin. This implies that a portion of the dune retreat was large enough to rise above even a high error threshold, confirming the reality of A2's foredune collapse. In summary, Area 2 experienced pronounced and unidirectional geomorphic change, steady foredune erosion and shoreline retreat with no appreciable recovery during the period of study.

5.2.2 Vegetation Changes:

The ecological response in Area 2 was one of initial vegetation expansion followed by widespread and sustained loss, paralleling the geomorphic trend of dune recession. In 2021-2022, despite the modest erosion at the back, A2 actually saw a net gain in vegetation cover. The vegetation change map for that interval reveals numerous green patches scattered especially in central and landward parts of the dune. These patterns imply that vegetation established in 2022 in places that were mapped as bare in 2021. Most gains appear in stable interior zones, and the areas that were previously sand-dominated. By contrast, only limited losses were observed in 2021-2022, mostly small isolated spots where perhaps some grass patches died off or were buried. Taken together, the map points to a short-lived increase in vegetation by the end of 2022, consistent with the "Gain" label reported for this interval in Table 14. This improvement does not persist. The 2022-2023 comparison shows a sharp contraction in cover, with red dominating much of the dune surface. In particular, a near-

continuous belt of loss develops along the seaward edge indicating that vegetation present in 2022 was largely absent by 2023. The few green gains in 2022-2023 were minimal and isolated, some small new growth patches inland of the main loss zone, but these were vastly outnumbered by losses. This indicates that 2022-2023 was a period of severe vegetative stress or disturbance for A2, likely due to the physical impacts of storm erosion and possibly salt spray or overwash that can accompany dune breaching. Much of the vegetation that expanded earlier did not persist through the harsher conditions of that year. The same loss-dominated pattern continues into 2023-2024. Red patches remain widespread, and they are evident along the already depleted dune front, where the vegetation boundary shifts further landward between 2023 and 2024. Smaller losses also appear within the dune interior, suggesting that some patches that were weakened in the previous interval continued to decline. A few new green spots do emerge in 2024, often just landward of the main loss belt, indicating limited re-establishment on newly exposed sand behind the retreating front. However, these gains are scattered and small and do not offset the ongoing reductions.

Across the full 2021-2024 comparison, the net change for Area 2 is strongly negative. The cumulative map is dominated by red, including a persistent strip along the seaward boundary, showing that much of the vegetation present in 2021 is absent by 2024, particularly along the foredune and in several interior patches. Green areas are comparatively few and tend to occur as small clusters toward the landward side. Overall, the mapped pattern indicates a landward contraction of vegetation coupled with additional internal losses, leaving large sections that were vegetated at the start of the period mapped as bare sand by 2024. The statistics underscore this, Table 14 shows a net loss status for 2021-2024, with vegetated area decreasing (roughly 12-13% of A2's area lost its vegetation cover over three years). This net decline aligns with our mapped observations that losses far outweighed gains in every year after 2022. The tight correspondence between morphological erosion and vegetation loss in A2 highlights their causal linkage. As the foredune eroded and lowered, any grasses or shrubs on that dune face were uprooted or buried. Subsequent landward erosion likely undermined vegetation that had expanded in earlier years, leading to interior losses. Moreover, the erosional disturbance (sand movement, saltwater intrusion) can create stresses that reduce plant survival even beyond the immediate scarp line. By 2024, Area 2's dune not only had receded in form, but its protective vegetative cover was greatly diminished. In management terms, this is alarming because vegetation is critical for dune stability and storm resilience. A2's condition suggests a vulnerable dune system where natural recovery of plant cover is not keeping pace with physical habitat loss. Without intervention or a change in conditions (e.g. an influx of sand or a lull in storm activity to allow regrowth), the trend in A2 could continue toward dune degradation and habitat decline.

5.3 Area 3: Geomorphological and Vegetation Changes

5.3.1 Geomorphic Changes:

Area 3 demonstrated a highly dynamic behavior with dramatic short-term changes but little net morphological change by the end of the study. Essentially, A3 went through a boom-and-bust cycle, a major sand deposition in one interval followed by almost equal erosion in the

next. In 2021-2022, A3 experienced a surge of sand accretion. The LoD1-filtered results show that approximately 24% of Area 3's surface saw elevation gains beyond the noise threshold, whereas virtually 0% registered significant erosion that year. Field interpretation suggests that a large volume of sand was delivered to A3 dune system in that year, potentially linked to favorable wind conditions or a temporary increase in sediment availability. In the main depositional zone, elevation gains reach roughly up to 1 m, indicating substantial aggradation. Elsewhere, the surface remains largely stable: around 76% of the area is classified as no change, and erosion affects only a negligible fraction (less than 0.1%). This gain is not sustained into the following year, the 2022-2023 results show a clear shift toward erosion. Under LoD1, the map is dominated by gray (no change) except for a large, continuous red patch covering roughly 15% of Area 3. This erosional zone closely matches the sector that accreted in 2021-2022, indicating that the same part of the dune that built up in one interval experienced lowering in the next. Accretion is almost absent in 2022-2023, with blue patches limited to scattered traces (<0.1% of the area). A large volume of sand that had been deposited was now removed. There is little evidence that this eroded sand was simply redistributed elsewhere within A3, no significant new blue accretion zones emerged landward of the red erosion patch that year. The implication is that the sediment was likely transported out of Area 3 entirely (e.g. carried further downcoast by alongshore drift or pulled seaward by storm surge), rather than just shifted to a different part of the area. The detailed analysis supports, the absence of concurrent large accretion signals means the sand removed in 2022-2023 did not settle within the boundaries of A3. Effectively, A3 experienced a boom (2021-22) and bust (2022-23) cycle, exchanging sediment with the broader coastal system rather than internally. By 2023-2024, the system calmed down considerably. The LoD1 results for 2023-2024 show the least amount of change among the intervals. The change map is dominated by gray, a small red patch of erosion and a small blue spot of accretion, each very localized. Only about 5-6% of Area 3 shows change above the LoD1 threshold (approximately 4% erosion and 2% accretion), while the remainder is classified as no change. These changes are so minimal and patchy that 2023-2024 can be considered a quiet interval in geomorphic terms. After the stronger adjustments seen earlier, the dune surface appears to have largely stabilized, with only minor local modifications. Over the full period from 2021 to 2024, Area 3 ended up with minimal net topographic change. When comparing the start and end states (2021 vs 2024 DEMs), the distribution of changes is balanced and small in extent, consistent with a near-zero net sediment budget by 2024. There were some lasting effects for example the specific area of major deposition and erosion might not have returned exactly to its original elevation but broadly, the gains of the first year were canceled out by the losses of the second, and the third year made little difference. We interpret that Area 3 may be influenced by episodic events or sediment pulses (for example, an Arno River mouth bar delivering sand one year, then a storm dispersing it the next). This behavior indicates a coupling with larger-scale coastal sediment dynamics, where it temporarily stores sand and then releases it. The fact that 2023-2024 was stable suggests the system had "reset" after the big changes, with no major new perturbations in that year.

5.3.2 Vegetation Changes:

Area 3 showed a notable trajectory, an initial decline in cover followed by a rebound and slight net increase by 2024. This trajectory is somewhat unique because the vegetation did not simply track the elevation changes one-to-one, rather, there was a lagged response and an overshoot in recovery. In 2021, vegetation in Area 3 is already limited overall. The seaward foredune is largely bare, and vegetated cover is mainly confined to a small number of patches, most of which occur toward the landward margin of the dune. These baseline conditions mean that A3 had a lot of unvegetated area to potentially colonize, but also that its existing vegetation was perhaps not extensive enough to stabilize newly deposited sand. By 2022, after the major sand deposition, the vegetation cover actually shrank compared to 2021. The VARI greenness maps show a decrease in green (high vegetation) areas from 2021 to 2022, and many zones that were moderately vegetated turned to low greenness (brownish) by 2022. In particular, some patches of vegetation present in 2021 appeared to have been lost or buried by 2022, as indicated by previously green areas fading to bare-sand tones. The seaward fringe remained almost entirely unvegetated (as it was initially), and even certain interior sections that had some plants in 2021 showed reduced vegetation index values in 2022. This decline in vegetative cover between 2021 and 2022 suggests an initial setback for vegetation, likely due to the disruptive influx of sand. Rapid accretion can smother existing plants, for instance, if dunes grow vertically or laterally very quickly, slow-growing shrubs and grasses may not survive being buried. Also, newly deposited sand creates bare surfaces that take time for vegetation to colonize (especially if the deposition happened over a single winter, plants might not have grown in yet by the survey time). As a result, 2022 saw A3 at its lowest vegetated extent in the study period.

After this dip, vegetation in Area 3 turns upward again. By 2023, the greenness of the dune increased significantly from the previous year. Many areas that were bare in 2022 turned to green, indicating that vegetation either regrew or newly established there. The strongest improvement is concentrated in the central and landward parts of the dune, where patches that had weakened earlier display higher VARI values in 2023. Vegetated areas also become more frequent and slightly larger than in 2022, even if the pattern remains patchy overall. High greenness areas reappeared on the backdune and interior zones, this widespread greening in 2023 implies that the dune had a chance to stabilize.

By 2024, the vegetative cover in A3 had improved further, cementing a net gain over the study period. The spatial pattern of greenness in 2024 was similar to 2023 but slightly more extensive and robust. Many of the new vegetation patches that appeared in 2023 persisted into 2024 and even expanded somewhat, with some bare spots turning green as late colonizers took hold. The VARI maps suggest that 2024 was the "greenest" year, vegetation was at its maximum extent and density in our record. This pattern is captured in Table 15, after the initial decline and the subsequent gains, Area 3 finishes with a small net increase in vegetated surface by 2024. The trajectory of A3's vegetation highlights a few important points; first, it underscores that massive deposition can temporarily reduce vegetation. In A3's case, the 2021-2022 sand inflow likely buried some existing plants, outpaced the immediate colonization, leading to a short-term decline in cover. Second, given a respite from further disturbance, the dune's vegetation was able to rebound quickly, showing the resilience of dune flora. By 2023 and

2024, plants had reclaimed not only their former extents but also colonized some areas that were previously bare, suggesting that the disturbance opened new niches for vegetation. Third, the interplay between topography and vegetation in A3 is evident, the initial loss of plants may have made the subsequent erosion in 2022-2023 even easier (no vegetation to hold sand), but then once the dune was stable, vegetation aggressively colonized and likely helped stabilize the surface against smaller changes in 2023-2024. In summary, Area 3's vegetation went through a boom-bust-recovery cycle analogous to the geomorphic changes.

5.4 Synthesis and Comparative Analysis Across Areas

Despite all three areas lying within the same coastal park and experiencing the same broad climatic events, their morphodynamic and ecological trajectories diverged significantly. These contrasts highlight that even within one dune system, local factors (geomorphic setting, exposure, sediment supply, vegetation feedbacks) can lead to markedly different outcomes. We synthesize the findings for A1, A2, and A3 to compare their behaviors and infer the reasons behind their differences:

5.4.1 Magnitude and Direction of Change

Area 1 remained in near-equilibrium, Area 2 underwent persistent net erosion, and Area 3 experienced large but compensating swings. Over 2021-2024, A1's net elevation change was negligible, essentially oscillating around a stable state. In stark contrast, A2 suffered a cumulative loss, its foredune receded and lowered progressively with each year. Area 3 had substantial short-term changes but minimal net change, effectively ending close to its starting topo-elevation profile (albeit after dramatic intervening shifts). This means A2 stands out as having the most severe permanent change (degradation), whereas A1 and A3, each in their own way, maintained overall stability (one by little change at all, the other by equalizing gains and losses). This indicates that disturbance in A2 was widespread and chronic, while in A1 and A3 it was limited either temporally or spatially.

5.4.2 Patterns of Accretion vs Erosion

A clear contradiction emerges in how accretion and erosion played out. Area 1 exhibited a balanced pattern, a phase of widespread accretion followed by a phase of widespread erosion. Importantly, these occurred in separate intervals, leading to a temporal alternation of process (accretion then erosion). Area 2, on the other hand, was dominated by erosion in every interval, it effectively lacked any accretion phase. Any minor accretion detected was sporadic and did not persist, indicating that A2 did not benefit from conditions or events that cause sand to accumulate on the dune. Area 3 uniquely had accretion and erosion in back-to-back intervals (a boom then bust) and then a lull, thus, its accretion and erosion were temporally segregated like A1's, but with much greater intensity in each phase. A3's initial accretion was far more substantial (relative to its size) than A1's, and similarly its erosion was intense, whereas A1's changes were more moderate. The comparative insight is that A1 and A3 both experienced oscillatory dynamics, but A1's oscillations were mild (indicating a stable dynamic equilibrium) while A3's were extreme (indicating sensitivity to episodic events). A2, lacking

oscillation, illustrates a unidirectional trend likely driven by an ongoing forcing (e.g. a sediment deficit or continuous high wave exposure) with no relief.

5.4.3 Vegetation Response and Coupling

Across the three sites, the results consistently showed that vegetation patterns and dune morphology are connected, although the form and intensity of that connection varied from area to area. Areas 1 and 2 provide the clearest contrast. In Area 1, vegetation increased across both intervals even though the shoreline shifted from accretion to erosion, largely because the main gains occurred on relatively stable interior surfaces, while the dune toe remained mostly unvegetated. In Area 2, the linkage is much more direct, progressive foredune erosion coincided with a marked reduction in vegetation, with plant cover retreating as the dune front lowered. In this sense, Area 1 reflects a weaker coupling between geomorphic adjustment and vegetation response, whereas Area 2 shows a stronger, erosion-associated decline in cover. Area 3 showed a looser coupling in the short term, its vegetation initially declined even during an accretion phase, then rebounded after the major geomorphic changes had occurred. This indicates a time lag, rapid geomorphic changes outpaced vegetation's ability to respond immediately in A3. The initial deposition didn't produce instant vegetation growth (likely because it was too fast/severe, burying plants), and the subsequent erosion removed sand that was largely bare, so vegetation loss was less visible at that moment (since it had already declined earlier). Only after things settled did vegetation reclaim and even improve its coverage, effectively catching up with and slightly surpassing the geomorphic recovery. By 2024, A3's slight net gain in vegetation suggests that plant life had capitalized on the post-disturbance environment to colonize more area than before, even though the dune's shape returned to status quo. In contrast, A2 by 2024 had lost both dune volume and vegetation cover dramatically, showing no such resilience. A1 by 2023 was essentially unchanged in both respects, reflecting its equilibrium. Therefore, we see three distinct eco-geomorphic regimes: A1 have stable dune & stable vegetation, A2 have erosional dune & declining vegetation, A3 have dynamic dune & recovering vegetation.

5.4.4 Influencing Factors

The divergent behavior likely arises from variations in local context. While our data do not explicitly include wave, wind, or human impact measurements for each area, we can hypothesize causes. Exposure to wave energy could differ, Area 2 might be more directly exposed to prevailing storm waves (e.g. a protruding part of the coastline or a narrower beach), causing consistent erosion, whereas Area 1 could be somewhat sheltered (by an offshore bar or wider beach) leading to milder changes, and Area 3 might be influenced by an external sediment source (like proximity to a river mouth or inlet delivering sand episodically). Vegetation differences might also play a role, A1 had an "unbroken" vegetative cover on the dune ridge which likely helped trap sand and limit erosion, whereas A2's vegetation (although present) was perhaps less continuous or less effective at the dune toe, and by mid-study it was severely reduced, further exposing the sand to erosion. A3 initially had low vegetation cover, which may explain why the first-year accretion did not immediately

yield vegetation gains and why erosion could remove sand without encountering much plant resistance, yet as vegetation increased in A3, it may help stabilize future events. Topographic differences such as dune height and width could matter too, if A1's dune was higher or broader, it could withstand moderate erosion without total loss, while A2's perhaps smaller dune could be wholly cut through by storms. If A3's dune was lower to start, adding a lot of sand created a bigger morphological perturbation relative to its size. Without introducing new external data, we rely on our observations to conclude that multiple interacting factors led to Area-specific trajectories. The key point is that management cannot assume a uniform behavior across the park's dune system, some sectors (like A2) are in active retreat, whereas others (A1) are stationary and some (A3) are cyclically changing. These findings echo the concept that coastal dunes can exhibit patchy responses to the same climate drivers, as found in other studies of alongshore variability in dune erosion and recovery.

5.4.5 Sediment Exchange and System Connectivity

Another comparative insight is how isolated or connected each area is in terms of sediment flux. In Area 1, gains in one interval are broadly offset by losses in another. Area 2 behaves differently, showing repeated net losses, which implies that sediment was exported out of the sector (either alongshore or offshore). Area 3 sits somewhere in between; it shows a strong gain in one year followed by a loss in the next. This suggests A3 might be a transient sink/source depending on conditions. It underscores that the three areas are not closed systems, especially A2 and A3 appear to be interacting with the broader coastal sediment system. The park's coastline likely has zones of divergence (net erosion) and convergence (net accretion) of sand, our results identify A2 as a divergence (net exporter of sand) and possibly A3 as a temporary convergence then divergence. A1 might lie near a nodal zone (neither gaining nor losing significantly over time). Recognizing these roles is important for coastal sediment management because it may be ineffective to address erosion in A2 without considering sediment processes upstream/downstream of it.

In summary, the three sites outline a clear range of behavior: Area 1 is comparatively stable, Area 2 shows persistent erosion, and Area 3 shifts noticeably from one interval to the next. This contrast highlights that, local setting and boundary conditions can strongly influence how the dune system responds to the same broader climatic and marine forcing.

5.5 Evaluation of Methodological Approaches

The integrated geomatic approach employed (combining multi-temporal UAV LiDAR surveys, RTK-GNSS bathymetric points, and remote sensing of vegetation) proved effective for capturing the fine-scale changes in dune morphology and ecology. Here we discuss the key methodological choices, DEM differencing with LoD thresholds, interpolation techniques, ground vs. vegetation separation, and data integration, and their influence on our results, as well as interpret the rationale behind them in light of the study's outcomes.

5.5.1 Change Detection and LoD Thresholds

A key step in our workflow was applying Level of Detection (LoD) thresholds so that mapped elevation differences could be separated from differences that are plausibly explained by measurement and processing uncertainty. For each DEM of Difference, we used two filters: LoD1, representing a minimal detectability level based on the combined DEM uncertainty, and LoD95, representing a stricter 95% confidence threshold. Using both thresholds made it possible to view the same DoD under a more sensitive criterion and under a high-confidence criterion.

In practice, the two thresholds produced distinctly different pictures. LoD1 retained many small adjustments and therefore generated more detailed change maps, whereas LoD95 removed most low-magnitude differences and highlighted only the strongest signals. This contrast is clear in Area 1 (2021–2022), where LoD1 suggested near-continuous accretion across the surface, while LoD95 retained changes only in more concentrated zones. A similar effect is visible in Area 2 (2023–2024): LoD1 identified roughly 15% of the area as changed, whereas LoD95 reduced that to about 1.9%, largely confined to the foredune margin. These examples show how strongly the selected threshold influences the mapped extent of change.

Methodologically, this approach follows standard practice in geomorphological change detection by explicitly incorporating uncertainty into the interpretation of DoDs. Rather than treating every cell-to-cell difference as real, we propagated DEM errors (RMSE) into a combined threshold that represents the expected "noise floor" of the comparison. This is particularly important in dune settings, where sandy surfaces, shoreline transitions, and interpolation effects can generate small offsets that look like change but are not necessarily geomorphic. Applying LoD thresholds improves reliability, even though a conservative filter like LoD95 can mask subtle but systematic trends if they remain below the confidence limit. Given that the focus of this study is on clear, management-relevant change, we considered that trade-off acceptable, while noting that intermediate thresholds could be explored in future monitoring where the objective is to track gradual, low-magnitude evolution.

5.5.2 DEM Construction and Interpolation (Kriging vs. IDW)

To create DEMs from our point cloud data, we evaluated two interpolation techniques, Inverse Distance Weighting (IDW) and Ordinary Kriging. Choosing the right interpolation was crucial because it affects DEM accuracy and thus the computed changes and LoD values. Our approach was to test both methods on each dataset and quantitatively compare their accuracy using cross-validation with withheld points (specifically using 30% of our RTK-GNSS bathymetric points as independent checks). The results (Table 4) showed a clear pattern, Kriging generally outperformed IDW in most cases, especially in areas or years where topography was complex or data distribution uneven. In flatter or more uniformly sampled cases IDW performed similarly (or even slightly better in one instance, e.g. A1 2021 where IDW RMSE was ~0.186 m vs. 0.286 m for Kriging). However, in highly variable terrain and at the land-water transition, IDW could produce large errors, whereas Kriging maintained much lower errors. Notably, in several area-year combinations where bathymetric data were sparse, IDW's error was exceedingly high (on the order of meters) while Kriging's error remained on

the order of decimeters. For example, in Area 3 2021, IDW interpolation yielded an RMSE over 4 m, whereas Kriging's RMSE was ~0.3 m. Such dramatic differences occurred typically in zones with poor point coverage (e.g. near the shoreline or in parts of the bathymetric survey), where IDW, which relies solely on nearby point averages, struggled to represent the terrain surface. Kriging, by contrast, leveraged the spatial correlation structure of the data (via variogram modeling) to provide more robust estimates even in data-sparse areas.

In essence, Kriging's geostatistical approach, accounting for trends and covariance in elevations, gave it an edge in our dune context, which features strong spatial gradients and heterogeneous data density. Consequently, we selected Kriging as the primary interpolation method for constructing our DEMs in almost all cases. This ensured that our final elevation models were as accurate as possible, thereby improving the reliability of the subsequent change detection. The choice of Kriging is further justified by the nature of our study area, coastal dunes have complex topography (steep foreslopes, undulating ridge, occasionally sharp berms) and our data integration (merging LiDAR and bathymetry) means point spacing isn't uniform, there are gaps in water, overlaps in LiDAR strips, etc. Kriging can handle such issues by interpolating in a statistically optimal way (essentially providing a kind of spatial smoothing that is informed by actual measured variability). IDW, in contrast, might over-smooth or under-smooth arbitrarily depending on point clustering. The rationale for ultimately adopting Kriging was to minimize interpolation-induced errors in our DEMs, errors which propagate directly into LoD calculations. The one caution is that Kriging is computationally heavier and requires statistical modeling, but given our area sizes, this was manageable. We used the RMSE of the chosen interpolation method to compute LoD for each pair of DEMs. By picking the lower-error method, we obtained smaller LoD thresholds, enabling more sensitive change detection. In summary, our interpolation strategy (test both, choose best) was validated by the results, it led to consistently accurate DEMs and reinforced the decision to use Kriging for its superior handling of complex dune morphology.

5.5.3 Handling of Shoreline and Bathymetric Data

A notable methodological challenge was capturing the dune–beach interface where LiDAR data end and bathymetric data begin. Airborne LiDAR, particularly near-infrared systems, cannot penetrate water effectively, so a data gap is inevitably present around the waterline. We addressed this by collecting in-situ bathymetric points in the nearshore shallows and merging them with the LiDAR point cloud to produce a continuous topographic–bathymetric DEM. However, the transition zone at the shoreline still required interpolation because point coverage in that strip is often sparse. We want to emphasize that interpolation was applied only at the shoreline, not arbitrarily across well-sampled dune surfaces. This approach ensured that almost all of the dune terrain in our DEMs is directly constrained by LiDAR observations, with interpolation uncertainty kept minimal on land. The downside is that the shoreline areas inevitably carry higher DEM uncertainty due to this interpolation and the potential temporal mismatch between LiDAR and bathymetric data (which might have been collected on different days or tidal conditions). Indeed, the largest DEM errors and hence the highest LoD values correspond to these shoreline regions. Overlap of LiDAR scan swaths in the surf zone and varying water levels can introduce vertical offsets or striping that inflate

error estimates. In our case, we suspect that some of the high RMSE values for IDW (and the larger combined LoD for certain year pairs) are attributable to difficulties in interpolating the topography and perhaps slight misalignments between data sources in that zone. We mitigated this by using Kriging (which handled the bathymetric gradients better) and by using ground control points near the shoreline for vertical referencing where possible. Still, we observed that the LoD thresholds were often on the order of ±0.3-0.6 m (for LoD1) and roughly double that for LoD95, varying per interval (Table 6 in Chapter 4 summarized these values). These numbers are relatively high for subtle dune changes, and the shoreline interpolation uncertainty is a major contributor. The implication is that changes on the order of a few tens of centimeters might go undetected at the very edge of the dune because they fall below LoD95. We accounted for this by carefully interpreting results near the shoreline, for example, some small apparent changes along the waterline could be artifacts of interpolation or tidal differences, so we treated them cautiously unless they clearly exceeded LoD95 and formed coherent patterns (as in Area 2's case). In retrospect, the methodological decision to integrate bathymetric data is a double-edged sword, it gives a more complete picture of the coastal system (dune to nearshore), but it introduces extra uncertainty and complexity. On balance, we consider it valuable, because understanding dune changes often requires knowing what happened at the toe (gain or loss of sand to the beach). Our approach yielded insight such as the continuity of erosion from dune to beach in Area 2, which would not be fully captured if we had truncated our analysis at the dune foot. Methodologically, future improvements could include increasing shore zone data density (e.g. using UAV photogrammetry or more GNSS profiles at the swash zone) to reduce interpolation distances, and performing more rigorous co-registration of LiDAR and bathymetry. Nonetheless, our handling of the shoreline data, with Kriging and error-thresholding, ensured that any "false changes" from interpolation were mostly filtered out, essentially, if our interpolation at the shoreline introduced spurious differences, those differences likely fell below LoD95 and were not interpreted as real change.

5.5.4 Ground-Vegetation Separation (CSF Filtering) and Vegetation Mapping

Another crucial methodological component was the separation of ground (bare-earth) from vegetation returns in the LiDAR data using the Cloth Simulation Filter (CSF). This allowed us to generate DTMs (Digital Terrain Models) for change detection that represent actual sand surface elevations, as opposed to DSMs that include the tops of vegetation. The CSF method worked by effectively "draping" a virtual cloth over the point cloud to identify the lowest points (ground) and classify higher points as non-ground (e.g. vegetation). We tuned the CSF parameters for our dune environment, which has gentle slopes in some parts and sharp breaks in others, to avoid misclassifying dune ridges as "non-ground" or low shrubs as "ground". The output was a set of ground points for DEM interpolation and a complementary set of vegetation points that we used for vegetation analysis. Overall, the CSF filtering was effective and indispensable, it enabled us to decouple topographic change from biomass change. Without this step, a simple DEM difference might confuse a change in vegetation height for a change in sand elevation (for instance, if a bush grows or is removed, a DSM differencing would show that as a surface change). By working with DTMs, we ensured that the elevation

changes we reported are predominantly due to sediment movement. However, this process introduced some uncertainties. No automated filter is perfect, especially in complex terrains like dunes where low vegetation and undulating ground can be hard to distinguish. It's possible that in some instances the CSF algorithm mislabeled ground as vegetation or vice versa. For example, a very dense clump of beach grass could be mistaken for ground (if the "cloth" rests on the top of the grass), causing the DEM to be slightly too high in that spot; conversely, a smooth sand surface with a uniformly low vegetation cover might see some of those vegetation returns left in the ground class. We did visually inspect and adjust obvious misclassifications (and the supervised classification of orthophotos further helped identify vegetation presence), but small errors likely remain. These classification errors would manifest as small elevation "changes" in the differencing if, say, a patch of vegetation was included in the 2021 ground DTM but excluded in 2022, it would look like the ground dropped there (when in reality it was just vegetation removal). We believe such effects were minor, one reason being that the vegetation in our areas (grasses, some shrubs) is relatively low in height, so even if misclassified, the vertical error introduced is on the order of decimeters at most. Additionally, we performed vegetation mapping separately using spectral indices and orthophoto classification, which acts as a check: if the DEM difference suggests a change and the vegetation map also shows vegetation loss/gain there, we can attribute it correctly. If there was a discrepancy (e.g. DEM change but no vegetation change or vice versa), it alerts to a possible classification artifact. By and large, our multi-pronged approach (CSF + VARI index + SVM classification) kept such uncertainties in check. The Cloth Simulation Filter's performance in our study underscores its value for dune surveys, but also its limitations. A known limitation is at the edges of dense vegetation clumps or in areas with tall vegetation, the filter can "leak" under vegetation or conversely catch on canopy. In future work, incorporating manual ground point editing or using supplemental data (like ground photos or more returns per pulse) might improve accuracy. We note that any residual misclassification would tend to be isolated to small patches and appear as noise, and indeed our LoD95 threshold likely filtered out any resultant spurious changes. Therefore, we are confident that the major changes we interpreted are real and not artifacts of CSF.

For vegetation change detection, we relied on a combination of the LiDAR-derived vegetation point cloud and high-resolution RGB imagery. We computed the Visible Atmospherically Resistant Index (VARI) as a proxy for vegetation "greenness" since our imagery did not include a NIR band. We then used a supervised classification (SVM) on the orthophotos (and VARI layers) to produce binary vegetation maps for each year. This method proved quite successful in delineating vegetated vs. non-vegetated areas, as evidenced by the clear separation of vegetation on dune crests vs. bare sand on beaches in our classification outputs. The multi-temporal comparison of these maps allowed us to identify vegetation expansion and contraction with fine detail. However, some methodological considerations must be noted:

(1) Using VARI (an RGB index) instead of a true NDVI (which requires NIR) is a compromise. VARI is designed to be somewhat robust to atmospheric effects and correlates with green biomass, but it can be fooled by certain conditions, notably, wet sand or driftwood might appear dark and be confused with vegetation, and seasonal color changes in plants might

affect the index. We mitigated this by using supervised classification with manually selected training samples (so the classifier learns the actual color-texture of vegetation vs sand in our scenes, not just index thresholds). Still, the lack of NIR data likely introduced a bit more uncertainty in vegetation delineation than an NDVI-based approach would. For instance, very sparse or senescent vegetation might not be picked up if it's not vividly green.
(2) Shadow and moisture: In early morning or late afternoon, flight images, shadows on the dune can be classified as "vegetation" due to darker hues. We tried to use imagery acquired with good sun angle to minimize harsh shadows, and our SVM classification would treat shadowed sand differently from plants. Moist sand can also appear darker and sometimes greenish on RGB, potentially confusing the index. In our area, wet sand is mostly at the beach foreshore, well outside the vegetated dune, so it was less of an issue, but could affect classification near the waterline.
(3) Georeferencing consistency: We assume our multi-year orthophotos and LiDAR are co-registered accurately with residual offsets expected to be only a few centimeters. Any larger misalignment could introduce artificial "change" at feature boundaries and create false edges in the maps. For this reason, careful attention was given to maintaining a consistent reference system and stable alignment across years, so that the spatial patterns interpreted in the change maps reflect real surface evolution rather than georeferencing artefacts.
In conclusion of this methodological evaluation, we find that our chosen approaches, thresholder DEM differencing, Kriging, interpolation, integrated LiDAR-bathymetry modeling, and independent vegetation mapping were appropriate and yielded reliable results. They allowed us to confidently parse out real geomorphic changes from noise, target the analysis on significant changes, and relate those changes to ecological shifts. Every method has its limitations, but by understanding and addressing those (through validation, error thresholds, and cross-comparison of data), we ensured that the study's findings rest on a solid technical foundation. This robust approach can serve as a model for similar dune monitoring efforts, where data accuracy and interpretation confidence are paramount.

5.6 Limitations and Uncertainties

It is important to acknowledge the limitations and uncertainties inherent in the data and methods. These factors could affect the precision of our results and should be considered when interpreting the findings or planning future work. We discuss the main sources of error, roughly in order of their significance, and how they may have influenced our analysis.

5.6.1 Survey Alignment and Systematic Errors

The most significant potential errors stem from any gross operational or georeferencing inaccuracies in the input data. Our analysis assumes that the multi-temporal datasets (LiDAR point clouds and bathymetric surveys from 2021-2024) are accurately co-registered in a common coordinate frame. Any residual misalignment, for example, a vertical offset between one year's LiDAR survey and another's, would produce an artificial "change" across the whole area. We took steps to minimize this risk (using RTK GNSS for LiDAR, and checking against ground control points, especially along stable features like the inland edge of the

survey area). However, small offsets on the order of a few centimeters could persist. Such a bias is difficult to detect in vegetated, dynamic terrain because there is no obvious invariant reference (like a paved surface). Nonetheless, the accuracy of co-registration is a limiting factor, our reported LoD1 thresholds (typically 0.3-0.6 m) incorporate the combined survey error and would cover small biases, but we cannot categorically rule out that part of the "zero-change" class contains a hidden uniform change below detection limit. Additionally, there could be orientation errors (e.g. if the LiDAR had slight pitch/roll calibration issues) that cause minor spatially varying errors. Overall, we estimate these systematic errors are low, on the order of a few centimeters, and thus do not change the qualitative findings, but they do set a floor on the smallest changes we can trust. In future iterations, a direct point cloud-to-point cloud alignment (using ICP or surface matching algorithms) could be performed to further refine relative orientation, which was beyond the current scope.

5.6.2 LiDAR and Optical Limitations in Wet or Low-Reflectivity Areas

Coastal surveys face particular challenges in wet or water-covered zones, which in our study translate to the beach and swash areas. Airborne LiDAR has an intrinsic limitation, it cannot penetrate water, and very wet surfaces can yield uncertain elevations due to specular reflection or lack of returns. Although we supplemented LiDAR with bathymetric points for submerged parts, the intertidal zone, is tricky. If the LiDAR was flown at a time when the sand was moist (e.g. just after a wave receded or shortly after rain), the laser reflectance could be reduced, potentially causing fewer ground returns or slightly erratic elevations. This could introduce higher noise in those fringe cells of the DEM. Moreover, on the optical side, our vegetation mapping could be confounded by wet sand or wrack, moist sand can appear darker and sometimes greenish, possibly leading to misclassification as "vegetated" in the RGB imagery if not carefully distinguished. We did address this in our classifier training (ensuring wet sand was labeled as non-vegetation), but some uncertainty remains. The NIR limitation is also relevant, since we lacked a NIR band, we could not use NDVI to more robustly pick out vegetation vs. wet sand or algae. VARI did a decent job, but NDVI would normally better separate green vegetation from others (because water and wet sand reflect very little NIR, making NDVI very low for those, whereas VARI might not separate them as cleanly). This is a limitation that could lead to slight under- or over-estimation of vegetation especially at the dune toe where seaweed or wet sand might confuse the classification. We consider any such misclassification to have a minor impact on our broad results (the major vegetation changes were large contiguous areas that are not explained by, say, a wet sand patch), but it's a source of uncertainty for fine-detail mapping. In summary, wet area issues likely increased our error margins at the interface of dune and beach, necessitating cautious interpretation of changes right at the shoreline.

5.6.3 Bathymetric Data Density and Interpolation Uncertainty

Integrating the bathymetric point data adds uncertainty because the measurements are unevenly distributed and must be interpolated to form a continuous nearshore surface. The GNSS-RTK elevations were collected as discrete points along transects across the land–sea

interface, and practical limits (tide windows, wave conditions, access and safety) restricted how densely the area could be sampled. As a result, gaps remain between transects, and small-scale features in shallow water (e.g., bars or troughs) may be only partly captured. These gaps can propagate into the interpolated DEM, so local depth errors are expected even with careful modelling. To reduce this effect, the bathymetry surface was generated using kriging and the shoreline was used to guide the transition at the boundary.

If a storm altered the sandbars between those surveys, then the "seam" between LiDAR DEM and bathy DEM could have a discontinuity. We did not detect obvious discontinuities (which would show up as strange change patterns at the extreme seaward edge), so this is likely minor. Nonetheless, temporal mismatches are a form of uncertainty, ideally, all data would be truly simultaneous. The LoD analysis partly accounts for interpolation error by using the DEM RMSE, but it assumes errors are random. Interpolation errors can be spatially structured (e.g. a bias over an unsurveyed area). Our use of Kriging helped by providing not just an estimate but also a smoother transition guided by variogram (thus likely reducing any bias compared to a blunt IDW guess). In practice, the largest bathy interpolation uncertainties coincided with areas that did undergo real big changes (e.g. A3's shoreline shift), but since those changes were large, they still registered above LoD95. Smaller genuine changes in the nearshore might have gone undetected due to these uncertainties.

5.6.4 CSF Filtering and Vegetation Classification Errors

We have partly discussed this in the methodology section, but to reiterate as a limitation, the Cloth Simulation Filter's classification of ground vs. non-ground points is not error-free. One source of error is at the boundary of vegetation patches, for example, the base of a shrub could be incorrectly marked as ground or the top of grass as ground if the cloth parameter is not perfectly set. We tuned the CSF with relatively conservative settings (including a stiffer cloth) so it could follow subtle dune undulations without over-smoothing the surface. The trade-off is that some very low vegetation can be picked up as "ground," especially at the edges of grass patches or around small shrubs. In that case, the DEM over vegetated zones may end up slightly higher because it carries a small vegetation component. When that cover thins or disappears in a later survey and is no longer included in the ground surface, the DoD could then show an apparent erosion that is not purely geomorphic. The reverse can happen too: if a shrub is excluded from the ground class in one year but partly included in another (for instance because local point density and penetration differ), the map may suggest a small, local accretion.

We expect these situations to be limited because the processing was kept consistent from year to year and the same CSF parameters were applied across the full time series. In addition, the vegetation mapping provides a practical check on whether a detected elevation signal is more likely a real terrain changes or a vegetation-driven artefact. Even so, the CSF contribution to uncertainty is greatest in dense vegetation and is plausibly on the order of ±0.1-0.2 m in those spots. This is smaller than our LoD1 in most cases, meaning it wouldn't drastically affect our significance masking, but it could contribute to the cluster of small changes around zero that we see in histograms. Similarly, the supervised classification of vegetation from imagery can have errors, e.g. classifying a patch of shadow as vegetation or missing a thin veil of grass on

sand. We likely slightly underestimated vegetation in mixed pixels (where sand and grass intermix, the classifier might lean one way). This would affect the absolute area of vegetation reported (in tables 13-15) by a small margin. Since we focus on net changes and patterns, and applied the same classification procedure each year, any bias is systematic and cancels out in change. Future work could quantify classification accuracy with ground truth vegetation surveys, but for our purposes the level of detail was sufficient.

5.6.5 Temporal Frequency and Event Impacts

Another limitation is the annual sampling interval of our data. Significant dune changes can happen in a single storm event and then partly recover within weeks. By surveying roughly once a year, we might miss the peak of erosion or the full extent of recovery. For instance, Area 3's big erosion occurred at some point between late 2022 and late 2023, if sand started to return later in 2023, our annual snapshot might under-report the intermediate worst condition or any short-term sand return. Similarly, vegetation could die back in winter and regrow in spring, depending on survey timing, the measured "loss" might partly be seasonal dieback rather than permanent loss. We scheduled surveys in similar seasons to mitigate seasonal effects, but some differences in timing (e.g. early vs. late summer) could introduce variability. Thus, our change calculations treat changes as if they occurred evenly over the interval, which might not capture intra-annual fluctuations. This is a limitation in interpreting causality, for example, we sometimes attribute changes to "the 2022-2023 winter," but it's possible that some recovery by summer 2023 had already occurred and we didn't capture the absolute nadir of dune condition. Higher-frequency monitoring (e.g. after major storms) would improve understanding of the short-term dynamics and extremes.

5.6.6 Statistical and Modeling Assumptions

For the LoD calculation, DEM errors were treated as random and approximately normal. In reality, some errors (especially near the shoreline where interpolation effects are stronger) can be spatially biased, so the LoD thresholds are best seen as practical cut-offs rather than strict guarantees. This leaves a small chance that very subtle changes are absorbed into "no change," or that occasional outliers pass the threshold.

The primary limitations of this study come down to data resolution and noise (especially at the dynamic dune toe), the difficulty of separating ground changes from vegetation and water influences, and the timing of surveys. These uncertainties mean that our quantitative values (areas, % change) have error bars, for instance, an "8% area eroded" could in reality be 7% or 9% if classification missed or added a percent, or "1 m of erosion" might be ± 0.1-0.2 m off. We are confident, however, in the qualitative patterns and the major conclusions, the scale of the changes we discuss far exceeds the noise level. For instance, A2's vegetation loss was ~8% of area, even considering the above uncertainties, there is no plausible scenario in which that area actually remained vegetated. Likewise, A3's accretion and erosion events are well above our uncertainty in elevation (a few cm). Thus, while one should not over-interpret very fine details, the broader findings are robust. Recognizing these limitations provides avenues for improvement in future monitoring, employing multi-temporal data fusion (optical, LiDAR,

possibly radar) to reduce gaps, increasing survey frequency for capturing transient events, and refining error models (perhaps even spatially variable LoD that accounts for higher uncertainty at shoreline vs interior). Ultimately, acknowledging uncertainties is crucial for informed management decisions, it allows managers to weigh the confidence in reported changes and perhaps prioritize responses to changes that clearly exceed the noise (which our analysis has highlighted).

5.7 Implications for Dune Conservation and Monitoring Strategies

The findings of this analysis carry several important implications for the conservation of the San Rossore coastal dunes and inform broader strategies for dune monitoring and management.

5.7.1 Differentiated Management by Area

The three study areas behave in markedly different ways, so a single "one-size-fits-all" management strategy would be inappropriate. Area 2 emerges as the clearest priority: the persistence of foredune erosion together with a pronounced decline in vegetation indicates a stressed sector where protective dune functions may be weakening. In practical terms, management in A2 could focus on stabilizing the foredune and supporting vegetation recovery, for example through sand-trapping measures (such as fencing or brushwood barriers) combined with targeted planting of native dune species to re-establish a protective cover. Because the mapped accretion zones tend to coincide with vegetation growth, reinforcing plant cover in A2 could help retain wind-blown sand and reduce the erosional feedbacks affecting the dune face. Any active intervention, however, should be assessed carefully in light of the park's protected status and natural dynamics. By contrast, Area 1 appears comparatively stable and can be managed primarily through preservation, limiting new disturbances and maintaining existing access controls. Area 3 shows a more variable but not strongly unidirectional behavior, suggesting that continued monitoring (rather than immediate engineering measures) may be the most appropriate response. If another large accretion or erosion event occurs, adaptive management could be needed, for example, if a huge deposition happens again and buries vegetation, managers might assist by planting on the new dune to speed up stabilization, thereby preventing the sand from blowing away or eroding as quickly. In summary, Area 2 likely needs active intervention and careful monitoring, Area 1 needs protection of its status quo, and Area 3 needs continued observation and potentially facilitation of its natural recovery cycles. The heterogeneous responses we documented caution against a uniform management plan for the entire park.

5.7.2 Vegetation as a Keystone for Dune Stability

Vegetation plays a central role in dune resilience, acting as both an indicator and agent of dune stability. Zones in which vegetation thrive generally zones of sand accumulation or stability, whereas vegetation loss often herald or accompany physical erosion. This implies that conservation of dune vegetation is not merely about preserving biodiversity, but is

directly tied to the structural integrity of the dunes. Implication for management, like protecting and enhancing vegetation cover can significantly bolster dune resistance to erosion. For instance, in areas like A2 where vegetation has been lost along the foredune, one might expect accelerated erosion because bare dunes are more easily blown out by wind and cut by waves (no roots to hold sand, no stems to dissipate wave energy). Conversely, A1's dense vegetative cover likely helped it withstand erosive forces, even when erosion occurred in A1, it was relatively shallow, possibly because plant root mats held the dune sand in place, preventing deep scouring. Therefore, management should prioritize vegetation health, this could include restricting activities that damage, controlling invasive species that might destabilize dune plant communities, and possibly irrigating or shading new plantings if needed to ensure they establish. The net "greening" observed in Area 3 by 2024 is encouraging and indicates that, where disturbance pressure is low, dune vegetation can recover without intensive intervention. Following major events, recovery could be supported with light, temporary actions aimed at stabilizing sand and helping plants re-establish. More broadly, the close coupling between vegetation patterns and morphological change means that vegetation cover itself can be used as a practical warning signal. A sudden drop in plant cover within a specific sector is often consistent with recent erosion or storm impacts and can highlight locations that deserve prompt inspection. For this reason, routine vegetation mapping can help flag emerging weak points before larger volume losses become obvious, supporting an integrated monitoring approach that tracks terrain and ecology together.

5.7.3 Continuous High-Resolution Monitoring

The study demonstrates the value of high-resolution geomatics tools (UAV LiDAR, photogrammetry) in capturing changes that would be missed by conventional surveying. The ability to pinpoint changes of 0.5-1 m in elevation and map vegetation shifts at sub-5 m scales allowed us to understand the dune dynamics in detail. This has implications for how the park should be monitored going forward. A practical recommendation is to make repeat surveys a routine part of park monitoring, ideally on an annual basis and again after major storm events. In this study, UAV-based LiDAR proved well suited to capturing the types of changes that matter for dune management. Establishing a consistent, year-by-year LiDAR survey programme would allow managers to build a longer, comparable record of change, rather than relying on isolated snapshots. With that longer time series, it becomes much easier to judge whether the patterns seen here are persisting, intensifying, or shifting direction under changing coastal conditions. It would also allow assessment of management interventions, e.g., if sand fencing is installed in 2025, LiDAR in 2026-27 could quantify how much additional sand was captured. Given the climate change context (rising sea levels and possibly more intense storms) continuous monitoring is essential to anticipate how the dunes will respond. The high detail ensures that even small precursors of big changes can be detected and addressed proactively. Our results specifically highlight some metrics to watch, dune toe position (a retreat indicates erosion), dune crest height (a lowering could indicate overwash or blowouts), and vegetation cover percentage on the foredune (a decline could signal vulnerability). By tracking these, rangers or scientists can identify degrading sections early. This is especially important for Area 2, which might reach a critical state (e.g. dune breach) if

erosion continues, early warning from monitoring could prompt emergency measures (like sand nourishment or temporary wave barriers) to prevent irreversible damage like barrier dune collapse.

5.7.4 Adaptive Management and Natural Dynamics

The differences observed among the areas also counsel an adaptive management framework that accommodates natural dune dynamics. For example, Area 3's big accretion then erosion might be part of a natural cycle, possibly influenced by river sediment pulses or alternating weather patterns. Managers should recognize that not all erosion is "bad" in the sense of requiring intervention, if it's preceded and followed by accretion, the system may be dynamic yet sustainable. Intervening in such a system (e.g. trying to "fix" the position of the dune) might actually do more harm than good, as it could interfere with natural sediment flows. In Area 3, a sensible approach might be to allow natural processes to continue but ensure that no critical infrastructure is at risk in the vicinity and that invasive species do not colonize the newly disturbed areas (which can hinder native vegetation return). On the other hand, Area 2's trend seems unidirectional, likely reflecting a perturbation (human or climatic) that the system cannot naturally compensate. Adaptive management means actively testing measures to stabilize it, but also being prepared to adjust or escalate efforts if initial steps don't work (for instance, if planting vegetation alone doesn't slow erosion, perhaps dune reinforcement or reducing wave energy with offshore measures might be necessary). Essentially, the data-driven insight allows managers to distinguish between natural variability and concerning trends, aligning interventions accordingly.

5.7.5 Enhancing Resilience to Climate Change

Coastal dunes are frontline defenses against storms and sea level rise. Our study's implications feed into climate change adaptation strategies for the park. The fact that Area 2 has experienced notable retreat from 2021 to 2024 could be an early indicator of how a segment of the coast responds to increasing erosive forces. By reinforcing vegetation and possibly dune elevation in such vulnerable segments now, managers can enhance the resilience of the dune system to future sea-level rise and storm surge. The results also encourage looking beyond the dunes themselves, if Area 2 is eroding due to lack of sand supply, it may require regional solutions (e.g. beach nourishment or restoring sediment flow from updrift sources). Protecting and restoring dune vegetation not only stabilizes dunes but also contributes to carbon sequestration and biodiversity, aligning with climate mitigation and ecosystem-based adaptation principles.

5.7.6 Community and Educational Outreach

The clear connection between vegetation cover and dune condition also offers a strong basis for outreach and public education. People understand dunes better when they can see what is happening. Most visitors won't notice a few centimetres of sand moving, but they do notice when a dune turns from green to bare. That's why linking dune health to vegetation cover is

useful for education: it helps explain, in a simple way, why rules like staying on paths, not walking on planted areas, and not removing driftwood or plants actually matter. For instance, showing images of Area 2 before and after, highlighting how the loss of plants led to dune damage. Engaging local stakeholders in monitoring (they could report unusual changes or assist in planting grasses) might also be fruitful.

Overall, the results provide a concrete basis for management in San Rossore Park, highlighting the value of maintaining dune vegetation, continuing regular high-resolution monitoring, and adapting actions to the specific behavior of each coastal sector. By implementing these insights, park managers can better protect the dune ecosystem in the face of both natural dynamics and global change pressures.

6 Conclusion

Over the 2021-2024 period, this study combined high-resolution geospatial surveys (UAV photogrammetry, LiDAR, RTK-GNSS, and nearshore bathymetry) to produce annual DEMs and orthophotos for three coastal dune sectors (A1, A2, A3) in San Rossore Park. By differencing the DEMs and applying "Level of Detection" thresholds to remove changes within the expected error, we quantified the main year-to-year geomorphic variations. In parallel, multi-temporal vegetation indices and image classifications were used to track changes in dune vegetation cover. Taken together, this eco-morphological framework offers a clear picture of how dune topography and plant communities evolved through the study period.

Area A1 remained in dynamic equilibrium. A year of widespread foredune accretion (2021-2022) was almost entirely offset by an erosional phase in 2022-2023, resulting in little net topographic change. Pioneer vegetation colonized the newly deposited sand, then receded when that sand eroded, leaving the overall vegetated area essentially unchanged. These balanced gains and losses highlight A1's resilience, as its dense vegetation and sufficient sediment supply allowed it to absorb short-term perturbations without lasting damage.

Area A2 underwent persistent foredune erosion with little or no compensating accretion, resulting in a clear sediment deficit and measurable dune retreat by 2024. A substantial portion of A2 showed significant elevation losses over the study period, and the vegetation gains observed in 2022 were quickly reversed by widespread die-back in 2023-2024, leaving much of the dune front exposed. Overall, the combined loss of sand and plant cover points to a particularly vulnerable sector that remained dominated by erosional conditions.

Area A3, in contrast, showed a pronounced boom-and-bust pattern but limited net change over the full period. A large accretion phase in 2021-2022 was largely removed by strong erosion in 2022-2023, so that by 2024 the dune had returned close to its 2021 configuration. Vegetation declined initially due to burial in 2022, but recovered once conditions stabilized, and by 2024 plant cover slightly exceeded its 2021 extent. This delayed rebound suggests that, despite short-term disruption, A3 retains a capacity for natural recovery when disturbances subside.

Interpretation of these changes was supported by careful uncertainty analysis. We applied Level of Detection thresholds (LoD1 at 1σ and LoD95 at 95% confidence) to ensure that only changes exceeding the DEMs' vertical error (a few decimeters) were considered significant. This filtering was crucial in high-uncertainty areas like the shoreline, where sparse LiDAR coverage and interpolation made small apparent changes unreliable. We also acknowledge that separating ground and vegetation with CSF filtering can introduce some classification error. However, we kept the workflow consistent across all years and used the vegetation mapping as a check, which helps reduce any systematic bias. A useful next step would be to monitor more frequently (seasonally, or immediately after major storms) so that short-lived episodes of erosion or deposition are not smoothed out between annual surveys and rapid dune responses are captured more clearly. In addition, deploying UAV photogrammetry or extra GNSS transects in the surf zone would improve shoreline coverage, and adding multispectral or field-based vegetation surveys would refine classification. Extending the

monitoring beyond 2024 is important to see whether current trends (such as A2's erosion or A1's stability) persist or shift under different conditions. Finally, linking geomorphic changes with ecological indicators (e.g. plant community composition or habitat quality) would provide a more holistic assessment of dune health and resilience. These efforts, building on the framework established here, would further deepen insight into coastal dune evolution.

7 References

Luijendijk, A., Hagenaars, G., Ranasinghe, R., Baart, F., Donchyts, G., & Aarninkhof, S. (2018). The state of the world's beaches. Scientific Reports, 8(1), 6641. https://doi.org/10.1038/s41598-018-24630-6

Jackson, DWT., Costas, S., González-Villanueva, R., & Cooper, A. (2019). A global 'greening' of coastal dunes: An integrated consequence of climate change? Global and Planetary Change, 182, 1-9. Article 103026. https://doi.org/10.1016/j.gloplacha.2019.103026

Duffy, J. P., Shutler, J. D., Witt, M. J., DeBell, L., & Anderson, K. (2018). Tracking Fine-Scale Structural Changes in Coastal Dune Morphology Using Kite Aerial Photography and Uncertainty-Assessed Structure-from-Motion Photogrammetry. Remote Sensing, 10(9), 1494. https://doi.org/10.3390/rs10091494

Flores-de-Santiago, F., Valderrama-Landeros, L., Villaseñor-Aguirre, J., Álvarez-Sánchez, L. F., Rodríguez-Sobreyra, R., & Flores-Verdugo, F. (2023). Detection of Beach-Dune Geomorphic Changes by Means of Satellite and Unmanned Aerial Vehicle Data: The Case of Altamura Island in the Gulf of California. Coasts, 3(4), 383-400. https://doi.org/10.3390/coasts3040023

Ma D, Tian Z, Zhu C and Wang Y (2024) A comprehensive approach to evaluate coastal dune evolution in Haiyang, China. Front. Mar. Sci. 11:1326317. doi: 10.3389/fmars.2024.1326317

Laporte-Fauret, Q., Marieu, V., Castelle, B., Michalet, R., Bujan, S., & Rosebery, D. (2019). Low-Cost UAV for High-Resolution and Large-Scale Coastal Dune Change Monitoring Using Photogrammetry. Journal of Marine Science and Engineering, 7(3), 63. https://doi.org/10.3390/jmse7030063

Christofi, D., Mettas, C., Evagorou, E., Stylianou, N., Eliades, M., Theocharidis, C., Chatzipavlis, A., Hasiotis, T., & Hadjimitsis, D. (2025). A Review of Open Remote Sensing Data with GIS, AI, and UAV Support for Shoreline Detection and Coastal Erosion Monitoring. Applied Sciences, 15(9), 4771. https://doi.org/10.3390/app15094771

Talavera, Lara & Costas, Susana & Ferreira, Óscar. (2022). A new index to assess the state of dune vegetation derived from true colour images. Ecological Indicators. 137. 108770. 10.1016/j.ecolind.2022.108770.

Belcore, Elena & Latella, Melissa & Piras, Marco & Camporeale, Carlo. (2024). Enhancing precision in coastal dunes vegetation mapping: ultra-high resolution hierarchical classification at the individual plant level. International Journal of Remote Sensing. 45. 4527-4552. 10.1080/01431161.2024.2354135.

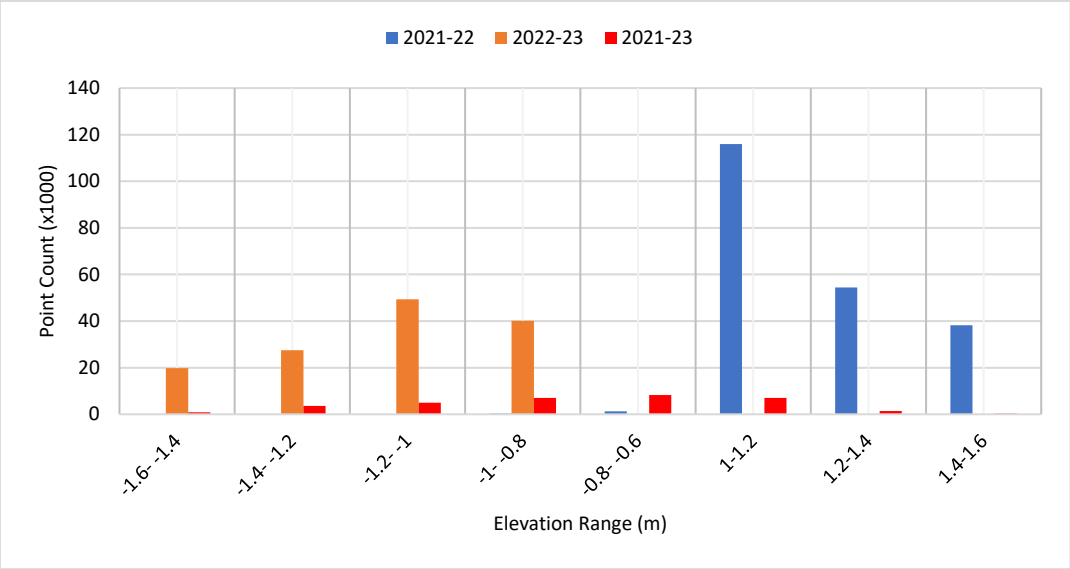
Laporte-Fauret, Q., Marieu, V., Castelle, B., Michalet, R., Bujan, S., & Rosebery, D. (2019). Low-Cost UAV for High-Resolution and Large-Scale Coastal Dune Change Monitoring Using Photogrammetry. Journal of Marine Science and Engineering, 7(3), 63. https://doi.org/10.3390/jmse7030063

Pinton, D., Canestrelli, A., Moon, R., & Wilkinson, B. (2023). Estimating Ground Elevation in Coastal Dunes from High-Resolution UAV-LIDAR Point Clouds and Photogrammetry. Remote Sensing, 15(1), 226. https://doi.org/10.3390/rs15010226

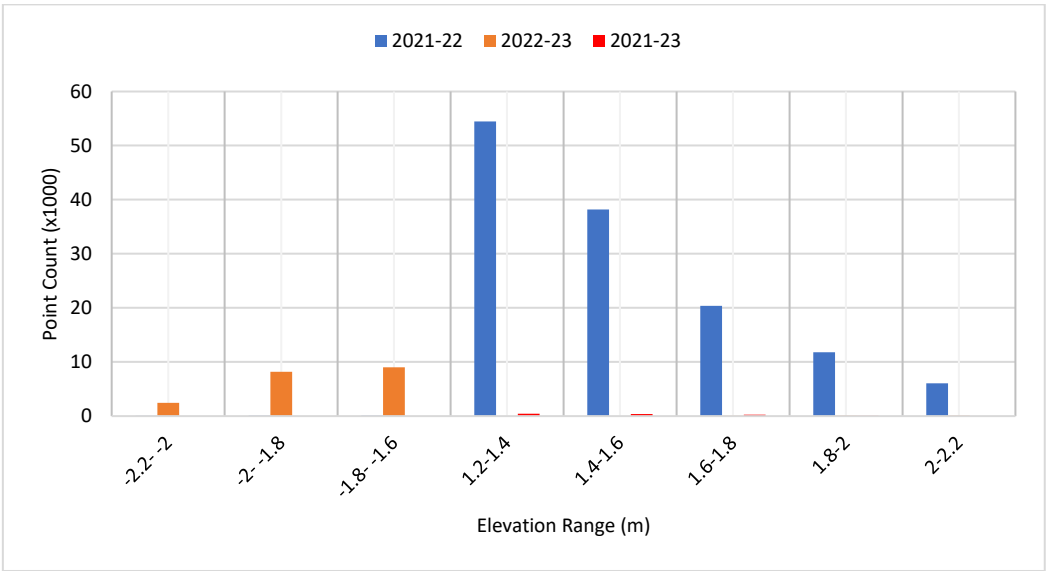
Flores-de-Santiago, F., Valderrama-Landeros, L., Villaseñor-Aguirre, J., Álvarez-Sánchez, L. F., Rodríguez-Sobreyra, R., & Flores-Verdugo, F. (2023). Detection of Beach-Dune Geomorphic

Changes by Means of Satellite and Unmanned Aerial Vehicle Data: The Case of Altamura Island in the Gulf of California. Coasts, 3(4), 383-400. https://doi.org/10.3390/coasts3040023
Bertoni, Duccio & Alquini, Fernanda & Bini, Monica & Ciccarelli, Daniela & Giaccari, Riccardo & Pozzebon, Alessandro & Ribolini, Adriano & Sarti, Giovanni. (2014). A technical solution to assess multiple data collection on beach dunes. Atti della Società Toscana di Scienze Naturali Memorie Serie A. 121. 5-12. 10.2424/ASTSN.M.2014.10.
Innangi, M., Di Febbraro, M., Balsi, M., Colonna, G., Finizio, M., Pontieri, F. and Carranza, M.L. (2025). A novel high-resolution eco-functional vegetation mapping of coastal dunes. Ecological Indicators, 171, 113157.
National Oceanic and Atmospheric Administration (NOAA). (n.d.). LiDAR 101: An introduction to LiDAR technology, data, and applications. Coastal Services Center, Coastal Geospatial Services Division, Coastal Remote Sensing Program
La Nazione. (2024, April 16). La sabbia di Viareggio destinata a noi. https://www.lanazione.it/pisa/cronaca/la-sabbia-di-viareggio-destinata-a-noi-67fea632?live
Pranzini, Enzo & Anfuso, Giorgio & Cinelli, Irene & Piccardi, Marco & Vitale, Giovanni. (2018). Shore Protection Structures Increase and Evolution on the Northern Tuscany Coast (Italy): Influence of Tourism Industry. Water. 10. 1647. 10.3390/w10111647.
Parco Regionale Migliarino San Rossore Massaciuccoli. (n.d.). Conservation of the coastal ecosystems of Northern Tuscany. Retrieved from https://www.yumpu.com/en/document/view/51825907/conservation-of-the-coastal-ecosystems-of-northern-tuscany-parco
Chirico, P., DeWitt, J., & Bergstresser, S. (2020). Evaluating elevation change thresholds between structure-from-motion DEMs derived from historical aerial photos and 3DEP LiDAR data. Remote Sensing, 12(10), 1625. https://doi.org/10.3390/rs12101625
Alfonso-Torreño, A., Gómez-Gutiérrez, Á., & Schnabel, S. (2021). Dynamics of erosion and deposition in a partially restored valley-bottom gully. Land, 10(1), 62. https://doi.org/10.3390/land10010062
Bailey, G., Li, Y., McKinney, N., Yoder, D., Wright, W., & Herrero, H. (2022). Comparison of Ground Point Filtering Algorithms for High-Density Point Clouds Collected by Terrestrial LiDAR. Remote Sensing, 14(19), 4776. https://doi.org/10.3390/rs14194776
Gitelson, A., et al. "Vegetation and Soil Lines in Visible Spectral Space: A Concept and Technique for Remote Estimation of Vegetation Fraction." International Journal of Remote Sensing 23 (2002): 2537–2562
Esri. (2025). ArcGIS Pro tool reference. Retrieved August 27, 2025, from https://pro.arcgis.com/en/pro-app/latest/tool-reference/main/arcgis-pro-tool-reference.htm
Esri. (2025). Tabulate Area (Spatial Analyst). ArcGIS Pro. Retrieved August 27, 2025, from https://pro.arcgis.com/en/pro-app/latest/tool-reference/spatial-analyst/tabulate-area.htm

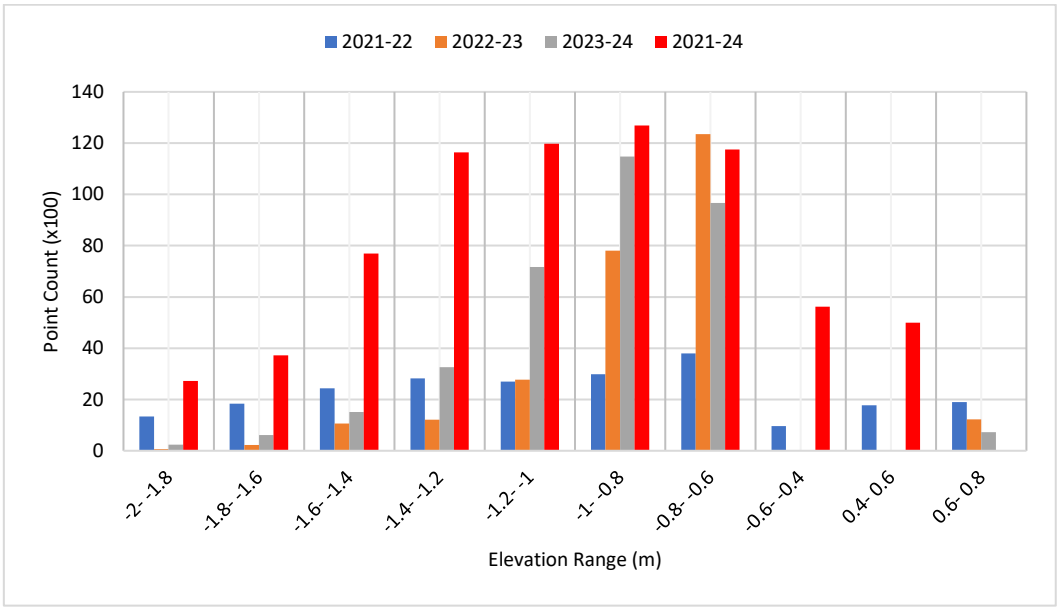
8 Appendix



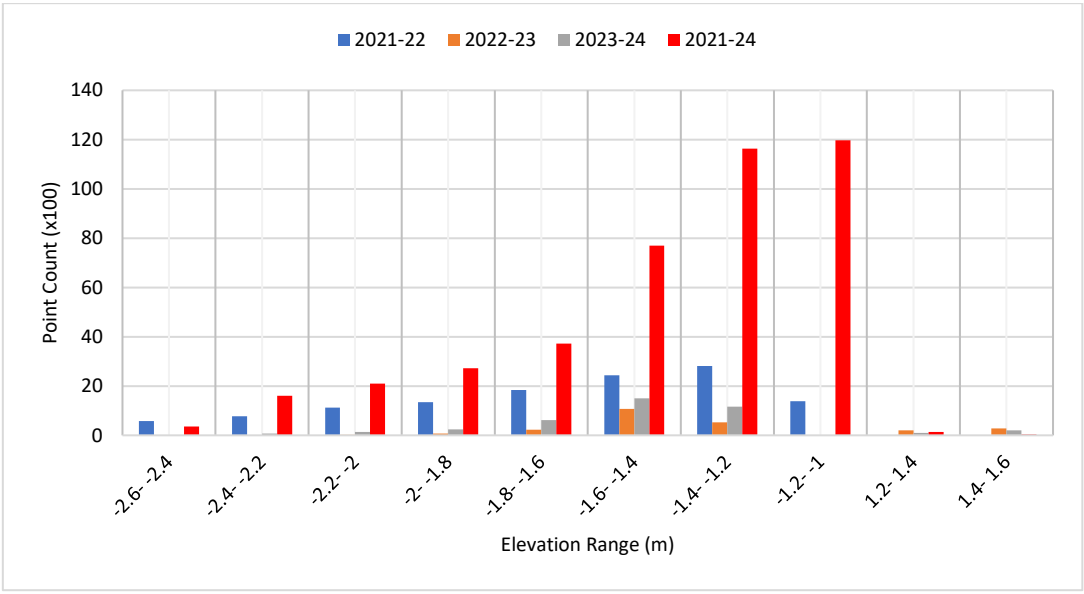
ANNEX 1 Histograms of Area 1 Elevation Changes excluding peak classes at LoD1



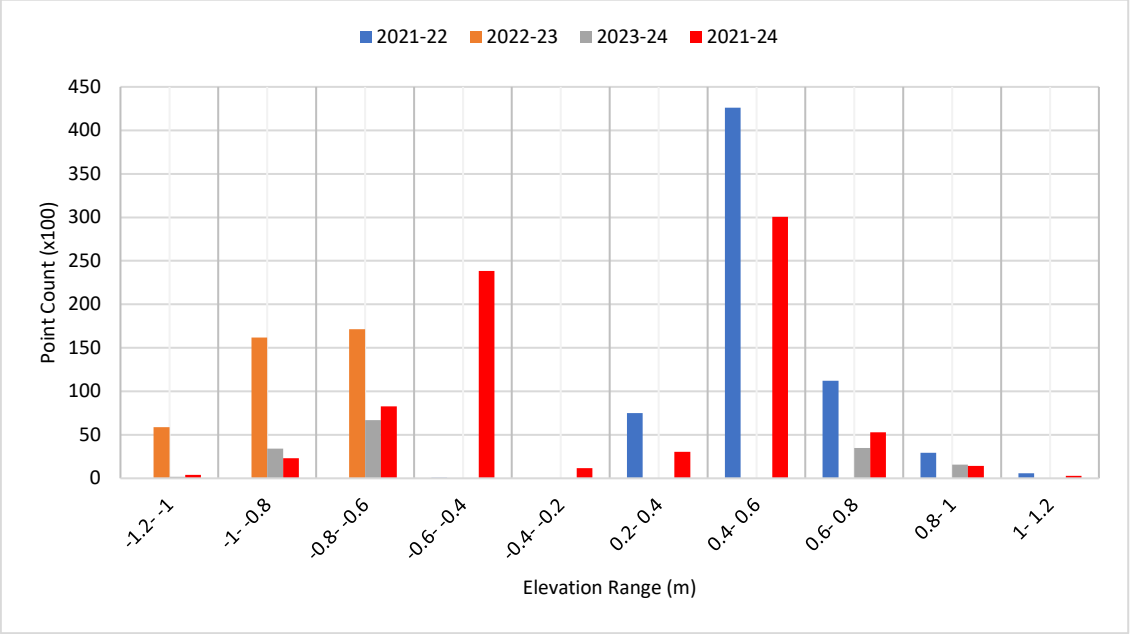
ANNEX 2 Histograms of Area 1 Elevation Changes excluding peak classes at LoD95



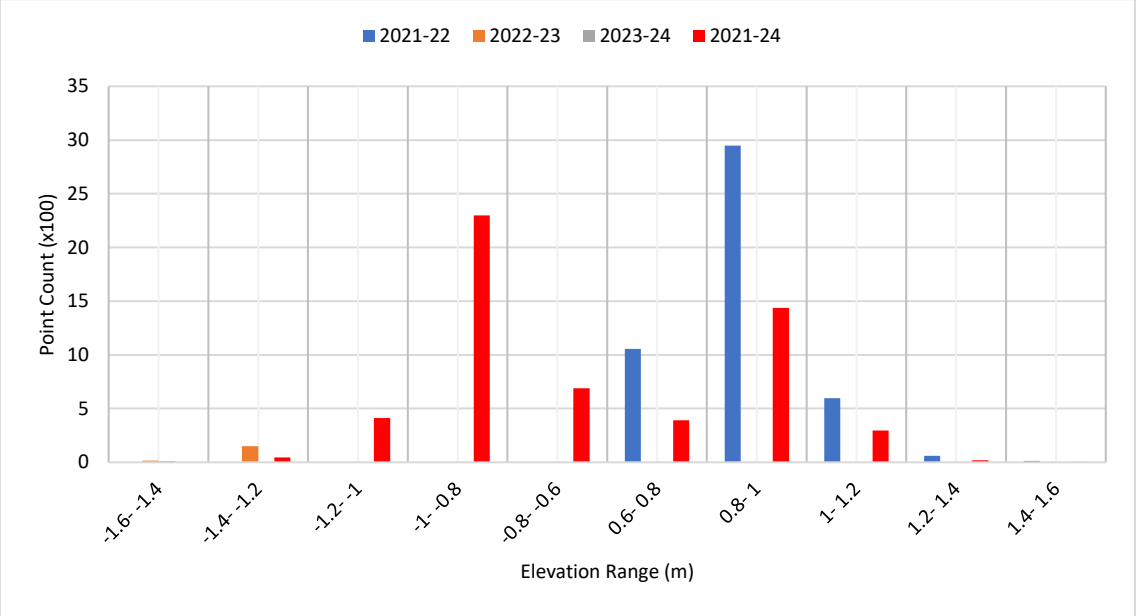
ANNEX 3 Histograms of Area 2 Elevation Changes excluding peak classes at LoD1



ANNEX 4 Histograms of Area 2 Elevation Changes excluding peak class at LoD95



ANNEX 5 Histograms of Area 3 Elevation Changes excluding peak class at LoD1



ANNEX 6 Histograms of Area 3 Elevation Changes excluding peak class at LoD95

A1	Erosion Area	No change Area	Accretion Area	Area Changed	Status
	m2	m2	m2	%	-
2021-2022	146.87	5322.79	118993.53	95.72	Accretion
2022-2023	10320.17	114100.17	69.97	8.35	Erosion
2021-2023	1551.16	118692.11	4219.99	4.64	Accretion

ANNEX 7 DoD Areal change summary of Area 1 at LoD 1

A1	Erosion Area	No change Area	Accretion Area	Area Changed	Status
	m2	m2	m2	%	-
2021-2022	46.67	115289.24	9127.28	7.37	Accretion
2022-2023	1303.15	123147.67	39.48	1.08	Erosion
2021-2023	141.43	124254.29	67.53	0.17	Erosion

ANNEX 8 DoD Areal change summary of Area 1 at LoD 95

A2	Erosion Area	No change Area	Accretion Area	Area Changed	Status
	m2	m2	m2	%	-
2021-2022	1384.73	13596.71	239.43	10.67	Erosion
2022-2023	1592.71	13335.37	292.80	12.39	Erosion
2023-2024	2131.37	12912.99	176.45	15.16	Erosion
2021-2024	4509.60	10100.40	610.88	33.64	Erosion

ANNEX 9 DoD Areal change summary of Area 2 at LoD 1

A2	Erosion Area	No change Area	Accretion Area	Area Changed	Status
	m2	m2	m2	%	-
2021-2022	819.23	14400.03	1.62	5.39	Erosion
2022-2023	119.78	15022.27	78.83	1.30	Erosion
2023-2024	233.19	14937.32	50.31	1.86	Erosion
2021-2024	2665.79	12522.07	33.02	17.73	Erosion

ANNEX 10 DoD Areal change summary of Area 2 at LoD 95

A3	Erosion Area	No change Area	Accretion Area	Area Changed	Status
	m2	m2	m2	%	-
2021-2022	6.30	12864.25	4047.79	23.96	Accretion
2022-2023	2502.52	14413.32	2.49	14.81	Erosion
2023-2024	639.33	15964.77	314.18	5.64	Erosion
2021-2024	2245.19	12168.69	2504.45	28.07	Accretion

ANNEX 11 DoD Areal change summary of Area 3 at LoD 1

A3	Erosion Area	No change Area	Accretion Area	Area Changed	Status
	m2	m2	m2	%	-
2021-2022	0.00	16627.03	291.30	1.72	Accretion
2022-2023	10.35	16907.99	0.00	0.06	Erosion
2023-2024	0.50	16917.84	0.00	0.00	Erosion
2021-2024	214.56	16570.12	133.65	2.06	Erosion

ANNEX 12 DoD Areal change summary of Area 3 at LoD 95